CP Rail

CA1
DTC800-
90
F278

41.D

CA1
DTC800-
90
F278

451875

41.D

TP 10215E
Feasibility Study of Utilizing a Synchronized Laser Scanner For Rail Inspection

Prepared For:
Transportation Development Centre
Policy and Coordination Group
Transport Canada

G. Izbinsky
Research and Development Dept.
CP Rail
Report No.: T-1029-90
February, 1990

DEC 10 '90

451875

The contents of this report reflect the views of the author and not necessarily the official view or opinions of the Transportation Development Centre, Policy and Coordination Group, of Transport Canada.

The work described herein has been partially funded by the Panel on Energy Research and Development administrated by Transport Canada

Un sommaire en français de ce rapport est inclus avant la Table des matières.

Transport Canada / Transports Canada

PUBLICATION DATA FORM

1. Transport Canada Publication No.	2. Project No.	3. Recipient's Catalogue No.
TP 10215E	7020	

4. Title and Subtitle

Feasibility Study of Utilizing a Synchronized Laser Scanner for Rail Inspection

5. Publication Date

February 1990

6. Performing Organization Document No.

T-1029-90

7. Author(s)

G. Izbinsky

8. Transport Canada File No.

D1465-523

9. Performing Organization Name and Address

C.P. Rail
Department of Research & Development
P.O. Box 6042, Station "A"
Montreal, Quebec H2Z 1X4

10. DSS File No.

19SD.T8200-7-7548

11. DSS or Transport Canada Contract No.

T8200-7-7548/01SD

12. Sponsoring Agency Name and Address

Transportation Development Centre (TDC)
200 René-Lévesque Blvd. West
Suite 601, West Tower
Montreal, Quebec H2Z 1X4

13. Type of Publication and Period Covered

May 17 '88-Feb '90

14. Project Officer

D.W. Dibble

15. Supplementary Notes (Funding programs, titles of related publications, etc.)

16. Abstract

The potential use of a laser vision camera as a non-contact transducer for inspections of rail was studied.

The camera developed for this purpose was based on a synchronized laser scanner. It was subjected to both laboratory tests which simulated the railroad environment and actual service trials.

During field testing, the camera was mounted under a railway car and used to monitor rail surface irregularities in the longitudinal direction. The results of these measurements, obtained at a track speed (50 Km/h), were successfully matched to measurements obtained with a high precision computerized reference instrument specially built for this project.

17. Key Words	18. Distribution Statement
Non-contact measurement, laser vision, synchronized scanning rail inspection - high speed, rail corrugations.	Limited number of copies available from the Transportation Development Centre.

19. Security Classification (of this publication)	20. Security Classification (of this page)	21. Declassification (date)	22. No. of Pages	23. Price
Unclassified	Unclassified	--		--

TDC/CDT 79-005
Rev 88

Canada

SUMMARY

A feasibility study of the possible use of a synchronized laser scanner in applications for rail inspection was initiated and carried out by the Research Department, CP Rail with financial support provided by the Transportation Development Centre of Transport Canada. Servo-Robot Inc., a supplier of synchronized laser scanners, was selected as a subcontractor for a portion of this work.

Non-contact measurement devices are preferred by railways and track maintenance contractors for safety-related inspections of rail. This preference is due to the fact that non-contact transducers do not require repair and replacement as frequently as their mechanical (contact) counterparts.

The specific properties of a synchronized laser scanner make it one of a number of possible devices to be used as a non-contact transducer on track inspection vehicles.

The commercial synchronized laser scanner was developed by Servo-Robot Inc. for a welding robot guidance. Application to high speed railway inspection requires, from a laser scanner, endurance to hostile environmental conditions including strong shocks and vibrations, wide ranging temperature fluctuations, and contrast illumination during day and night operations, etc.

In the initial stage of this project, the standard commercial laser scanner was tested in a simulated railroad environment (a vibration bench, a refrigerator, an oven).

Based on the results of laboratory testing, a number of modifications were incorporated in the laser scanner design to enable it to perform satisfactorily on a railway inspection car.

Performance characteristics of a synchronized laser scanner permit use for a number of railway inspection tasks to replace contact transducers and strong competition with other non-contact transducers. The capability to scan the field of view makes it unique in applications where target tracking is required. One of these applications - inspection of the longitudinal rail profile - was chosen for testing of a laser scanner under field conditions.

In order to determine a preferred mounting position of a scanner on the rail car, a series of preliminary tests was carried out during which car body vibrations were measured in different locations; rail vibrations caused by passing wheels were also analyzed. A position in front of the leading axle of the trailing track was selected for the test.

A high precision reference instrument was designed and built for evaluation of performance of a laser scanner. This instrument is capable of performing measurements of rail corrugations in the range of 3" to 48" wavelengths on relatively long segments of track (several hundred feet).

Field tests of a synchronized laser scanner were conducted on CP Rail tracks in Montreal and also at Smiths Falls. The test zones were measured with the reference instrument. The test car, equipped with a laser scanner, passed over the same zones at different speeds collecting data which represented the distance from the car body to the rail surface sampled at 1.5" intervals. This raw data was processed utilizing specially written software which removed from the signal the wavelengths outside of the range of interest (3" to 48"). The result obtained was compared to the result of the reference measurement and showed satisfactory correlation between the two measurements.

Field testing has indicated the capability of a synchronized laser scanner to satisfactorily perform in the railway environment. Further testing is required and will be performed in order to verify the ability to sustain the performance characteristics over longer distances and in extreme weather conditions.

Transports Canada Transport Canada

FORMULE DE DONNÉES POUR PUBLICATION

1. N° de la publication de Transports Canada	2. N° de l'étude	3. N° de catalogue du destinataire
TP 10215E	7020	

4. Titre et sous-titre	5. Date de la publication
Feasibility Study of Utilizing a Synchronized Laser Scanner for Rail Inspection	Février 1990
	6. N° du document de l'organisme exécutant T-1029-90
7. Auteur(s) G. Izbinsky	8. N° de dossier — Transports Canada D1465-523
9. Nom et adresse de l'organisme exécutant C.P. Rail Service de recherche et développement B.P. 6042, station "A" Montréal (Québec) H2Z 1X4	10. N° de dossier — ASC 19SD.T8200-7-7548
	11. N° de contrat — ASC ou Transports Canada T8200-7-7548/01SD
12. Nom et adresse de l'organisme parrain Centre de développement des transports (CDT) 200 ouest, boul. René Lévesque Tour ouest, suite 601 Montréal (Québec) H2Z 1X4	13. Genre de publication et période visée 17 mai '88-fév '90
	14. Agent de projet D.W. Dibble

15. Remarques additionnelles (Programmes de financement, titres de publications connexes, etc.)

16. Résumé

L'objet de cette recherche a été de vérifier les possibilités d'une caméra au laser utilisée comme dispositif d'inspection à liaison non matérielle pour l'auscultation superficielle des rails.

La caméra utilisée, comportant un capteur à balayage synchrone au laser, a été soumise à des essais en laboratoire simulant l'environnement ferroviaire, et des essais en service.

Montée sous le wagon d'auscultation, la caméra a enregistré les irrégularités longitudinales à la surface des rails, à la vitesse de 50 km/h. Les données recueillies ont été comparées à celles d'un instrument témoin de haute précision, assisté par ordinateur, qui avait été conçu et réalisé exprès.

17. Mots clés	18. Diffusion
Capteur à liaison non matérielle, vision laser, balayage synchrone, contrôle des rails, grande vitesse, usure ondulatoire.	Le Centre de développement des transports dispose d'un nombre limité d'exemplaires.

19. Classification de sécurité (de cette publication)	20. Classification de sécurité (de cette page)	21. Déclassification (date)	22. Nombre de pages	23. Prix
Non classifié	Non classifiée	--		--

CDT/TDC 79-005
Rev 88

Canada

Project Team

The project team for CP Rail was:

- G. Izbinsky
- D. D'Aoust
- J. Gillanders
- H. Schrekinger

The project team for Servo-Robot was:

- J.P. Boillot
- B. Beranek
- D. Villeneuve
- E. McConney
- F. Lapinski

SOMMAIRE

Le service de recherche de CP Rail a lancé, avec le concours financier du Centre de développement des transports, de Transports Canada, une étude sur la faisabilité et les possibilités d'un capteur à balayage synchrone au laser pour l'inspection des rails. Une partie de cette recherche a été confiée en sous-traitance à Servo-Robot Inc., fournisseur de ce type de capteurs.

Les sociétés ferroviaires et les entreprises de sous-traitance en entretien des voies ferrées donnent leur préférence aux dispositifs d'inspection à liaison non matérielle parce qu'ils sont plus fiables que les dispositifs mécaniques (à liaison matérielle) qui nécessitent des interventions plus nombreuses.

Les caractéristiques particulières d'un capteur à balayage synchrone au laser placent celui-ci au rang des dispositifs d'inspection à liaison non matérielle propres à cet usage.

La Servo-Robot Inc. avait mis au point ce capteur à balayage synchrone pour qu'il serve au guidage d'un robot de soudage. Or, sa transposition au domaine ferroviaire, notamment l'inspection à cadence rapide des rails de chemins de fer, nécessite des qualités particulières : endurance dans des conditions d'exploitation sévères, résistance à des niveaux élevés de chocs et de vibrations, aptitude à fonctionner à des extrêmes de température et d'éclairage, la nuit, le jour, etc.

La première étape de la recherche a consisté à éprouver un capteur de série dans des conditions simulant l'environnement ferroviaire (générateur de vibrations, réfrigérateur, four).

Les essais en laboratoire ont montré la nécessité de modifier le modèle de série de manière à lui permettre d'accomplir les fonctions de contrôle exigées de lui, ce qui fut fait.

Le capteur à balayage synchrone au laser possède les aptitudes nécessaires pour accomplir plusieurs tâches de contrôle dans le domaine ferroviaire et pour prendre la relève des dispositifs à liaison matérielle utilisés jusqu'ici, en plus de pouvoir concurrencer les autres dispositifs à liaison non matérielle. L'aptitude de ce capteur à balayer le champ visuel à sa portée le rend imbattable dans les applications où l'appareil doit suivre une cible ininterrompue. Parmi ces applications, la profilométrie du champignon des rails a été choisie pour éprouver ce capteur au laser dans des conditions d'exploitations réalistes.

Il a fallu d'abord trouvez le meilleur endroit où poser l'appareil sur le wagon d'auscultation. Après une série d'essais durant lesquels les niveaux vibratoires du wagon ont été déterminés en plusieurs endroits ainsi que les vibrations des rails lorsqu'ils sont sollicités par le passage des roues, l'endroit choisi, aux fins de l'essai, a été devant l'essieu directeur du bogie arrière.

Un instrument témoir de haute précision a été conçu et réalisé dans le but d'apprécier les performances du capteur à balayage. Il s'agit d'un dispositif pouvant mesurer l'usure ondulatoire des rails dans la plage de longueurs d'onde allant de 3 à 48 pouces, et ce sur des tronçons de voie relativement longs (plusieurs centaines de pieds).

Les essais du capteur ont été réalisés sur les voies appartenant à CP Rail à Montréal et à Smith Falls. Le mesurage s'est fait d'abord avec l'instrument témoin, puis avec le capteur au laser. Dans ce dernier cas, le mesurage a été répété sur les mêmes cibles à des vitesses différentes; la variable mesurée est la distance par rapport à la surface des rails, relevés faits à intervalles de 1,5 pouce. Les données brutes ainsi recueillies ont été analysées à l'aide d'un logiciel permettant d'éliminer les signaux dont la longueur d'onde se trouve de part et d'autre de la plage visée : 3 à 48 pouces. La comparaison des deux séries de résultats a fait ressortir une corrélation satisfaisante.

Ces essais ont montré que le capteur à balayage au laser fonctionne bien dans un environnement ferroviaire. Mais d'autres essais seront nécessaires pour s'assurer qu'il peut donner les mêmes bonnes performances de manière soutenue et dans des conditions météorologiques extrêmes.

Table of Contents

	Page
1. Introduction	1
2. Synchronized Laser Scanning	4
3. Areas of Possible Applications	8
4. Development of a SLS Camera For Longitudinal Rail Surface Inspection	12
4.1 Environmental Testing and Camera Protection	12
4.2 Location of the SLS Camera on a Test Car	14
4.3 Vibration of the SLS Camera on a Test Car	16
4.4 Reference Rail Surface Inspection System	20
4.5 Field Testing of the SLS Video System	25
5. Conclusions	36
References	38
Appendix	39

1. Introduction

Modern track geometry cars are sophisticated measurement systems; they are widely used for safety-related inspections and for track maintenance purposes.

Railway-users of track geometry cars and track maintenance contractors state that as much as 90% of track measurement service costs are due to the mechanical transducers that frequently require repairs and replacement.

Recent advances in the fields of machine-vision and high-speed data processing made it possible to build non-contact measurement systems for railway inspection needs. Such systems are rapidly finding their way into the railway industry in Australia, Europe, Japan, and North America. They are used for a variety of measurements such as gauge, curvature, rail cross-section, etc.

Vision systems found on track geometry cars vary in the principle of operation. The oldest group of vision systems for rail inspection use a high intensity flash lamp as a light source projecting a thin strip of light on the rail head, a high resolution camera to capture the image and a fast data processor. Usually, this type of a system delivers moderately accurate measurements at quite low sampling rates (3-5 frames/sec).

Rail profile information is collected in a very short time interval, practically instantaneously, rendering measurements virtually immune to noise generated by rail and car dynamics. Better performance from railway vision systems is expected with the use of laser light sources. At CP Rail, the first experiments with a laser vision system were carried out in 1984: a cylindrical lens was used to transform a laser beam into a thin strip of light. At present, systems using an identical type of light source are commercially available. Laser vision systems can operate in the presence of bright ambient light, project a sharper image, and deliver sampling at much higher frequencies than the systems using a flash lamp.

One of the latest additions to the family of laser vision systems - a synchronized laser scanner - is based on the work of Dr. M. Rioux at NRC, Canada. Although this type vision system requires a longer time interval for data collection across the field of view than the systems described above, the scanning feature opens new opportunities in the area of rail inspection.

This report summarizes preliminary work undertaken by CP Rail on a contract basis with the Transportation Development Centre of Transport Canada, the purpose of which was to evaluate the application potential for synchronized laser scanning technology to high speed rail inspection in order to support railway's safe and efficient operation.

2. Synchronized Laser Scanning (SLS)

The basic idea of Synchronized Laser Scanning, as described by its originator M. Rioux, NRC Canada (Ref. 1), is synchronization of the projection of a light spot with detection. This is realized by using two scanners: the first one projects a beam on the surface to be measured, and the second is coupled to a receiving sensor to follow the spot. Both scanners operate at the same frequency. An exact synchronization is achieved by using a galvanometer driven double-sided mirror, the optical arrangement of which is shown on Fig. 1.

This arrangement was used by Servo-Robot Inc., a company located in Boucherville, Quebec, for the first commercial application to robot guidance in arc welding.

The Research Department of CP Rail approached Servo-Robot Inc. in 1985 to explore the potential use of the SLS camera for the railway industry. The main motivations for our interest in the SLS technology were the following:

Although using a principle similar to the traditional triangulation technique, the SLS provides better resolution without reduction of the field of view, and reduces the shadow effect.

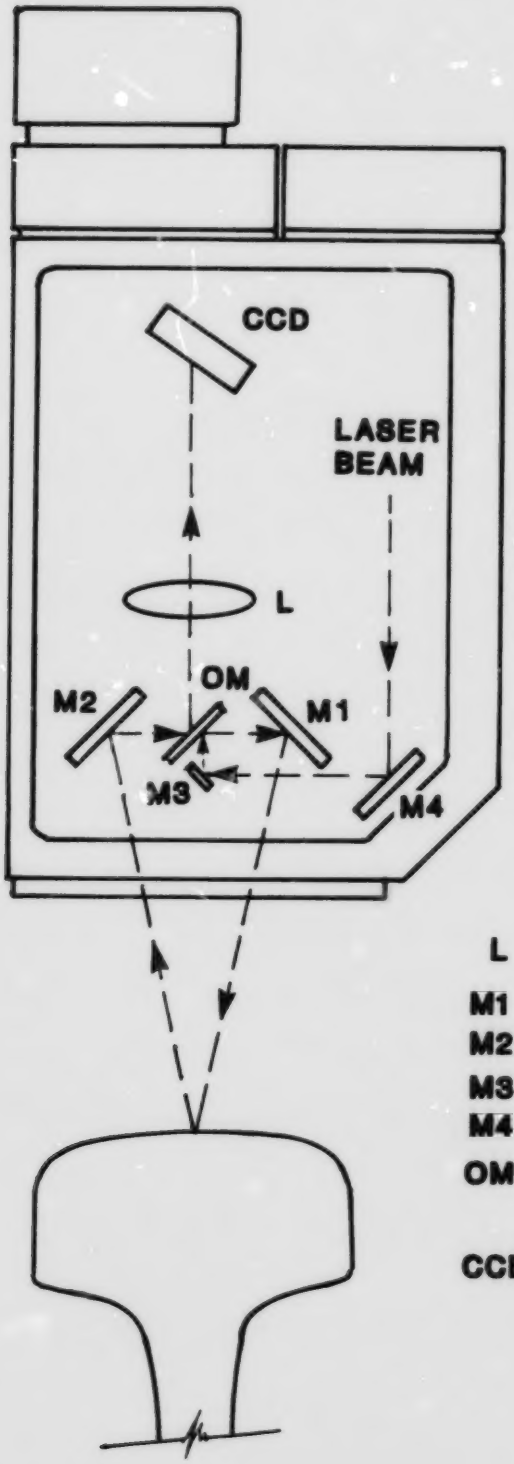

L - LENS

M1, M2, M3, M4 - FIXED MIRRORS

OM - ROTATIONAL MIRROR

CCD - CHARGE — COUPLED DEVICE

PRINCIPLE OF THE CAMERA

FIGURE 1

While the other types of vision systems used for rail cross-section measurement employ 2-dimension cameras with area image sensors, the SLS device operates with a charge-coupled device (CCD) linear array sensor having 256 pixels. Not only does it process a much smaller quantity of data, without compromizing resolution, but it also actually measures, without ambiguity, the surface profile of the objects under examination, not a projection as with 2-dimension cameras. In the SLS vision camera, the amplitude of the output signal is related to geometrical characteristics of the object, whereas in 2-dimension cameras the amplitude of an output signal represents the surface reflectance properties of the object combined with ambient light conditions, intensity, and spectral characteristics. Use of a coherent light source and control of the power from point to point along the surface being measured, and the use of an interference filter, allow the SLS cameras to carry out measurements in a wide variety of combinations of ambient light and background.

The first commercial SLS camera was developed by Servo-Robot (Montreal) for robot guidance and was used with a welding robot. It demonstrated the following characteristics;

- high accuracy,
- robust construction,
- immunity to very bright ambient light,
- moderate scanning and frame rate. *

* Technical specifications for an SLS Camera are presented in the Appendix.

Application to high speed railway inspection imposes even more demanding performance characteristics:

- endurance to shock and vibration,
- ability to withstand an extremely hostile environment (dust, moisture, snow, wide range of temperature, etc.),
- large field of view while maintaining high accuracy, high scanning rate, high frame rate (number of complete scans per second),
- adaptation to different reflectivity of rail surface,
- target (rail) tracking to compensate for changes in the relative position of rail and the camera caused by car dynamics.

In order to achieve these performance characteristics development work was carried out within the limits of this project.

3. Areas of Possible Applications

Some possible applications of the SLS camera became initially evident. The SLS camera may successfully compete with the existing vision systems in measurement of the rail cross-section and the track gauge.

At an early stage of this project the ability of the SLS camera to measure rail profiles was verified with the Servo-Robot unmodified camera. Fig. 2 illustrates traces of rail profiles (raw data) taken in the laboratory. It can be seen that the rail profile is clearly outlined.

Existing rail profile systems perform at the rate of 3-5 frames per second. The optimum rate, considered to be 15 frames/sec (see Ref. 2), is easily achievable with the SLS camera. Actually, the maximum rate (at present) of approximately 50 frames/sec is great enough to provide track gauge measurement with sampling every .5 m at a train speed of 100 Km/h. This measurement can be accomplished with the help of two cameras mounted under a car which monitor the gauge side of both rails in one reference frame.

In the applications listed above, the SLS camera faces strong competition from existing vision systems using

CAMERA ORIENTATION

CAMERA ORIENTATION

RAIL PROFILES, RAW DATA

FIGURE 2

2-dimension area sensors. Its scanning feature may be seen as a drawback because of a finite time interval required to scan an object across the field of view. But this same feature makes the SLS camera unique for applications such as monitoring the rail surface in the longitudinal direction. The undulations of the rail surface in this direction, observed on different North American railways, occupy a broad range of wavelengths (see Ref. 3). In order to accurately reproduce the rail surface, measurements have to be made at approximately 1" intervals along the surface of the rail. Even though it is theoretically possible to extract the longitudinal rail profile from the rail cross-sections, in reality, the sampling rate required (approx. 1000 frames/sec) at 100 Km/h) is unachievable with modern conventional vision systems.

The SLS camera can deliver a sampling rate required by modifying the regular mode of operation: instead of repetitive scanning, it can use periodical scans during which the target point on the rail profile is tracked (see Fig. 3, line 2-1), following which the rotational mirror at the point Y_t) is fixed in the target position (angle θ_t), and a series of single-point measurements is performed with the frequency required.

This particular mode of operation was subjected to a thorough investigation in the course of this project.

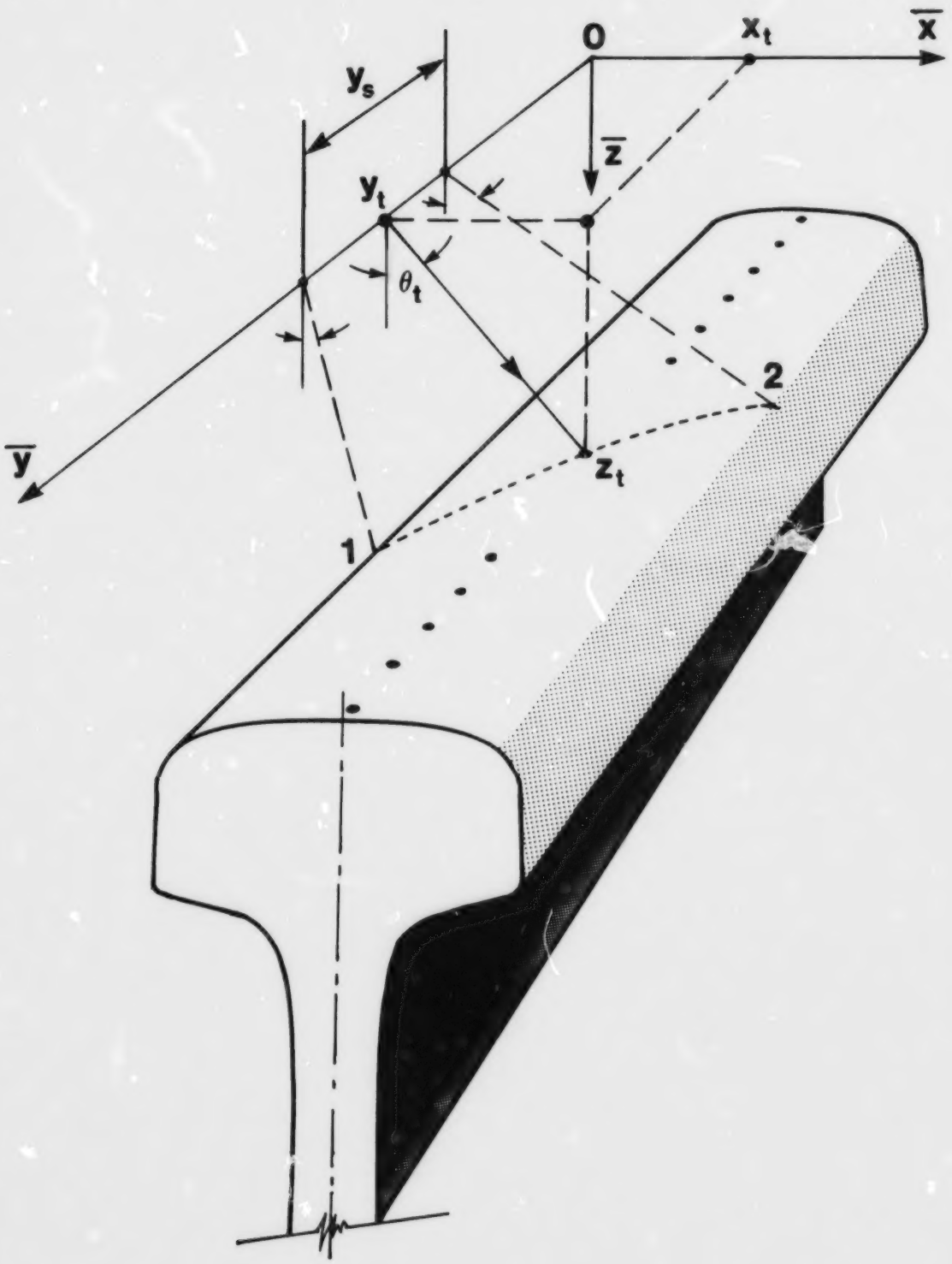

LONGITUDINAL RAIL SCANNING

FIGURE 3

4. Development of a SLS Camera System for Longitudinal Rail Surface Inspection

In the course of the program a test system was developed and tested both in the laboratory and in the field.

4.1 Environmental Testing and Camera Protection

In the initial stage of development, the standard unmodified Servo-Robot camera was tested on a computer controlled fatigue bench to simulate vibrations and mechanical shocks usually encountered in the railroad environment. Ambient temperature fluctuations were simulated by placing the camera in a refrigerator and subsequently in an oven. (Details on the environmental testing, see Appendix). Based on the results of the testing, a number of changes were incorporated in the design of the camera for railroad applications.

For field testing, the SLS camera was mounted in a heavy duty protective enclosure, oil and dust tight, intended for installation under a test car (Fig. 4). The enclosure was connected to an air compressor to air-cool the heat sinks of the camera components and also to maintain a positive pressure in the enclosure for keeping the viewing window clean (see Appendix for details).

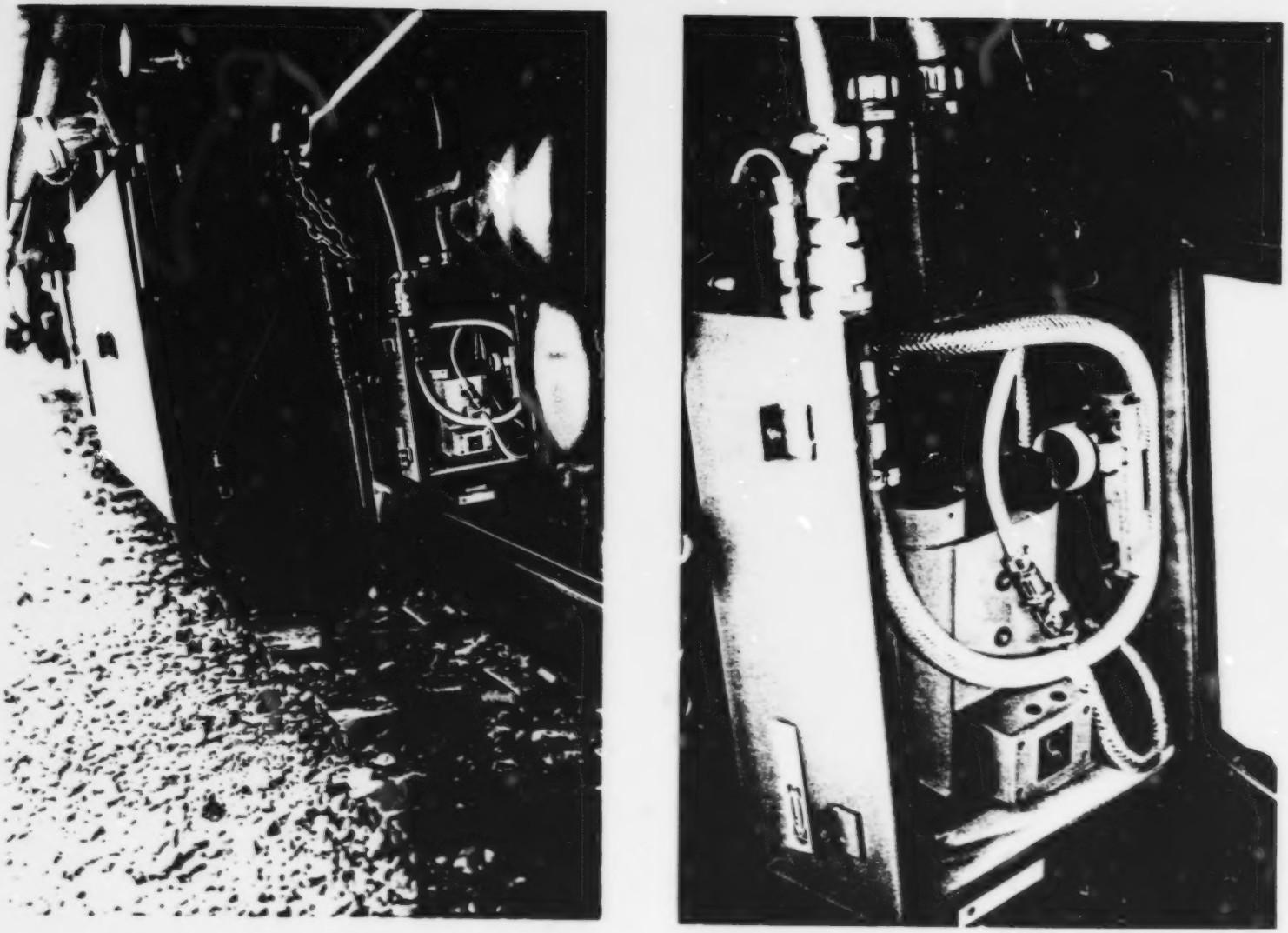

VIEW OF CAMERA ON TEST CAR

FIGURE 4

4.2 Location of the SLS Camera On a Test Car

A vision system installed on a railroad car will experience shocks and vibrations resulting in rail movements in the field of view. Especially large displacements will be observed when the measurement car goes around a curve. Moving on a curve, the car body follows a chord. This results in lateral movement of rail relative to the measurement instrument attached to the car body (see illustration on Fig. 5). In the top portion of Fig. 5, the three positions for location of the camera are marked: 0, 1, and 2. In the position 0, between the truck axles, the camera has practically no lateral movement with respect to the rail; but this position is usually obstructed by truck components, and therefore does not allow a clear view of rail. It is easy to see in Fig. 5 that in position 2 the lateral movement of the camera in relation to the rail is smaller than in position 1.

The extent of the relative lateral and vertical movement, and the field of view of the vision system have to be taken into account when choosing a preferred mounting position of the camera on the rail car.

Position "2" on Fig. 5 was selected for field testing. In this position, the rocking of a car body, when negotiating a curve, also assists in keeping the target in sight.

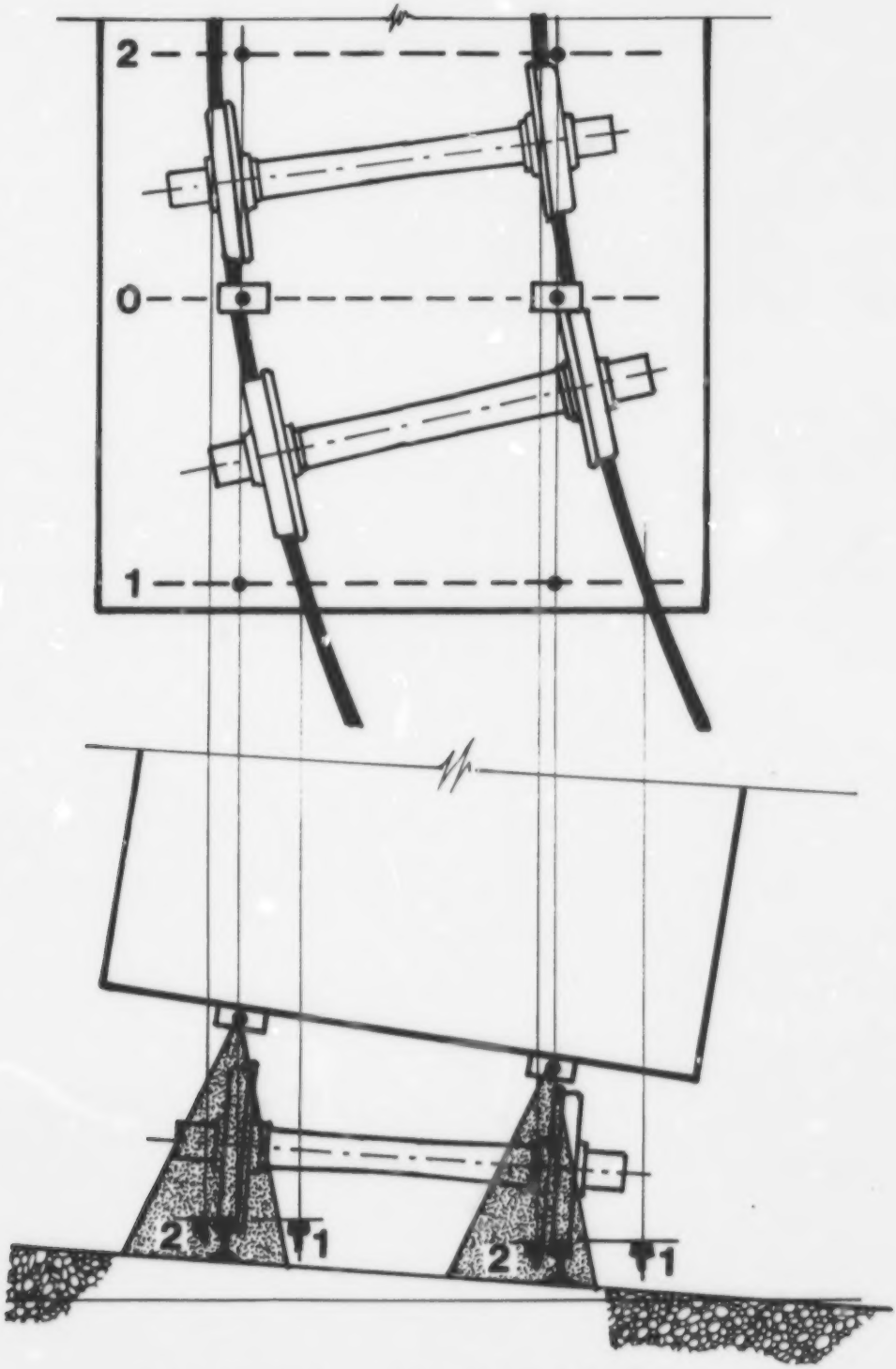

CAMERA LOCATIONS AND FIELD OF VIEW

FIGURE 5

4.3 Vibration of the SLC Camera On a Test Car

Besides the relatively slow (up to several cycles per sec.) movements of the rail-target in the field of view caused by the rail-car dynamics, the vision system on a rail vehicle is subjected to vibrations and shocks of much higher frequencies.

Several field tests were made in order to assess the vibration level of the SLS camera when it is mounted on the car, and also to estimate rail vibration under a test consist. These vibrations may interfere with the measurement process and may affect the results.

The instrumentation for the rail vibration test consisted of an accelerometer (B&K 4371), a charge amplifier (B&K 2635), an FM tape recorder and a wheel detector. The accelerometer was mounted on the base of the rail, and aligned to measure the vertical component of the rail vibration. The filters of the charge amplifier were adjusted to provide a passband of 2 Hz to 1 KHz.

The instrumentation for the car mounted SLS vibration measurement test consisted of two accelerometers that were mounted on the SLS body and aligned to measure the vertical and lateral components. The accelerometers and charge amplifiers were the same as used for the rail vibration test.

The recorded data was first played back onto a strip chart recorder (Asto-Med MT-9500). The accelerometer data was also analyzed with a dynamic signal analyzer (HP 3561A).

The SLS controller expects a pulse for each measurement taken. For our tests, we required a sample at every inch of travel, independent of the speed of the test car. A device was developed that accepted the output signal of an axle mounted wheel encoder, and produced a sampling pulse for the SLS controller. The sampling distance was user selectable, for our initial tests a one inch sampling interval was used. The device also accepted the output signal of an optical proximity sensor. The sensor was mounted under the car body and "looked" between the rails. The sensor produces a signal only when a special reflective target is in its field of view. Two targets were used to define the start and the end of a test zone. Upon receipt of the first signal indicating the start of the test one, the device would toggle the inch pulse on, and the SLS controller would acquire data, one sample per inch, until the next target when the device would toggle the inch pulse off.

Some typical results of the vibration measurements are shown on Figs. 6 and 7. The analysis of the vibration test results show that it is feasible to design a signal processing system which would "isolate" the car body

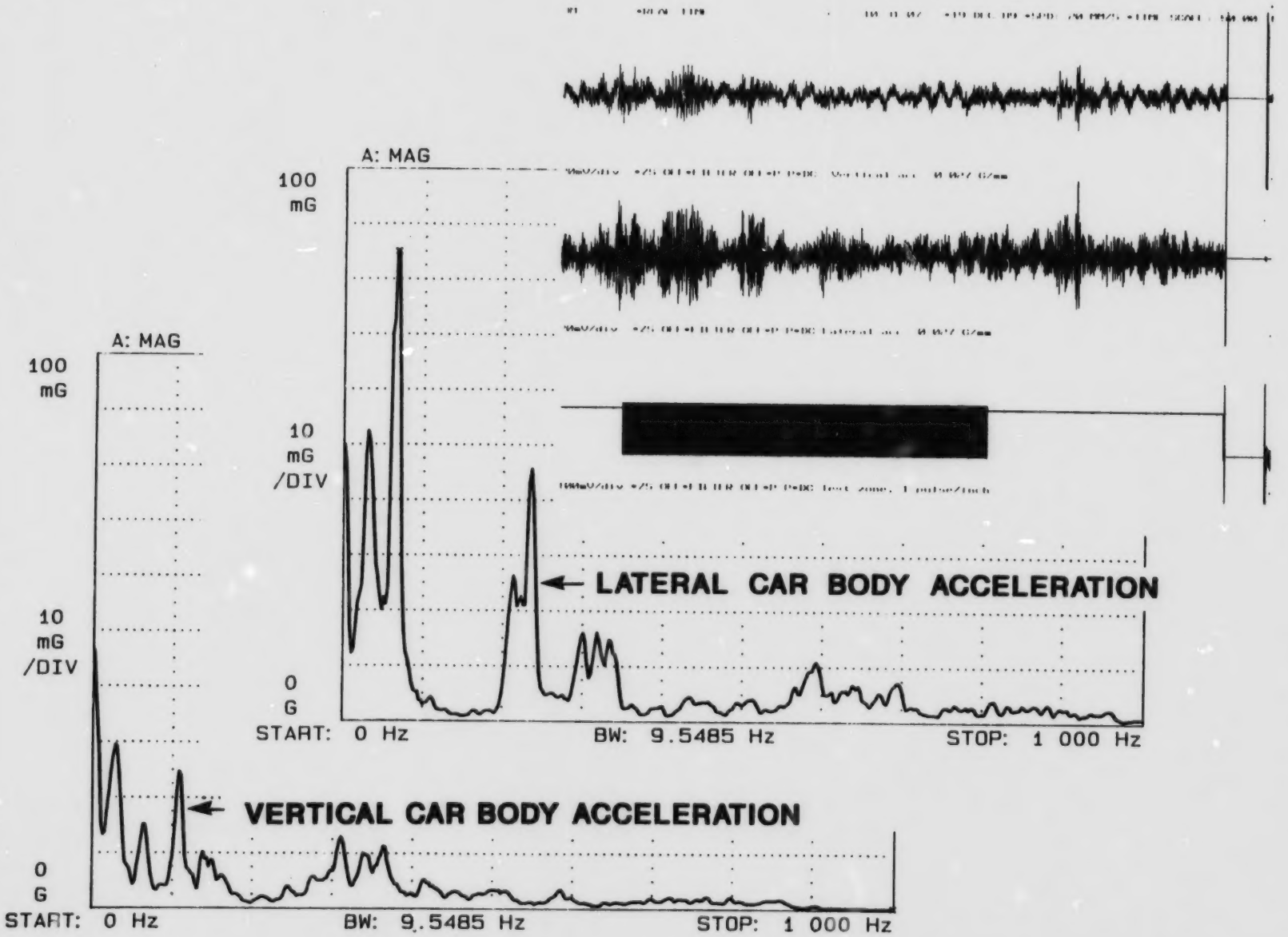

VIBRATION TEST: SMITH FALLS, run #3, 30 mph

FIGURE 6

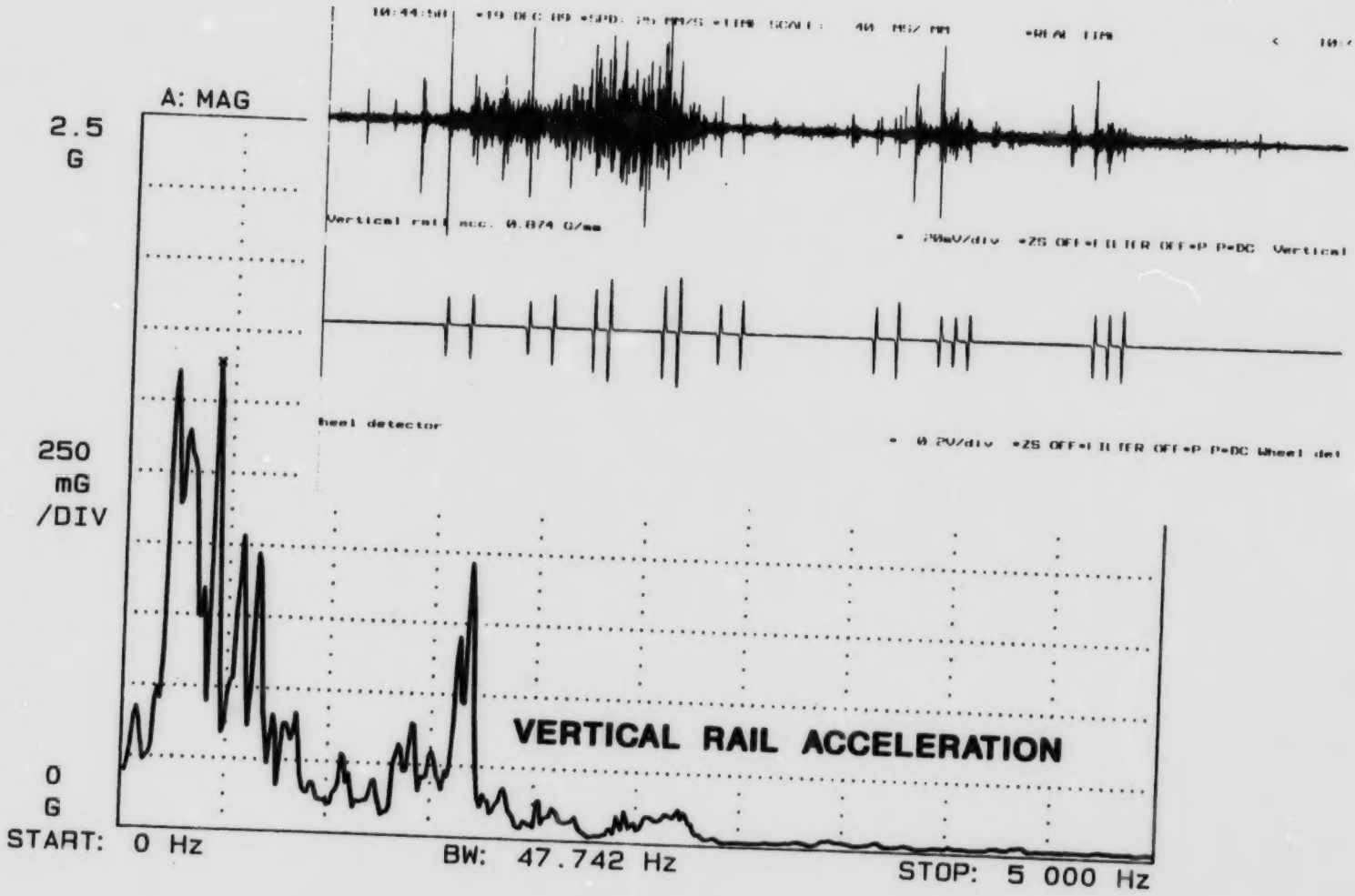

RAIL VIBRATION TEST **SMITH FALLS, 30 mph**

FIGURE 7

movement without any significant distortion of the video system output. The rail vibration, however, may present a problem, the severity of which depends on the intended application of the system. In the tests described, the average rail vertical displacement peaks obtained by the double-integration of the accelerometer signal observed under the test car were approximately .2 mm.

4.4 Reference Rail Surface Inspection System

The rail surface as an object of visual inspection has a very simple shape. But movements of the target rail in the field of view, rail vibrations combined with instability of a platform (car body) on which the video system is mounted, makes it difficult to predict the rate of success of inspection. For evaluation of the quality of inspection, a reference device capable of the high accuracy fast measurements of the longitudinal rail profile was required. The choice of instrumentation for a reference manual measurement in the past had been limited to a "straight-edge-dial-indicator". This method is time consuming and physically demanding; it would be impractical to use it for the reference measurements even on a minimal length test zone (150-200 ft) chosen for the high speed on-board measurements. An appropriate reference instrument - Reference Rail Surface Inspection Systems (RRSIS) - developed by the Department of Research, CP Rail, consists

of a measuring frame, a data logger, and a software package for data processing. A general view of the measuring frame and the data logger is presented in Fig. 8. A 72" linear ball slide is held above the rail head surface by end brackets that rest on the base of the rail. The assembly is stabilized by toggle action clamps that push against the rail's head web fillets (Fig. 9). The ball slide is sufficiently rigid to assume that it forms a straight reference line. The length of the slide is chosen as a compromise between mechanical rigidity, the longest wavelength that can be detected in a single pass, weight of the instrument, and cost.

An LVDT (linear variable differential transformer) displacement transducer is mounted on the carriage of the slide (Fig. 10). The transducer tip is fitted with a ball point to allow it to glide over the rail head surface. It is spring-loaded to ensure constant contact with the rail surface. The measurement range of the transducer is +/-15 mm with .3% linearity.

The transducer can be adjusted laterally across the rail head. The longitudinal position of the transducer with respect to the end bracket is measured with a string potentiometer displacement transducer which has a 75" range with .05% linearity.

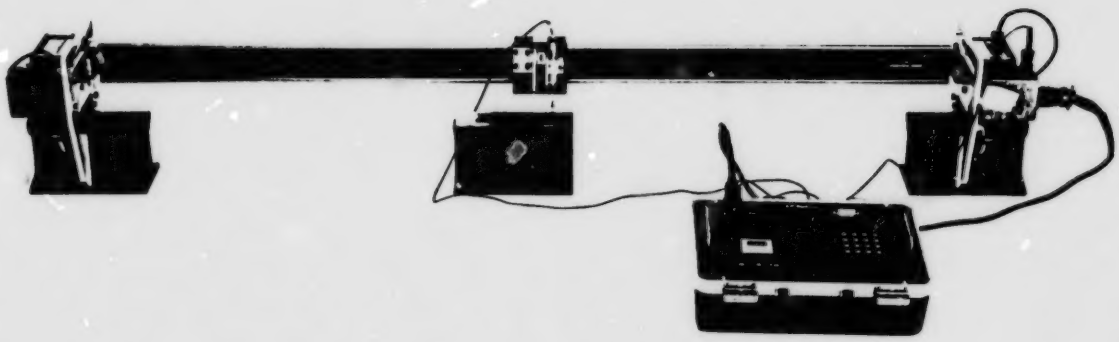

GENERAL VIEW OF RRSIS

FIGURE 8

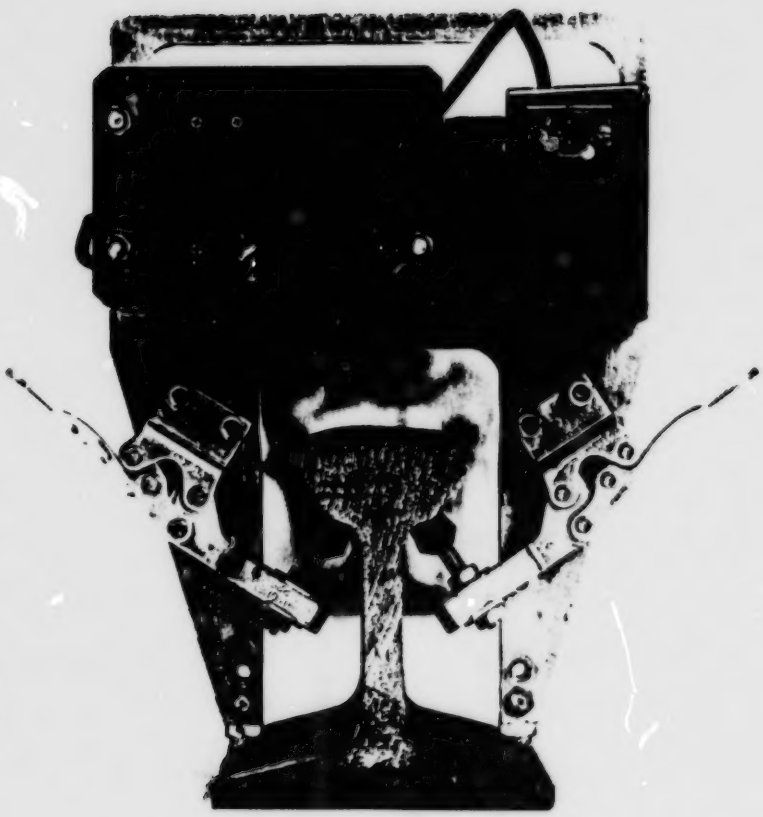

SIDEFRAME AND CLAMPING ARRANGEMENT

FIGURE 9

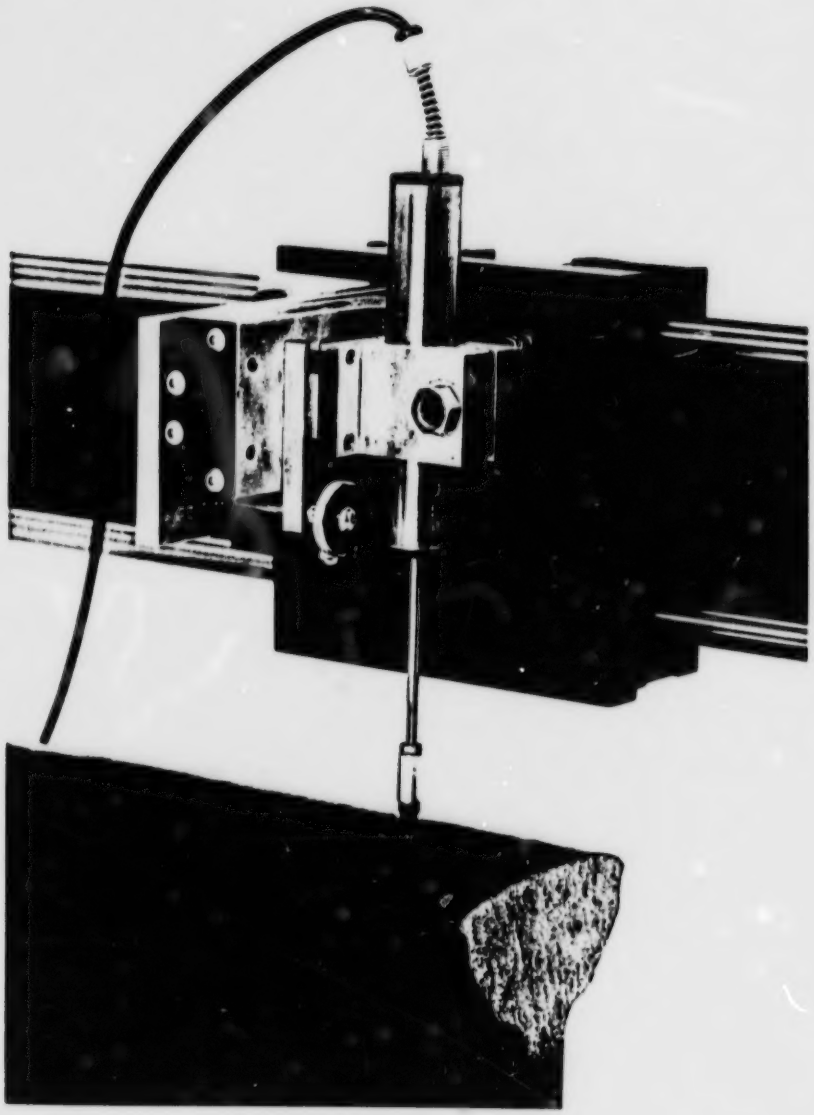

Y COORDINATE MEASURING CARTRIDGE

FIGURE 10

Both transducers are powered by the internal battery of the Data Logger in combination with a battery mounted on one of the end brackets. The output of the transducers are sampled and stored by the Data Logger on a magnetic tape. (Details on the Data Logger, see in Ref. 4).

For a meaningful test comparison with the video system measurements, a rail length much longer than the length of the RRSIS frame has to be measured. For this purpose, the RRSIS is clampled on the rail such that each consecutive position would overlap the previous one. The overlapped region is then used to align the rail sections measured relative to each other. This procedure illustrated on Fig. 11 allows an accurate reproduction of the rail's "space curve". Two examples of measurements made with the RRSIS are shown in Fig. 12. Both sites on this illustration were measured before and after rail grinding. Even though some of the surface undulations were removed as a result of grinding, the preserved "space curve" allows one to identify and match the traces.

4.5 Field Testing of the SLS Video System

For the field tests, the camera, in its protective enclosure, was installed under the track geometry car, in front of the leading axle of the trailing truck (Position "2" on Fig. 5).

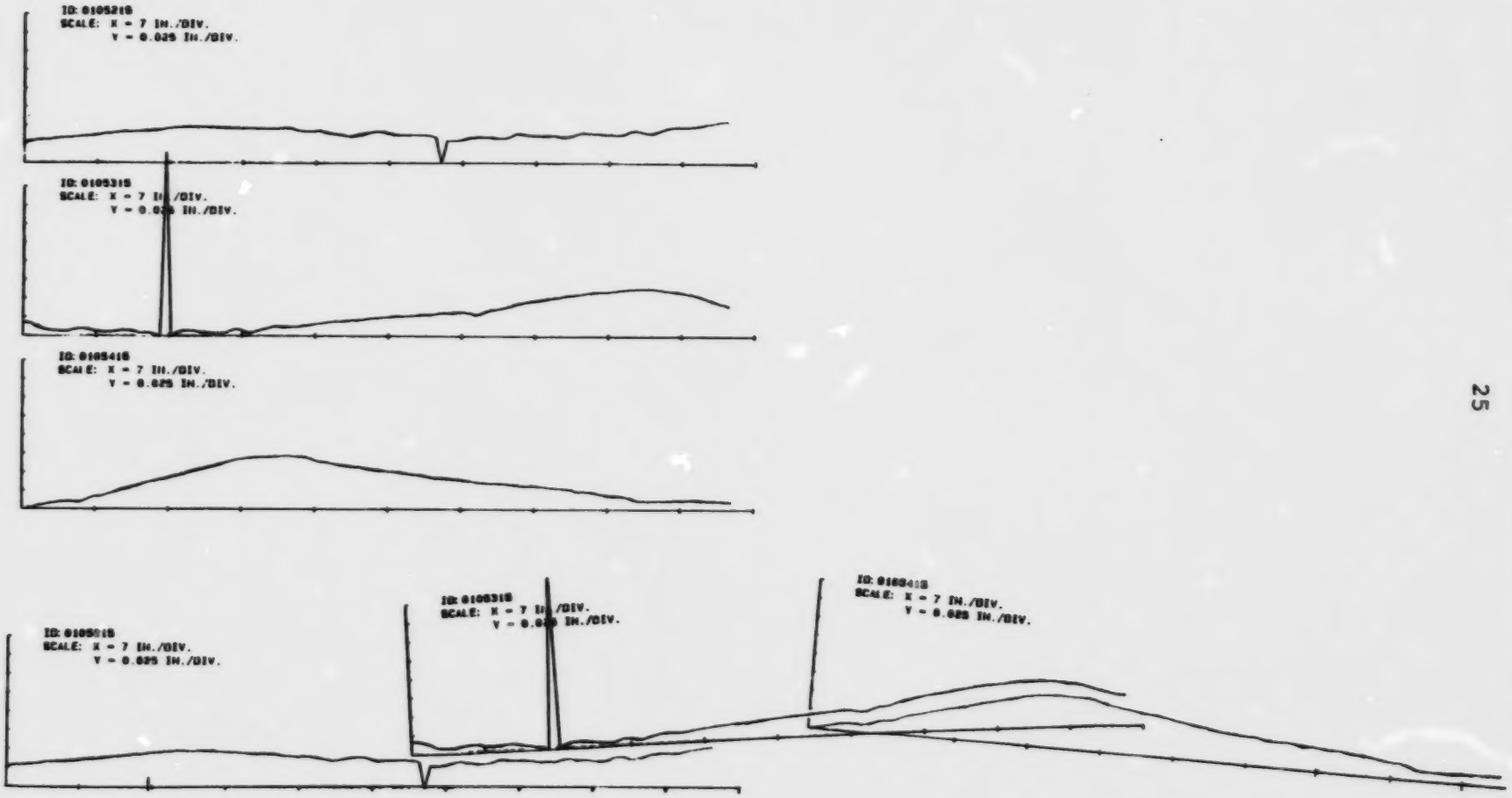

RAW DATA AND FRAME ALIGNMENT

FIGURE 11

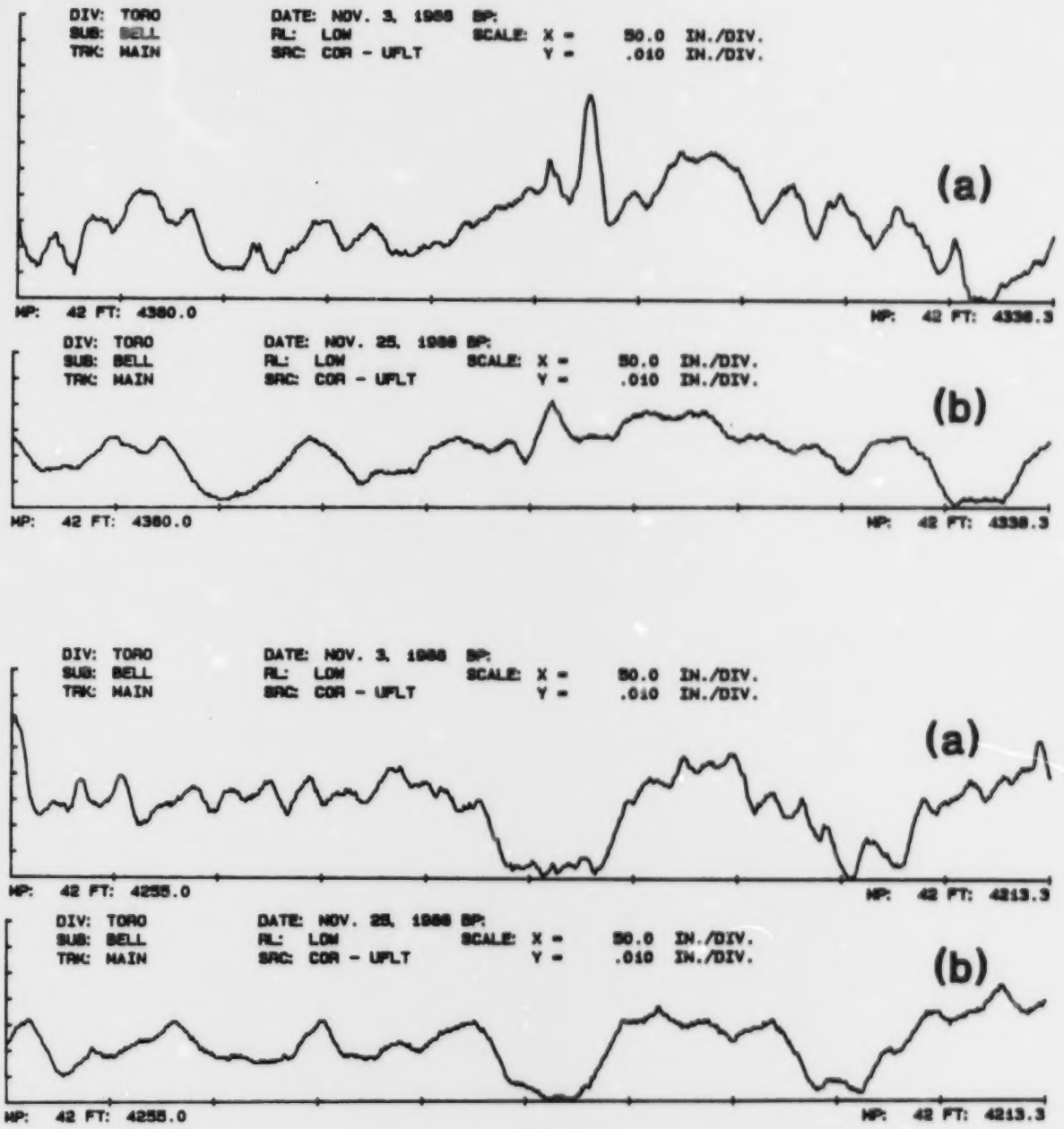

SPACE CURVE OF A RAIL SECTION BEFORE (a) AND (b) AFTER GRINDING

FIGURE 12

The test system consisted of the SLS camera, a controller and a portable PC computer. The controller and the computer were installed inside the car.

The controller, connected to the camera via a 10 M cable, managed all the operating parameters of the camera (sensitivity, scanning frequency, laser power, etc.). It also digitized the video signal and stored the data in memory buffers.

An IBM-compatible computer, connected to the rest of the test system via an RS-232 serial link, served as the user interface. From the interface program the user could operate the camera, change parameters of operation, display collected data, etc.

The rail tracking software enabled the camera to follow a target point on the rail surface. Normally, this point would move laterally and vertically in the field of view of the camera as a result of the rail-car interaction. The version of the tracking software tested made the laser beam of the camera follow the middle of the wheel-rail contact zone (Fig. 3, points with coordinates X_t, Y_t, Z_t) defined by using the reflectivity data collected during the cross-scan (a line between points 1 & 2 on Fig. 3).

Several test runs were performed on the CP Rail main line at Smiths Falls and in Montreal. The test zones of 150 to 200 feet with noticeable corrugations were measured with the reference instrument (RRSIS). The resulting traces of the filtered data are presented on Fig. 13. The bandpass filter removed the wavelengths longer than 48 inches and shorter than 3 inches. The choice of the filter's range was based on the previous observations of corrugations on the main North American railways (see Ref. 3).

The test train passed over the test zone at different speeds. Raw data (Zt-coordinates representing distances from the camera to the rail surface sampled at every inch along the rail) is plotted on Fig. 14. The plots of 4 runs made at 30 mph are superimposed and show repeatable results. Identical results were obtained for all the runs at the same speed. Fig. 15 illustrates the camera-rail surface distance measured on these passes over another test zone at the speed of 10 mph.

These results reflect the dynamics of the car body caused by the local track parameters and track geometry.

Before comparison to the reference measurement can be made, the raw data collected with the on-board SLS camera has to be processed. This processing is broken into two steps:

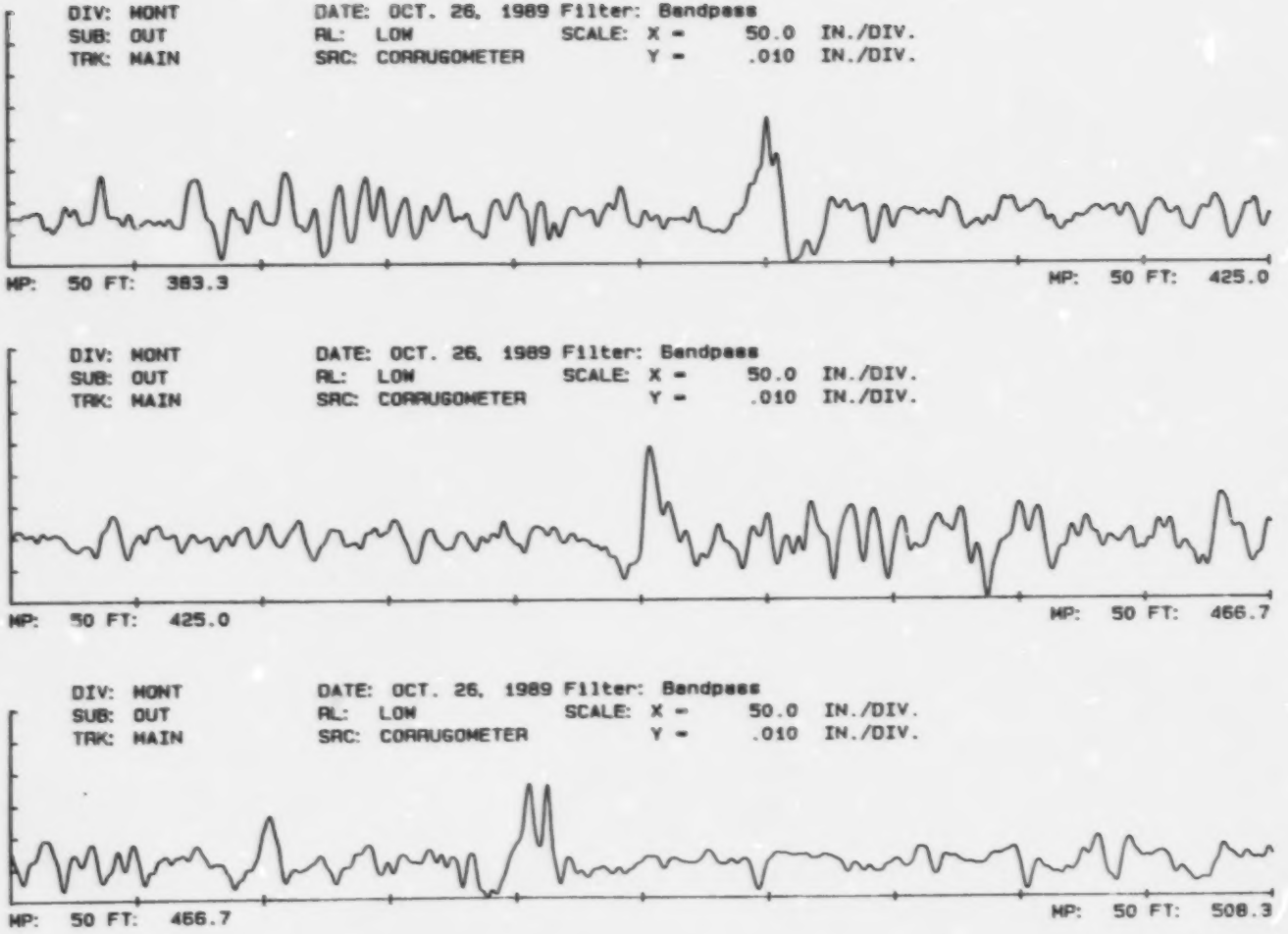

RAIL SURFACE - REFERENCE MEASUREMENT

FIGURE 13

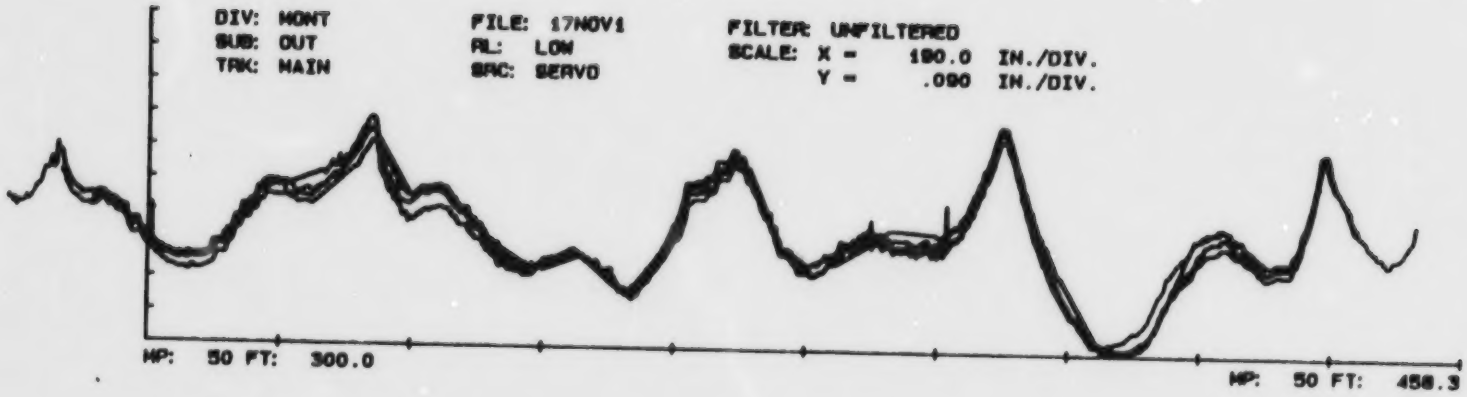

z_t - RAW DATA , 30 mph

FIGURE 14

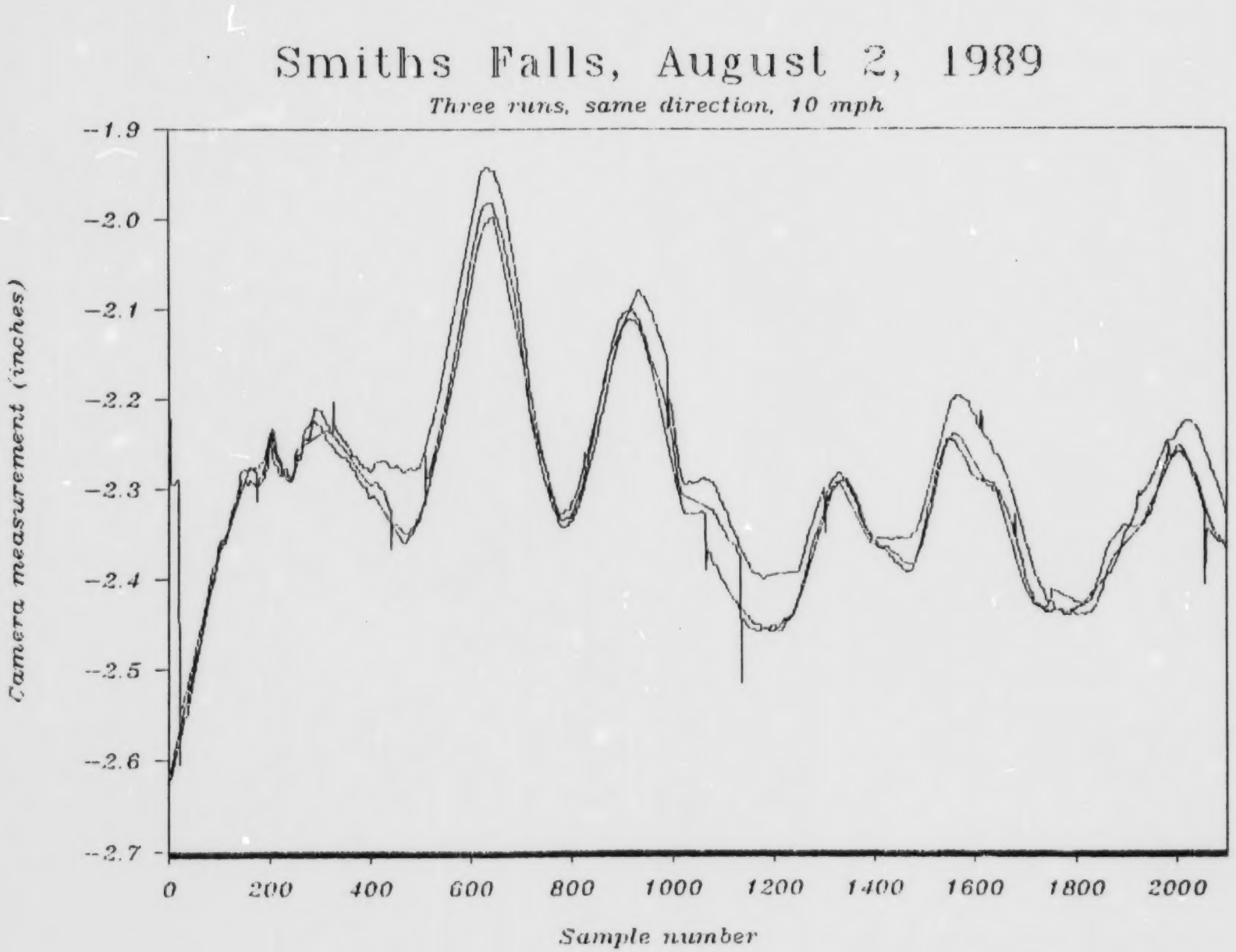
Smiths Falls, August 2, 1989
Three runs, same direction, 10 mph
Camera measurement (inches)
-1.9
-2.0
-2.1
-2.2
-2.3
-2.4
-2.5
-2.6
-2.7
0
200
400
600
800
1000
1200
1400
1600
1800
2000
Sample number

FIGURE 15

The first step removes the effect of the laser repositioning interval. During this interval, when the laser scans across the rail top, measurements of the distance between the camera and the rail surface, otherwise continuous along the rail, are not available. This interval is replaced by a straight line interpolation from the last point measured before the target tracking to the first point measured after tracking. The exact length of the lost interval is a function of the train velocity. It is taken into account when restoring the space curve.

The second processing step eliminates the effect of the "unstable platform" from which the measurements are made. The longitudinal rail profile is measured by the vertical distance from the camera attached under the car to the rail surface. The trajectory of the camera moving along the track serves as a reference line. During normal operation, this trajectory is influenced by car body dynamics. The vertical excursions of the camera are much larger than undulations of the rail surface, but limited to low frequencies. They superimpose long wavelength distortions on the image of the rail surface, and are usually much longer than the wavelengths of interest. For data collected at a train velocity faster than 15 mph, the effect of car body movement is removed by filtering the wavelengths longer than 48 inches. Also rejected by the filtering are wavelengths shorter than 3 inches.

The raw data collected during the test run at 30 mph were processed as described above. An example of the resulting trace with the superimposed reference trace (as on Fig. 13) presented on Fig. 16 shows satisfactory correlation between the two measurements.

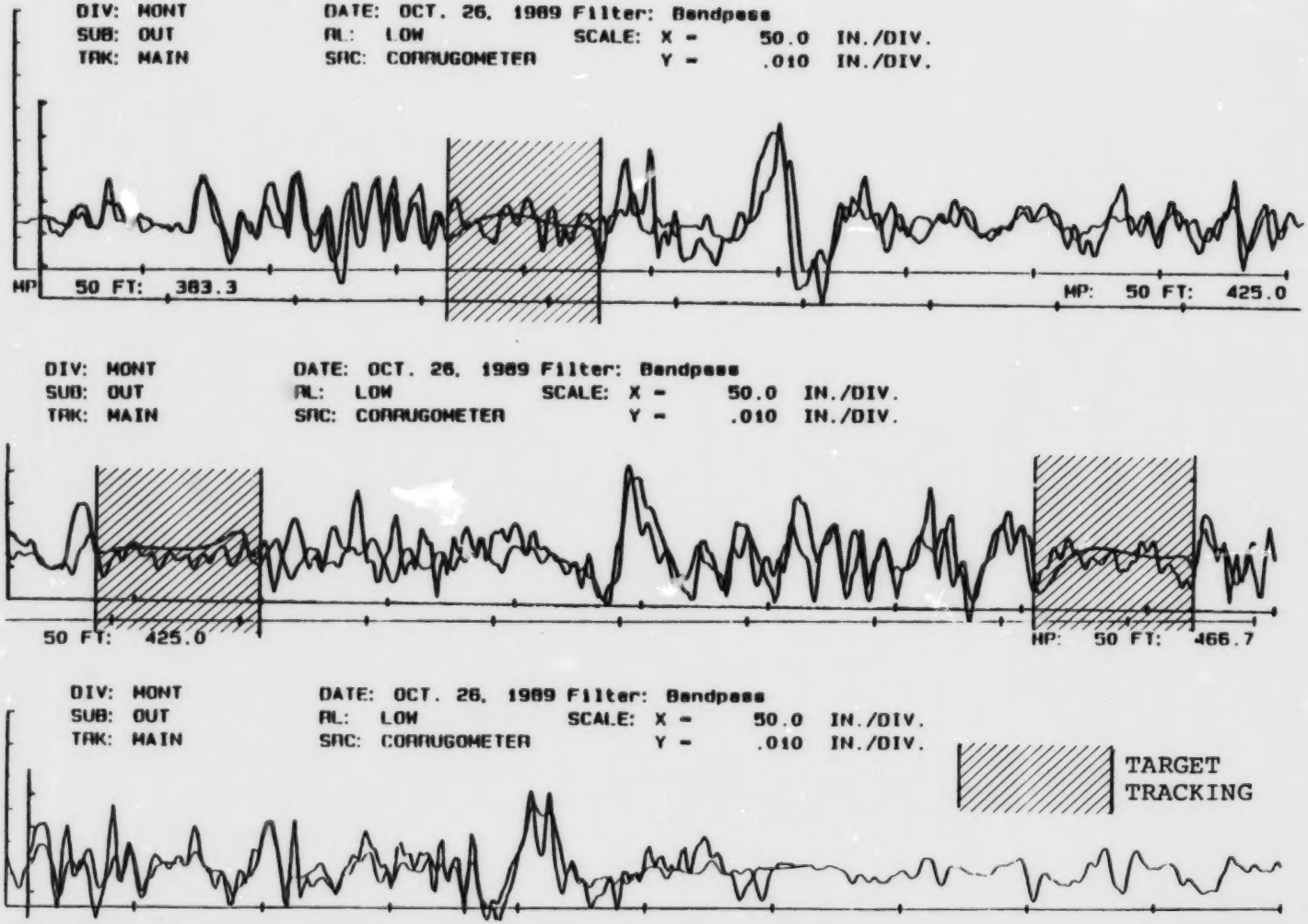

COMPARISON OF REFERENCE AND ON-BOARD MEASUREMENTS

FIGURE 16

Conclusions

1. The SLS camera, modified and reinforced for field testing on a railroad car, demonstrated the ability to operate in the presence of lateral and vertical vibrations typical of the railway environment.

2. The data collected during the test runs indicate repeatable performance of the camera and controller.

3. Due to a limited number of test runs, no attempt was made to statistically evaluate the final accuracy of the camera.

4. Further testing is required and will be conducted by CP Rail to verify the ability of the SLS camera to operate under the extreme temperature conditions outlined in Appendix A.

5. The results of testing obtained so far indicate that the SLS video system can be used in a number of applications for railroad inspection:

   - rail cross-section monitoring,
   - rail gauge measurement,
   - train-ground speed measurement,
   - rail corrugation measurement,
   - rail profile grinding evaluation,
   - rail-car dynamics study,
   - evaluation of track maintenance.

6. As expected, the cost of the test equipment used in this project was high. It will have to be reduced in order to make applications listed practical.

References

1. M. Rioux. Laser range finder based on synchronized scanners. Appl. Optics, Vol. 23, No. 21.

2. G. Izbinsky, D. Holfeld. Requirements for an on-board rail profile measurement system. AREA Symposium on Automated Track Measurement, Chicago, Ill., March, 1988.

3. A. Zarembski, G. Izbinsky, S. Handal, W. Worthington. Corrugation behaviour in the freight railroad environment. AREA Bulletin 712, Vol. 88 (1987).

4. H. Soares, H. Schrekinger, L. Feiter. A Battery Powered Data Logger and Acquisition System for Wheel/Rail Profile Measurements. Track/Train Dynamics, V. 5, 1989, T&O Research, CP Ltd.

Appendix

The Synchronized Laser Scanning Camera for Rail Inspection

Prepared by: Servo-Robot Inc.

TABLE OF CONTENTS

1. INTRODUCTION 1

2. STANDARD JUPITER CAMERA 2
2.1 Optical configuration 2
2.2 Optical Characteristics of the Standard Jupiter Camera 3

3. GENERAL APPLICATIONS 4

4. SPECIAL VISION SYSTEM FOR RAIL MEASUREMENTS 5
4.1 CP Requirements 5
4.1.1 Optical Characteristics 5
4.1.2 Mechanical Characteristics 5
4.1.3 Environmental Requirements 5
4.1.4 Software Requirements 7
4.2 Summary of Differences between SRI Standard Vision System and CP Requirements 7
4.3 Special Vision System for Rail Measurements . . . . .
4.3.1 Optical Characteristics 7
4.3.2 Mechanical Characteristics 8
4.3.3 Software 8
4.3.4 Environmental Protection 9

5. INSTALLATION 12

6. TESTING 12
6.1 Vibration Tests 12
6.2 Laboratory Tests 12
6.3 Field Tests 14

7. CONCLUSION 15

ENCL. 1 - VIBRATION TESTS 16

References 17

1. INTRODUCTION

The purpose of this report is to give a general description of the vision system used to perform various rail geometry measurements. The results of the extensive vibrations and temperature resistance tests which were conducted by Servo-Robot Inc. will be found in Enclosure 1.

During the first phase of the development of a rail geometry measurement system, Servo-Robot produced a special version of its Jupiter camera, with a reduced field of view for higher resolution. The camera used during the vibrations and temperature resistance tests was a Saturn camera, which has a smaller field of view, but is built using the same basic components. The results can be considered as showing the performance of any one of our standard Jupiter and Saturn cameras. The camera built especially for this project performs equally well under the same conditions.

This camera has been installed under a track geometry car for field tests. The results were used to improve the system.

2. STANDARD JUPITER CAMERA

2.1 Optical configuration

The camera is based on the principle of autosynchronized scanning (Rioux 1984), where the basic idea is to synchronize projection of the laser beam with its observation as shown in Figure 1.

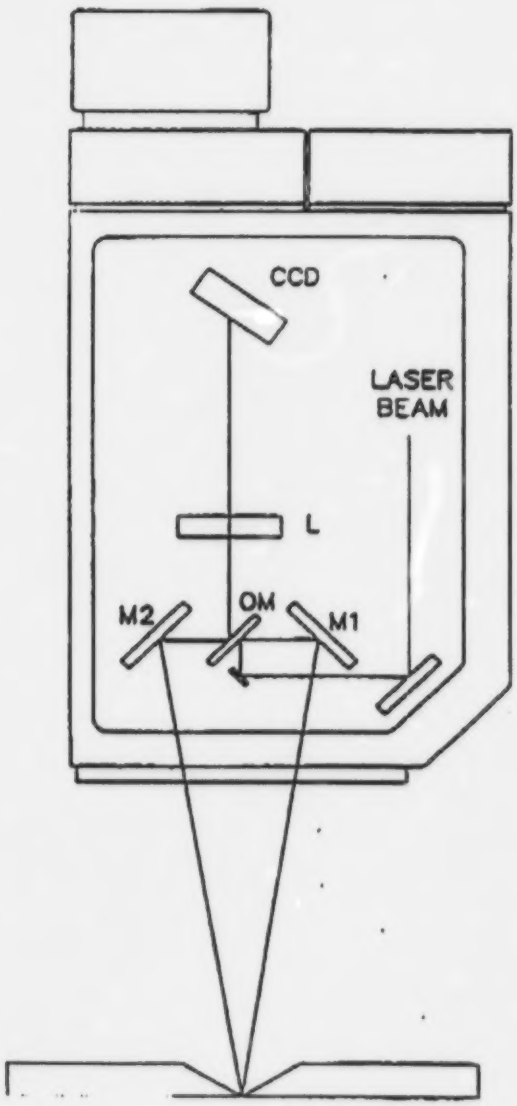

FIGURE 1 - Principle of the camera.

Referring to the diagram in Figure 1, the beam is deflected by one side of the driven mirror (OM) onto a fixed mirror (M1), from which it is deflected (and thus scans) onto the object. The reflected beam is picked up by another fixed mirror (M2) on the other side of the driven mirror. From there it falls on the opposite facet of the driven mirror (OM) and is deflected through a set of optics (L) onto a CCD position sensor. The position of the spot on the CCD array is proportional to the Z coordinate of the scanned profile; the Y coordinate is abstracted from the scanning angle of the driven mirror. The principal advantage of this optical arrangement is that, despite the sharp angle of observation, the resolution is much better in comparison with traditional triangulation techniques. If we had chosen a non-synchronized scanning approach, we would have had to sacrifice the compact size of the sensor in order to achieve the same resolution.

2.2 Optical Characteristics of the Standard Jupiter Camera

Light source	solid-state laser 30 mW minimum
Stand-off	165 mm
Depth of field	1005 mm
Field of view	
near plane	108 mm
far plane	579 mm
Resolution, Z axis	
near plane	0,03 mm
far plane	1,4 mm
Resolution, Y axis	
near plane	0,42 mm
far plane	2,3 mm

The resolution along the Y axis is based on a scan with 256 points.

3. GENERAL APPLICATIONS

The Jupiter camera includes a coherent light source (infrared laser) whose collimated output produces a spot on the object. Distance between this spot and the camera is obtained from triangulation with a precision to allow the resolution of 4096 depth levels. A scanning mechanism sweeps the spot across the object at a programmable frequency and amplitude. This allows the calculation, in real time, of coordinates of 256 sampling points on a slice of the object. The acquisition system is fast enough to repeat this scheme up to 56 times per second. The whole volume of the scene can be covered by mounting the camera on a translation or rotation device such as the arm of a robot.

The Jupiter camera owes its performance to the high quality of its optomechanical-optoelectrical components, and to sophisticated techniques for acquisition and real-time processing of the image formed on the sensor. The dynamic range of the camera is obtained by instantaneous control of the laser power and of the sensor's exposure time. This renders possible the simultaneous observation of surfaces with varying reflectivities.

The Jupiter camera is a high-precision instrument designed to resist the most hostile environments. It maintains the same performance when moved from the laboratory to the factory floor. The interferential filter used in this camera offers good immunity to surrounding light.

The Jupiter camera is mainly used for inspection and surface mapping tasks. In one application, it is installed on a motorized linear slide, over an object to be scanned. The movement of the slide, combined with the scanning of the camera, produces a full 3-D image of the top surface of the object. This image can then be observed on the screen of a PC with different viewing angles, using the USER-2000 software. Measurements can also be easily made on the displayed image. With some special software, this data could be sent to a CAD system to be used as a model, and combined with 3-D images taken from other sides of the object to provide enough information about its full volume.

4. SPECIAL VISION SYSTEM FOR RAIL MEASUREMENTS

4.1 CP Requirements

The following specifications are taken from the CP Rail Document of 87-09-29, entitled "Specifications - One-Rail Longitudinal Surface Profile".

4.1.1 Optical Characteristics

Stand-off	No equipment closer than 4 inches (102 mm) from top of rail.
Depth of field	120 mm
Field of view	275 mm
Acccuracy, Z axis	Not less than 0,003" (0,076 mm)

4.1.2 Mechanical Characteristics

The camera and its protective enclosure must be small enough to be installed under the Track Geometry car and stay within limits set for the distance above the rail top and outside of the rails laterally.

4.1.3 Environmental Requirements

The camera in its protective enclosure must withstand and impact with track debris weighing 150 lbs. (68 kg) at a speed of 65 m.p.h. (104 km/h), and maintain continuous operation in presence of dust, moisture, snow, ice particles and usual railway ambient light conditions.

Operating temperature	-25°C to +45°C
Storage temperature	down to -45°C

Vibrations and shocks, with temporary loss of signal

Shock (1/2 sine):

	Lateral	Vertical	Longitudinal
Peak Amplitude	5 g	5 g	10 msec
Duration	10 msec	10 msec	10 msec

Vibration:

	Lateral	Vertical	Longitudinal
5 Hz to 30 Hz	0.5 g	0.5 g	0.5 g
30 Hz to 150 Hz	1.0 g	1.0 g	1.0 g

Vibrations and shocks, without degradation of accuracy

Shock (1/2 sine approximation of signal waveform):

	Lateral	Vertical	Longitudinal
Peak amplitude	0.2 g	2.0 g	2.0 g
Duration	0.3 sec	30 msec	0.4 sec

Vibration:

	Lateral	Vertical	Longitudinal
1 Hz to 5 Hz	0.1 g rms	0.3 g rms	0.1 g rms
5 Hz to 50 Hz	-	0.1 g rms	-
50 Hz to 100 Hz	-	0.8 g rms	-

4.1.4 Software Requirements

The Z coordinates of the top of the rail should be taken at the center of the wheel/rail contact area, which can be identified as highly reflective segment of the rail head top surface, or as some distance from a side of the rail head. Those two coordinates will be measured at intervals of 1 inch along the rail when moving at up to 65 m.p.h. The lateral and vertical coordinates should be sent to the host computer through a standard interface.

4.2 Summary of Differences between SRI Standard Vision System and CP Requirements

The standard Jupiter camera has a depth of field much too large for this application and, because of this, cannot meet the requirements for accuracy everywhere in the usable depth of field. The camera by itself could not withstand some of the environmental conditions specified, such as the -25°C minimum operating temperature or the impact of a 68 kg track debris at 104 km/h. The scanning frequency cannot be set high enough to provide one scan for each inch along the rail at a speed of 104 km/h, which would be a frequency of 1,144 images per second.

4.3 Special Vision System for Rail Measurements

4.3.1 Optical Characteristics

Light source	solid-state laser 30 mW minimum
Stand-off	157 mm
Depth of field	93 mm
Field of view	
near plane	135 mm
far plane	192 mm
Resolution, Z axis	
near plane	0,02 mm
far plane	0,04 mm
Resolution, Y axis	
near plane	0,53 mm
far plane	0,75 mm

The resolution along the Y axis is based on a scan with 256 points.

4.3.2 Mechanical Characteristics

Dimensions	115 x 180 x 95
Weight	2.40 kg
Case material	Cast aluminum alloy
Link to controller	10 m cable

Operating Conditions

Temperature	-25°C to +45°C (outside the camera's protective enclosure)
Relative humidity	0 to 90%
Vibrations of	0.5 g from 5 Hz to 30 Hz and 1.0 g from 40 Hz to 150 Hz
Shocks	2 g of 10 msec duration
Environment	Dust, snow and ice particles

Non-Operating Conditions

Ambient temperature	-45°C to +45°C

4.3.3 Software

We developed special software to support the requirements for data rate and tracking. Instead of getting one full profile for each inch of the rail, which is not possible, one full profile is used periodically to detect the center of the highly reflective part of the rail top surface. This information is then used to position the scanner so that the laser spot is maintained on the measurement position, while 255 coordinates are acquired with a 1-inch spacing along the rail. This tracking/acquisition cycle is repeated continuously as the car moves. For such cycle, apart from the tracking data, 256 values are stored as the depth measurement block, the first value bring the inch-count and the next 255 values being the depth data. The one-inch spacing is defined by a signal coming from equipment inside the car through a digital input of the CSR-2000 controller.

Until now, for the field tests, the data has been stored inside the vision system during the acquisition process and transfered to a PC at the end, for storage on disks and analysis.

4.3.4 Environmental Protection

The camera is mounted inside a heavy duty protective enclosure. The design is done in such a way that the camera is easily accessible.

The protective enclosure is positioned under the car 63 or 65 as shown in Fig. 2. The camera is mounted inside this enclosure in such a way that:

- the top of the rail is located in the center of the field of view of the camera,
- the mechanical axis of the camera forms with the rail the geometrical configuration shown in Fig. 3.

The protective enclosure is of the NEMA 12 type, oil and dust tight. To allow an adjustment of its height above the rail, it is attached to an external bracket designed with many mounting positions. The bracket is equipped with a specially designed extension nozzle facing the viewing window of the protective enclosure. This nozzle has the following functions:

- mechanical protection of the viewing window against minor objects,
- protection against a dust deposit on the window during operation, by the means of an air flow around this window.

To make possible the removal of the camera from its enclosure, the latter is mounted on a rigid steel inner panel with a small support. This support is inclined 8° relative to the back panel of the enclosure, which gives to the optical plane of the camera an angle of 8° relative to the vertical axis when it is installed under the car. The purpose of this angle is to eliminate the possibility of direct light reflexions from the rail. Once assembled, the protective enclosure and the bracket constitute an integral unit.

To the car body, above the rail, as shown in Fig. 4, is welded a rigid steel plate to which the bracket is attached. To prevent any major damage to the system, should this attachment fail, the bracket is secured in its position with steel chains. The distance between the rail and the extremity of the nozzle is 12,5 cm to 13 cm.

The air flow required to correctly operate the system (supplied by a separate compressor unit) is divided into two streams, one which is used to cool the heat sink of the heat pump of the laser module, and the other which goes directly to the nozzle of the protective enclosure. The air from the first stream leaves the camera and gets into the enclosure where it maintains a positive pressure of 1 psi before going out through the one-way pressure sensitive valve installed on the enclosure. Both streams circulate in an open-loop fashion. In order to keep the design as compact as possible, the tubing for air distribution is incorporated inside the protective enclosure. Quick disconnect connectors are used to facilitate the maintenance.

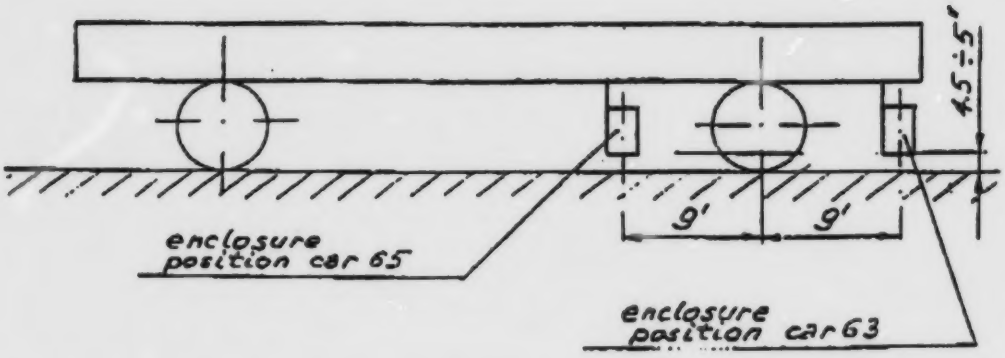

FIGURE 2 - Position of the protective enclosure.

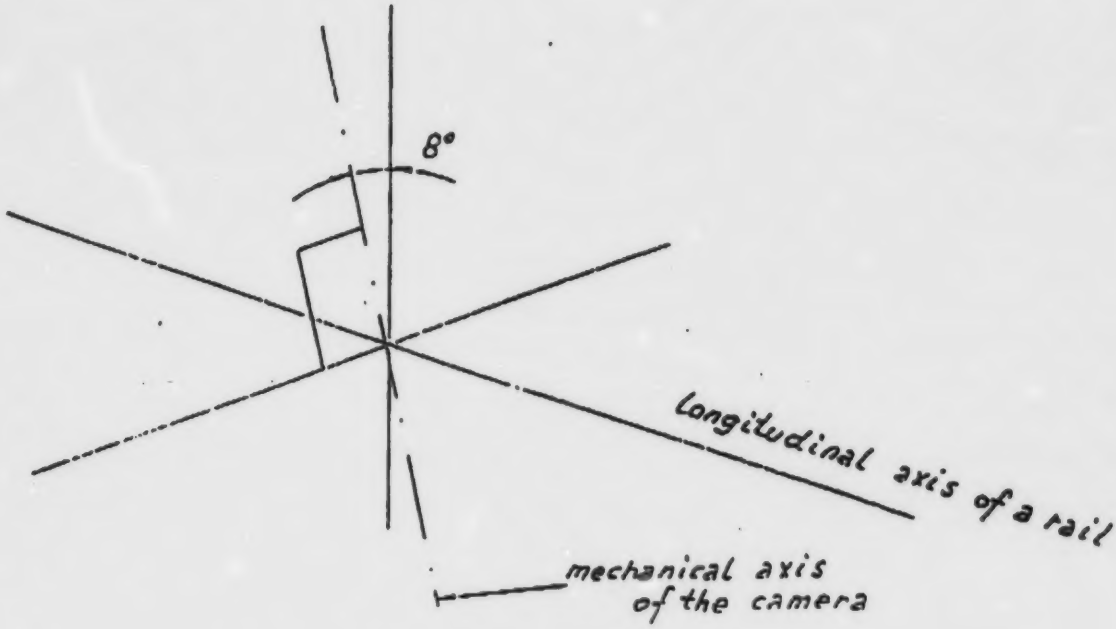

FIGURE 3 - Geometrical configuration.

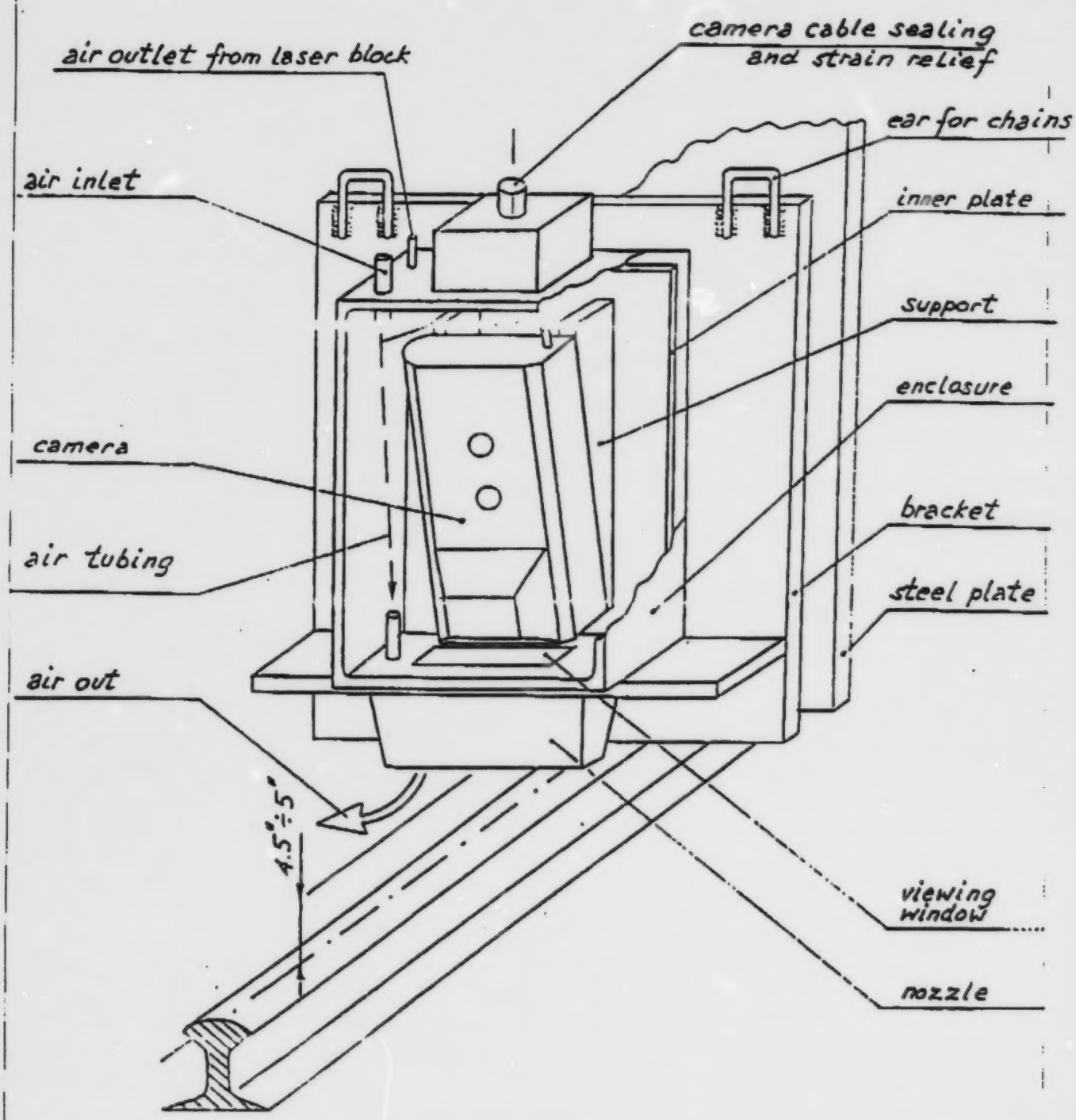

FIGURE 4 - Protective enclosure.

The enclosure is equipped with an electrical heater controlled by a thermostatic switch in order to keep the temperature of the camera above the minimum operation level required for its electronics when the outside temperature is too low.

5. INSTALLATION

The measurement system consists of one camera which is mounted above the rail head, inside of a thermally controlled enclosure, one controller and one IBM-PC compatible computer installed inside of the track geometry car. All the functions of the camera are controlled by the controller connected via a 10 m cable. The vision system has the ability to track a defined position on the top of the rail head and provide measurement of this particular point at a rate determined by a synchronization signal provided by some other equipment in the track geometry car.

To install the rail measurement system, first attach the protective enclosure at the proper position under the car as described in the previous section. Then plug the 10 m cable going from the camera to the controller and the air tubes from the compressor to the protective enclosure. The controller must be plugged to a 115 Vac outlet and, through a serial communication cable, to the PC used as the terminal. Finally, an "inch" signal must be provided at the USER I/O port of the controller.

6. TESTING

6.1 Vibration Tests

You will find a copy of a previous report describing the vibration tests in enclosure 1.

6.2 Laboratory Tests

Before installing the vision system aboard the track geometry car, we performed laboratory tests on three rail sections. CP personnel first measured the longitudinal profile of the rails with a mechanical measurement device and recorded the data. We then installed the camera on the linear slide which was part of the measurement device used by CP. We used a data acquisition board in a PC to measure the longitudinal (X) position of the slide in order to be able to associate one X position with each depth (Z) measurement taken by the vision system. The depth measurements were taken while the camera was in the fixed mode (not scanning) to observe the center of the top surface of the rail head. Our data matched the CP data as shown by the curves displayed on the following pages.

Servo-Robot

13a

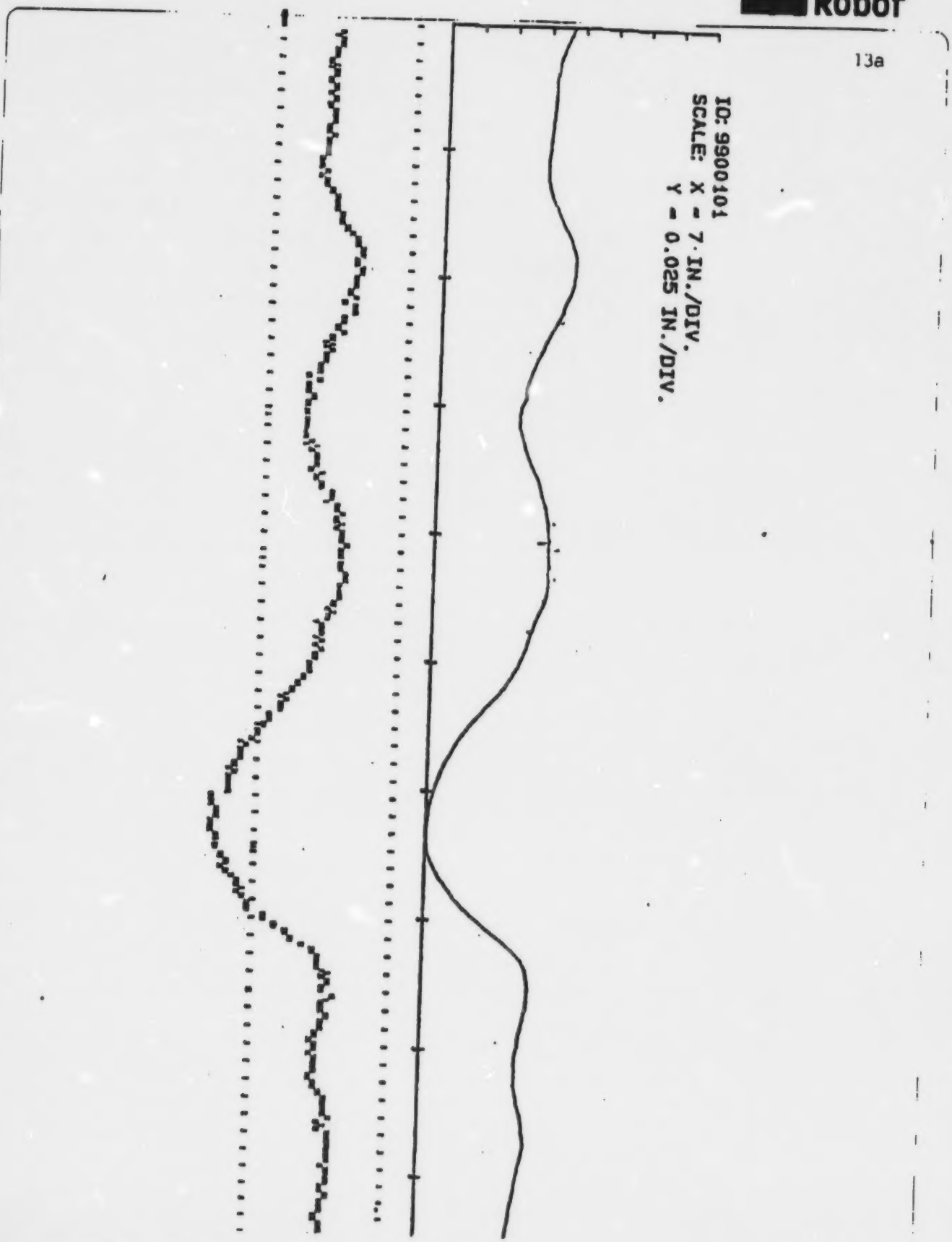

Servo-Robot

13b

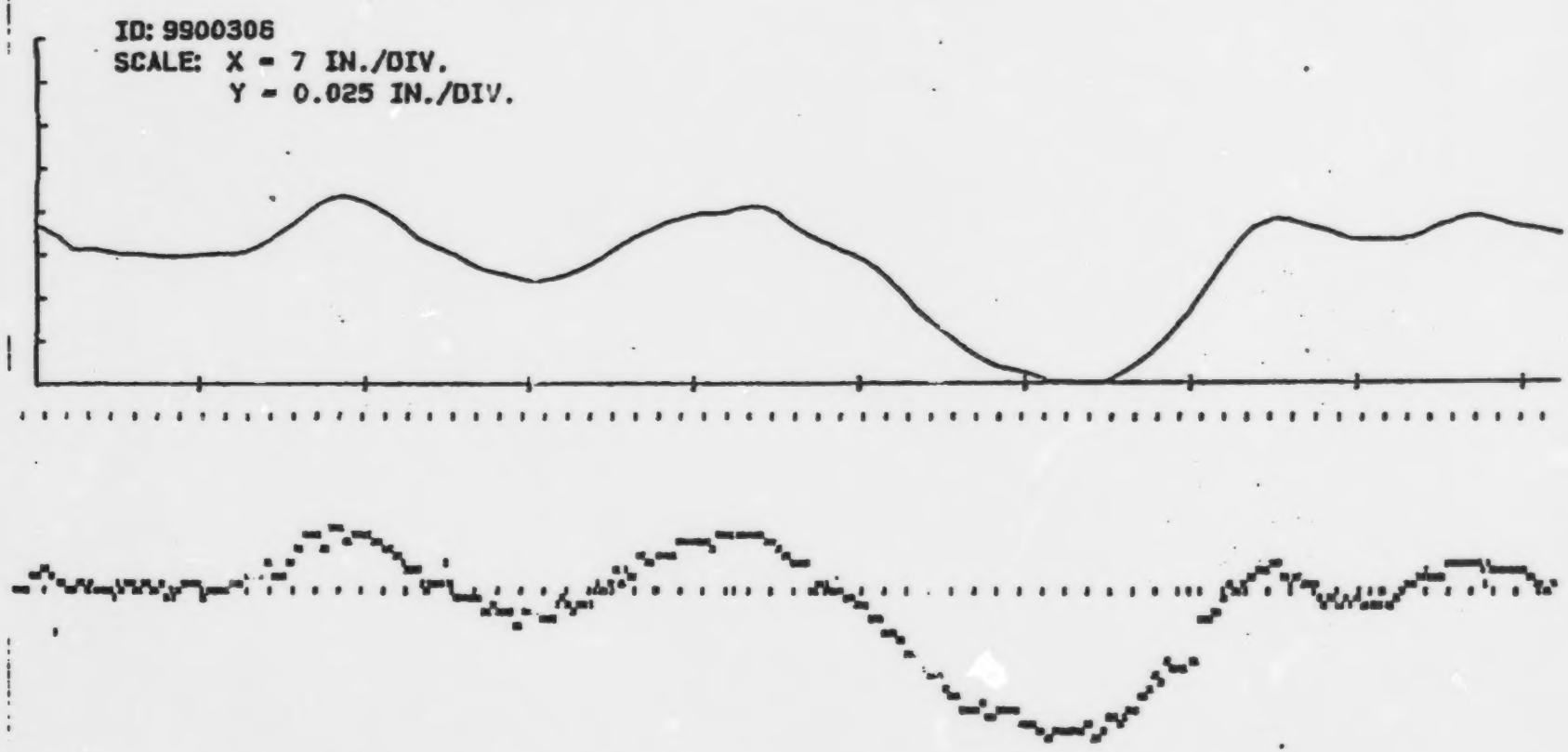

Servo-Robot

13c

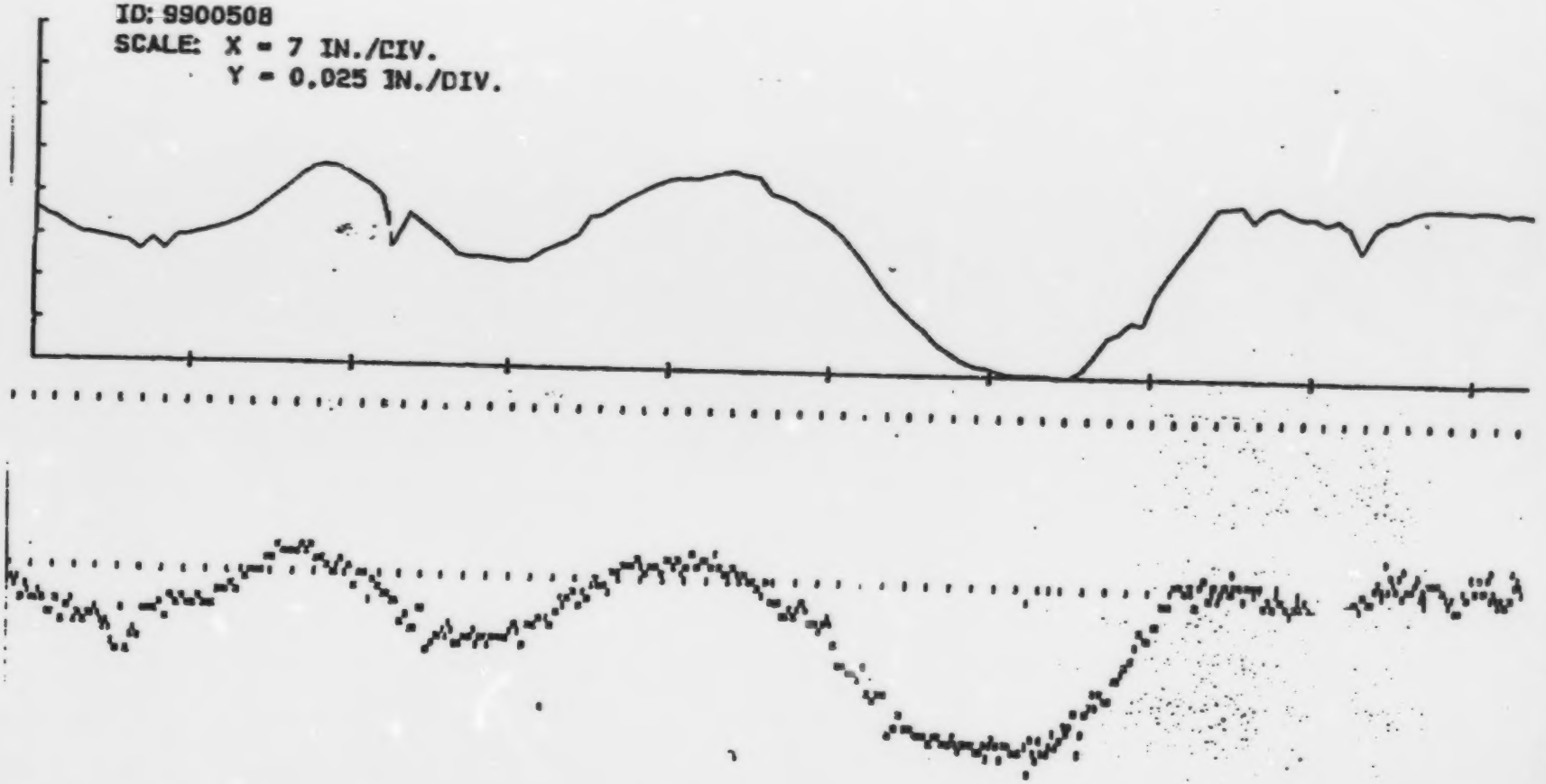

6.3 Field Tests

Many field tests were needed to help uncover and/or solve some of the problems with the special software designed for this system. The tests were also used to demonstrate that the rail geometry measurement system will perform as needed once its development is completed and all its functions fully implemented.

For the field tests, the camera was installed, in its protective enclosure, under the track geometry car, the top of the rail head being close to the center of the field of view when the car is on a straight rail section. The controller was installed inside the car, with the PC used as an interface.

For the measurement tests, the car moved at speeds up to 50 miles/hour over a rail section on which the corrugation measurement had previously been performed manually by CP. The results from both measurements were then compared by CP, after the oscillations caused by the movements of the car were removed from our data.

For certain tests, CP was providing an "inch-count" signal, coming from an encoder placed on the wheels, to the controller of the vision system, in order to associate each point measured on the rail with a longitudinal position along it and to facilitate the comparison process. For some of the tests, a true "inch" signal was not available. A signal generator was then used with an oscillation frequency corresponding to a speed of 30 miles/hour, which is close to the real speed of the car.

During the field tests, the PC was used to control the functions of the system and to store the measurement data after each run over the test section of the rail. Some of this data was the corrugation measurement data given to CP for the comparison, and the rest was used by us to analyse the performance of the system.

The software running on the PC was an extension to the standard user's interface of our vision system, designed to ease the use of the system and minimize the number of commands needed to operate it. With the software, it was also possible to display the corrugation data after each run to check its validity.

One of the improvements that was made following field tests served to eliminate some of the bad data present right after the tracking function, as the first values of each measurement group, mainly at high speeds. It was found that not enough time was spent waiting for the laser beam to stabilize over its measurement position after a tracking scan. The power control algorithm was also improved at this time and we plan to further improve it to be able to get a precise profile of the full top surface of the rail head during the tracking scans.

The corrugation measurements made during the first field tests were showing a large permanent drop in depth after each tracking operation on the curves traced by CP. After studying the data, we found that this was caused by the first depth value being very large. This bad data point was leading CP's curve tracing software in producing a permanent drop (offset), when it should simply have shown a spike. This bad data point was part of the bad data eliminated by the software improvement.

The measurements performed during the last field test were correlated with reasonable accuracy to the manual measurements made by CP.

7. CONCLUSION

Sections 4.1.1 and 4.3.1 show differences between CP requirements and the delivered camera insofar as the camera's depth of field and field of view are concerned. The difference in depth of field should not cause any problem for the rail measurements.

The reduced field of view of the real camera caused the image of the rail head to be lost over curves during the field tests, but it may prove to be large enough if a way could be found to install the camera closer to the pivoting point.

Even if the vision system is general enough to perform various rail geometry measurements, the first tests were performed specifically to address the problem of on-board measurement of the longitudinal rail surface profile. The results showed that our laser vision system is able to successfully cope with the harsh environmental conditions typical to train operations.

ENCL. 1 - VIBRATION TESTS

Please refer to our Report No. Q71014-31-R1 January 25, 1988, Revised March 17, 1988.

References

Marc Rioux, "Laser Range Finder Based on Synchronized Scanners", Appl. Opt. 21, 3837 (1989)

Marc Rioux, G. Bechthold, D. Taylor and M. Duggan, "Design of a Large Depth of View Three-Dimensional Camera for Robot Vision", Opt. Eng. 26, 1245 (1987)

ENCL. 1 - VIBRATION TESTS

Servo-Robot

TABLE OF CONTENTS

		Page
	EXECUTIVE SUMMARY	
	SYMBOLS AND ABBREVIATIONS	1
1.	CP Rail specifications	2
2.	CAMERA EVALUATION	5
2.1	Description of the signal representation	5
2.2	Camera resolution along Z coordinate and accuracy	6
3.	TESTS DESCRIPTION	8
3.1	Preliminary tests	9
3.2	Main tests	10
3.2.1	The vibration tests in LG and LT directions	10
3.2.2	The vibration tests in VR direction	11
3.2.3	The shocks tests	12
3.2.4	The temperature resistance tests	12
4.	OBSERVATIONS	13
4.1	Vibration and shocks	13
4.2	Temperature	14
5.	CONCLUSIONS	15

Servo-Robot

EXECUTIVE SUMMARY

The purpose of this report is to give the results of the extensive vibrations and temperature resistance tests which were conducted by Servo-Robot Inc.

The major goal of this first phase was to evaluate if a synchronized laser scanner is capable to cope with the severe conditions of railway transportation and to decide if this tool could be used for corrugation measurement.

The vision head should be mounted under the rail geometry measurement car which runs with a speed of up to 65 mph.

The results of the experiments indicate that our laser vision system will be able to successfully cope with the harsh environmental conditions, typical to train operations.

SYMBOLS AND ABBREVIATIONS

f	-	Frequency of vibrations of the camera in Hz
FOV		Field of view of the camera
DOF		Depth of field of the camera
a		Acceleration in terms of g rms
d	-	Approximate resolution in Z coordinate
g	-	9.806 ms $^{-2}$
VR	-	Vertical direction as shown in fig. 4
LT	-	Lateral direction as shown in fig. 4
LG	-	Longitudinal direction as shown in fig. 4
SMC	-	Static mechanical condition, no vibration, a = 0
t	-	Total time in min.
$\bar{Z}$ (average)	-	Characterizes the distance between the camera and the target
σ (deviation)	-	Standard deviation
t_d	-	Dry-bulb temperature (temperature of the atmosphere) in °C
r	-	Relative humidity in %
t_{cam}	-	Temperature inside the camera °C
t_{las}	-	Temperature of the laser in °C
t_{pel}	-	Peltier effect temperature in °C
I_{pel}	-	Peltier effect current in A
I_{las}	-	Laser current in A
P	-	Laser power in W
1/2 T	-	Duration of a shock in s

1. CP RAIL SPECIFICATIONS

The values of the vibrations, shocks and ambient temperature typical for railway operation were given to us by CP Rail in a document dated September 29th, 1987.

PARAMETERS OF THE VISION SYSTEM REQUESTED BY CP RAIL:

Field of view	275 mm
Depth of field	120 mm
Accuracy along Z axis	0.075 mm

The system will consist of one camera with the associated controller, interfaces to a host computer, and the mounting enclosure.

- The camera in the mounting enclosure is to be located under the Track Geometry car and be protected from an impact with track debris weighing 150 lbs. when tracking at a speed of 65 m.p.h.

- The optical system must be protected to permit continuous operation at ambient temperatures of minus 25° C to plus 45° C and must be capable of assuming operation after a non operating cold soak at -45° C.

- The optical system must maintain continuous operation in presence of dust, moisture, snow or ice particles and ambient light conditions usually encountered in the railway environment.

- No part of the equipment can be installed closer than 4 inches from the top of rail; higher position is preferable.

- AAR Plate C and C-1 clearance must not be exceeded for any installed equipment.

- All components must be capable of surviving, with temporary loss of signal, when attached to the underside of a carbody that has a maximum vibration environment that can be characterized as:

Shock (1/2 sine):

	Lateral	Vertical	Longitudinal
Peak amplitude	5 g	5 g	5 g
Duration	10 msec	10 msec	10 msec

Vibration:

	Lateral	Vertical	Longitudinal
5 Hz to 30 Hz	0.5 g	0.5 g	0.5 g
30 Hz to 150 Hz	1.0 g	1.0 g	1.0 g

- The optical system must be capable of operating without degradation of accuracy when subjected to the following shocks and vibrations.

Shock (1/2 sine approximation of signal waveform):

	Lateral	Vertical	Longitudinal
Peak amplitude	0.2 g	2 g	2 g
Duration	0.3 sec	30 msec	0.4 sec

Vibration

1 Hz to 5 Hz	0.1 g rms	0.3 g rms	0.1 g rms
5 Hz to 50 Hz	-	0.1 g rms	-
50 Hz to 100 Hz	-	0.8 g rms	-

The above mentioned parameters require partial modification of the standard Servo-Robot's camera. Additionally, the camera will be mounted in a special enclosure in order to maintain the vision head at a reasonable ambient temperature. In order to prove that the vision system will be capable to successfully function in severe environmental conditions typical to railway operations, we decided to conduct experiments simulating vibrations, mechanical shocks and temperature fluctuation with our standard camera. This camera has the following parameters:.

Light source	-	15 mW IR laser diode
Detector	-	Linear array 256 elements
Field of view (FOV)	-	30 mm
Depth of field (DOF)	-	30 mm
Distance of closest approach (DCA)	-	80 mm
Resolution	-	At the center DOF 0.12 mm along Y axis 0.007 mm along Z axis
Dimension	-	115 x 144 x 55 mm 40 mm protrubing scanner case
Weight	-	1.5 Kg
Scanning frequency	-	Up to 28 Hz
Case material	-	Aluminum alloy

2. CAMERA EVALUATION

The main method for evaluation of the camera is to observe the 3-D signal during all phases of the experiments and to quantify the deviation of the signal during SMC. In order to do this kind of quantification, we made a program calculating the standard deviations of the measured distance Z.

2.1 Description of the signal representation

All 3-D figures of the target profile are shown as follows:

The left side of the picture shows the raw data Y-Z which represents the 3-D profile of the scanned object.

"Average" means the relative Z positions of points, distributed uniformly on the object along a beam path, in the DOF. The deviation characterizes σ (one standard deviation) of $\bar{Z}$ measurements. In order to have reasonable statistical sample, one hundred scans are taken to compute the average and deviation. The right side of the picture shows the intensity of the signal taken by the sensor. No other values appearing on the picture have a meaning for that project. The pictures are prints of the computer screen. Our computer graphic was designed for a general use.

One scan contains 256 points. A value associated to each one represents the Z coordinate. We choose 32nd, 64th, 96th, 128th, 160th, 192nd and 224th points for calculation of the standard deviation.

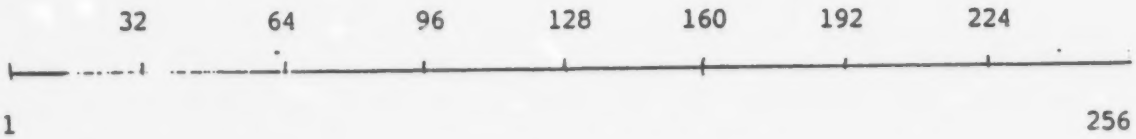

Figure 1.1

Choice of points on a scan

Depending on the value of the parameter which characterizes the averaging process, the point can be taken in account alone or with its neighbourhood. The window size depends on the level of the signal averaging. All our calculations were done with the window size 0 in order to demonstrate only the accuracy of the optical system without influence of possible software improvement. For each measurement, we took 100 scans and then we calculated the mean value. So we have for every scan 7 mean values. For 100 scans, we compute, besides the average values, the standard deviations using the following formulas:

$$\bar{Z} = \left(\sum_{i=1}^{N} Zi \right) / N$$

$$\sigma = \sqrt{\sum_{i=1}^{N} \left(Zi - \bar{Z} \right)^2} / N$$

where Zi, is a mean value for a given group of points on i-th scan position and N=100.

Values are read in and treated by INTSAT software in real time.

2.2 Camera Resolution along Z Coordinate and Accuracy

The DOF is divided into equal section (pixels). The assumption that DOF is equally divided can be used for camera evaluation, especially when the DOF is not large.

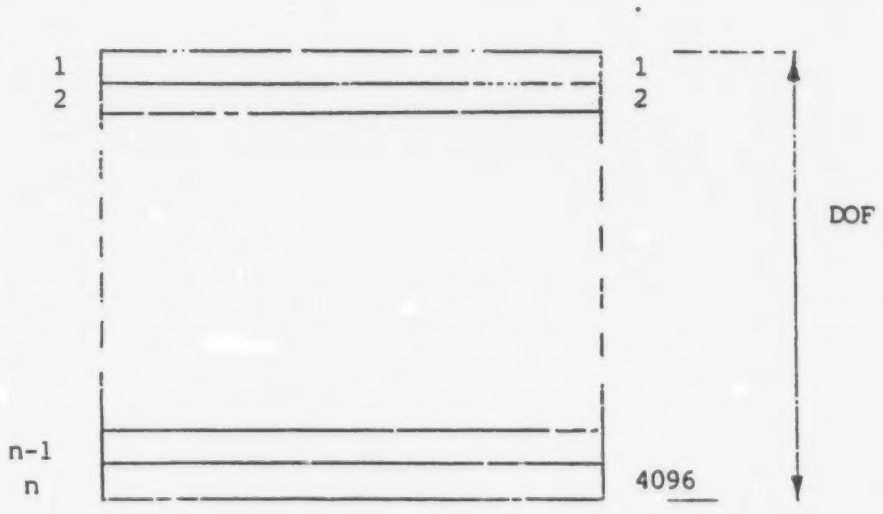

Figure 2. Division of depth of field

The number n can be chosen by the software among 2^{9}, 2^{10}, 2^{11}, 2^{12}. For all the tests, we used n = 12. One pixel (section) corresponds to

$$d = \frac{DOF}{n} = \frac{30}{4096} = 0.00732 \text{ mm} = 2.88 \cdot 10^{-4} \text{ "}$$

The above mentioned formula represents the resolution of the vision system. The accuracy is defined by the value of 3σ according to statistical mathematics.

3. TESTS DESCRIPTION

A series of mechanical vibration tests were made on programmable hydraulic fatigue benches. Fig. 3, 4, and 5 show the schematic of the measurement system. After mechanical vibration tests, the temperature resistance tests were done. The vision head underwent testing in a refrigerator and in an oven as well.

At the beginning, a preliminary test was performed in three orthogonal directions VR, LT and LG. It was carried out without scanning. The objective was to verify:

- mechanical and electrical connections inside the camera,
- quality of the signal from the camera in static mechanical conditions (SMC) after series of vibrations tests.

The following test was performed in three orthogonal directions LT, LG and VR. It was made with a scanning camera and had the objective to verify that the camera performs and keeps its accuracy in the simulated railway environment.

The VR, LT and LG directions in comparison with the camera position are shown in Fig. 6.

The target to be scanned was attached to the camera front (Fig. 7). The camera was mounted on a special supporting device designed and manufactured by Servo-Robot (Fig. 8).

Before the beginning of the tests on the vibration stands, the camera was adjusted and checked on the optical bench to verify the CP specifications. The conditions on the optical bench are called static mechanical conditions (SMC). The Z coordinate of the target was measured with an accuracy better than 0.055 mm.

To fulfil the conditions encountered in a train, we have manufactured a special bracket set for attaching the camera which allows us to use the available hydraulic actuators to simulate both vibrations and shocks in all required directions.

Since the vibration stands are generally intended to fatigue tests and do not permit to obtain great displacements for very low frequencies and then high level accelerations, we manufactured the bracket set in such a way that we can use the possibility of the mechanical resonance to achieve the required accelerations for the frequencies in the range of 1 to 5 HZ. As a generalization of that concept, we use the same set to simulate the shocks on the same vibration stands when we apply one cycle sine signal (single wavelength).

For each series of vibrations, we calculated the actuator's piston displacement which is the input parameter for the stand and used the accelerometer to be sure that the correct values were reached.

3.1 Preliminary Tests

The vibration tests without scanning were performed with the parameters shown in tables 1, 2, 3, 4, 5 and 6. After each series (VR, LI, LG) of these vibrations (operating, survival), the camera was taken back to the optical bench to measure the signal in SMC. No changes in accuracy in comparison with the measurements performed before the tests were detected. Figure 14 shows the typical signal shape for SMC.

These preliminary tests had one more very useful result: we detected that the adhesive (Loctite Speed Bonder 312 with primer NS-Locquic) we used to join together the scanner mirror and its fork was not very appropriate to work under the vibrations (glass/Al or glass/Ti joints).

We changed that adhesive for the epoxy one and then carried out the vibration tests of the working galvanometer with the mirror under the following conditions:

- frequency of actuator: 100 HZ,
- acceleration: 7 g,
- frequency of galvanometer: 10 HZ,
  100 HZ,
- duration of one test for each galvanometer frequency: 20 hrs.

The objectives of the tests were as follows:

- verification of the choice of the adhesive,
- verification of the influence of high scanning speed on the galvanometer.

The tests did not alter neither the joint nor the selected galvanometer of the camera scanner.

3.2 Main Tests

3.2.1 The Vibration Tests in LG and LT Directions

The vibration tests with the working camera were made with the same vibration equipment and the same conditions as indicated in Table 7, Table 8, Table 9 and Table 10.

For the operating conditions specified by CP in LT and LG directions, we obtained very satisfying results. The results are analysed in details in chapter 4. Observations.

Fig. 9, 10, 11, 12 and 13 show typical signal shape for LT vibrations of 2, 4, 10, 25, 50 HZ respectively and acceleration of 0.183, 0.159, 0.194, 0.140, 0.128 g respectively. The similar but better results were obtained for LG vibrations.

For the survival LT and LG vibrations, we have never lost the signal and the typical signal shape is shown on Fig. 14 and 15. Figure 16 shows the typical signal shape for SMC. We want to stress the fact that for the operating conditions specified by CP for LT and LG vibrations, the system operates with required accuracy and without the distortion of the signal described later in the report.

In order to check the camera performance for more severe conditions than specified, we undertook the tests for LT and L vibrations within the range of frequencies from 1 to 150 HZ with the accelerations within the range from 0.1 to 3.150 g rms. (See Table 11, Table 12)

The reason for these additional tests was a problem encountered during the LG and LT vibrations in the range 50 to 100 Hz (see section 4.1). After improvements the phenomena was not visible at all for conditions specified by CP and we ran the test with greater accelerations than required. It allowed us to observe the efficiency of the modifications. The quality of the signal was better than required. The typical shape of the signal is shown in Figure 17 and Figure 18.

3.2.2 The vibrations test in VR direction

In order to improve the stability of the camera-target assembly, the target for the vertical vibrations/shocks tests was changed (see Figure 31).

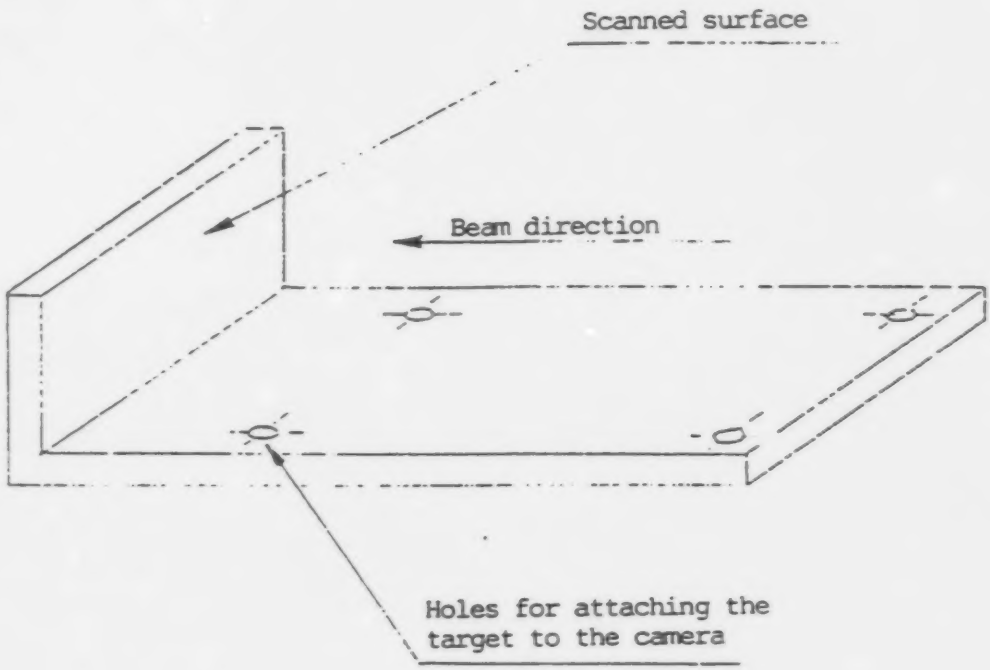

Fig. 2 Bracket for VR tests

Figure 19 shows the SMC signal before the VR test started. The VR vibration tests conditions are indicated in TAB 13 and TAB 14. Figures 20, 21, 22, 23 and 24 show typical shape for VR operating vibrations of 5, 20, 50, 50 and 100 Hz respectively and acceleration of 0.326, 0.116, 0.130, 0.818 and 0.809 g respectively.

Figures 25, 26, 27, 28, 29 and 30 show the signal shape for VR survival vibrations.

3.2.3 The shock tests

The shock tests were carried out on the same equipment used for the vibration tests. In order to simulate the shock condition, we put 1/2 I signal of the actuator in such a way that it fulfilled the CP requirements (peak amplitude and duration). This method was very convenient for continuous observation of the signal and, from the mechanical point of view, it was equivalent to the classical shock test methods, and it allows to pass several thousands of cycles.

Figures 32 and 33 show the signal shape for LG shocks, figure 34 for LT shocks and Figures 35 and 36 for VR shocks. We stress the fact that the signal was never lost for the survival shocks and that for the operating conditions, the signal was better than required by CP.

3.2.4 The temperature resistance tests

These tests were carried out in a range of temperatures from + 1°C to + 44°C as shown in the tables 15 and 16. The ambient temperature means the temperature to which the camera was exposed without any external protection. Before the tests, the camera was left in the non-operating temperature of - 25°C during 24 hours.

We operated the vision system from + 1°C despite the fact that operating lower temperature limit for the galvanometer is + 10°C. The figures 37 to 47 show the results (signal shape and accuracy) obtained.

4. OBSERVATIONS

4.1 Vibrations and shocks

In the process of testing, suddenly a severe degradation of the camera signal occurs after 50 hours of non stop operation. This is represented in figure 51. The misfunction happened because of improper assembly of the laser module. The laser module was modified in order to eliminate the possibility of a similar failure in the future.

During vibration tests L1 and L6, we observed some fluctuation of $\bar{Z}$ values after we changed the direction of vibrations for which we had to mount the camera in different places on the holder. After analysing the problem, we came to the conclusion that due to the limited space inside the camera, one cable was squeezed between the laser module and the cover. When the camera was attached in a new position, the laser module was forced to slightly different positions through the system camera holder-cover - cable - laser module. The distortion of the laser module from the correct position had an effect on the variation of $\bar{Z}$.

After the above mentioned discovery, we solved the problem and we modified the camera assembly in such a way that it could not happen again.

After fixing all the problems, we continued with the tests and we always experienced a better signal than required by CP. In figures 48, 49 and 50, we can see that even the values of 3σ for operational conditions are below CP requirements.

There is only one exception in figure 50 -- Vibrations - VR direction for operating conditions with acceleration 0.8 g rms. In this case, the value of 3σ would go above the limits set by CP Rail requirements. It can be seen from figure 19 that the standard deviation for SMC were relatively high (around 3 pixels). For most of the vertical vibration tests, the standard deviation stayed in the same vicinity as in SMC. In case of operating conditions with 0.8 g rms, the increase of the value σ is around 60%. It means that our effort has to be targeted for the reduction of σ. The avenues which lead to this goal are described in chapter 5. Conclusion.

4.2 Temperature

The camera operates in the given temperature range with the required accuracy. We have not observed the degradation of accuracy linked to the temperature and humidity changes.

The temperature stability of the camera is demonstrated by figure 52.

In some cases, the camera operated in condensation conditions. Even during this condition, we received a good signal from the camera. Despite this fact, we highly recommend not to operate the camera above the condensation point.

5. CONCLUSION

All experiments were done with the standard camera which has a smaller depth of field and field of view as we mentioned at the beginning of the report.

For the DOF = 120 mm which is required by CP, we have a resolution of = 0.0293 mm = 1.153 . 10 $^{-3}$".

For DOF = 120 mm, the accuracy required by CP would correspond to the standard deviation value of 0.856.

This indicates that we have to take some measures in order to decrease the value of the standard deviation σ . There is a way to do it in the vision system which will be built for CP Rail.

The standard camera used in our experiments is normally utilized for welding applications and therefore the interference filter has to be built in. The interference filter obviously cuts great amount of light coming back to the sensor. That is why we are forced to use a very high amplification for the video signal. In our experiments, we had a very strong signal due to the removal of the interference filter . We could therefore run the vision system with a very low laser power.

In the dedicated camera for rail inspection, we will implement a 40mW laser (instead of 15mW) and we should be able to dramatically decrease the gain of the video signal which has a positive effect on the standard deviation σ .

We will also incorporate different optical components in the vision head which will help to increase the intensity of the receiving signal. This will also have a good influence on the reduction of the standard deviation σ .

After the tests described in the report, we again improved the vision head and for SMC, a standard deviation in the order of 0.3 - 0.5 for a DOF = 30 mm was reached (see figure 53).

If we are able to maintain the standard deviation σ in the vicinity of 0.3 - 0.5 pixel, we will be in a good position to meet the accuracy set by the CP requirements.

It should be noted that we experienced some changes in the value of $\bar{Z}$ from one test to another (even if the target was in exactly the same position). This was due to the temperature drift of the galvanometer.

This phenomena is known and the vision system built for CP Rail will incorporate a module which will compensate and control this drift.

The results of the temperature resistance test indicate the following facts:

- During the operation of the camera, the ambient temperature in the protective enclosure must be maintained in the range of + 10° to + 40°C if the standard scanning device is used. There is a possibility to incorporate in the vision head a military version of the galvanometer type G120DM. In this case, an ambient temperature variation of 0° to + 40°C would be acceptable.

- The ambient temperature in non operating conditions could be - 10° to + 70°C in case of the standard galvanometer and - 40° to + 70°C supposing the military one is used.

In order to prove the resistance of the camera to railway conditions, we used more severe conditions than the one defined by CP and we always received a better signal than specified in the CP Rail conditions (except one case indicated in chapter 4.1).

The experience gained from the tests will be used to improve the new version of the camera. This will give us a better tool for the measurement of the longitudinal surface profile.

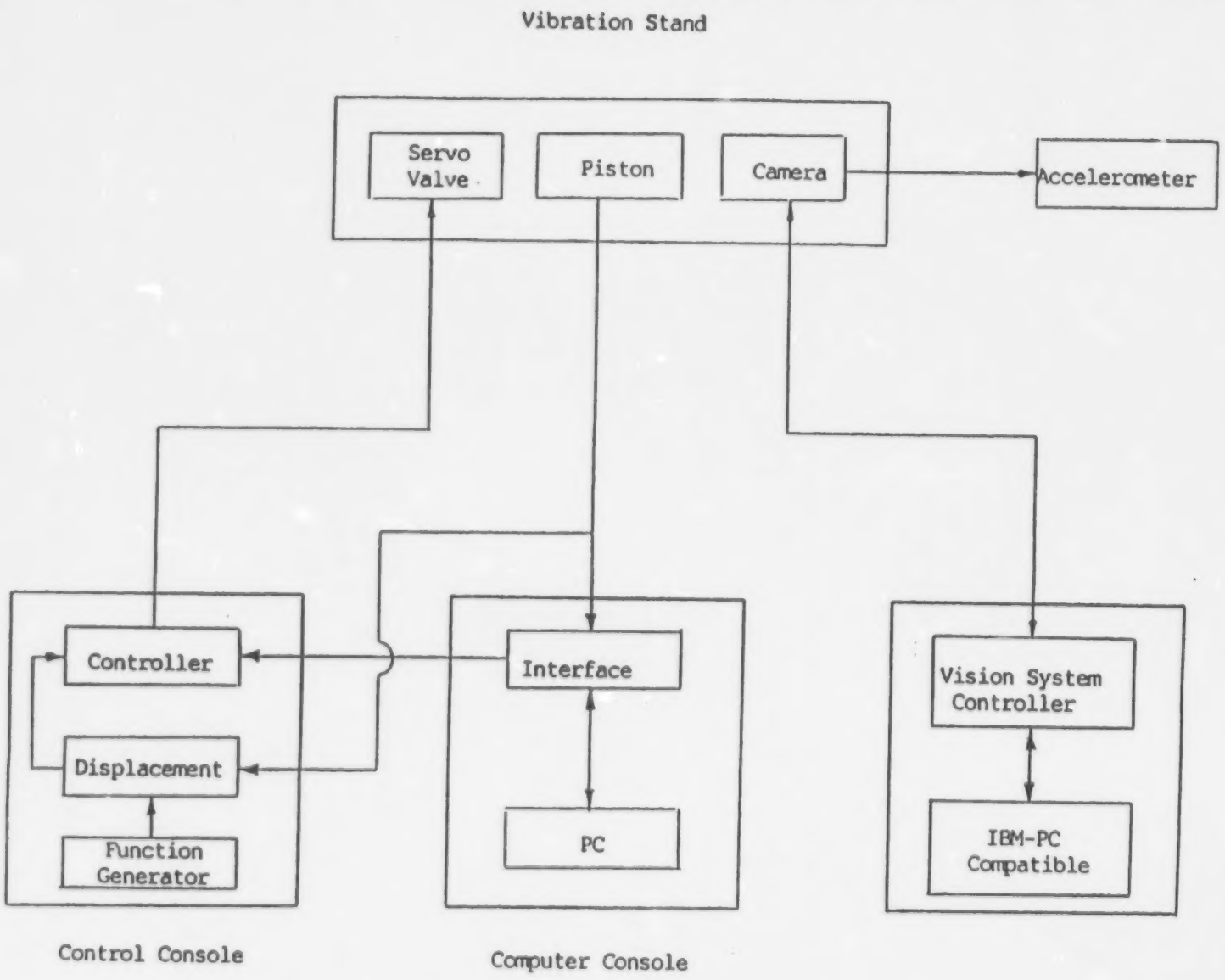

Fig. 3 General Description of the Measurement System

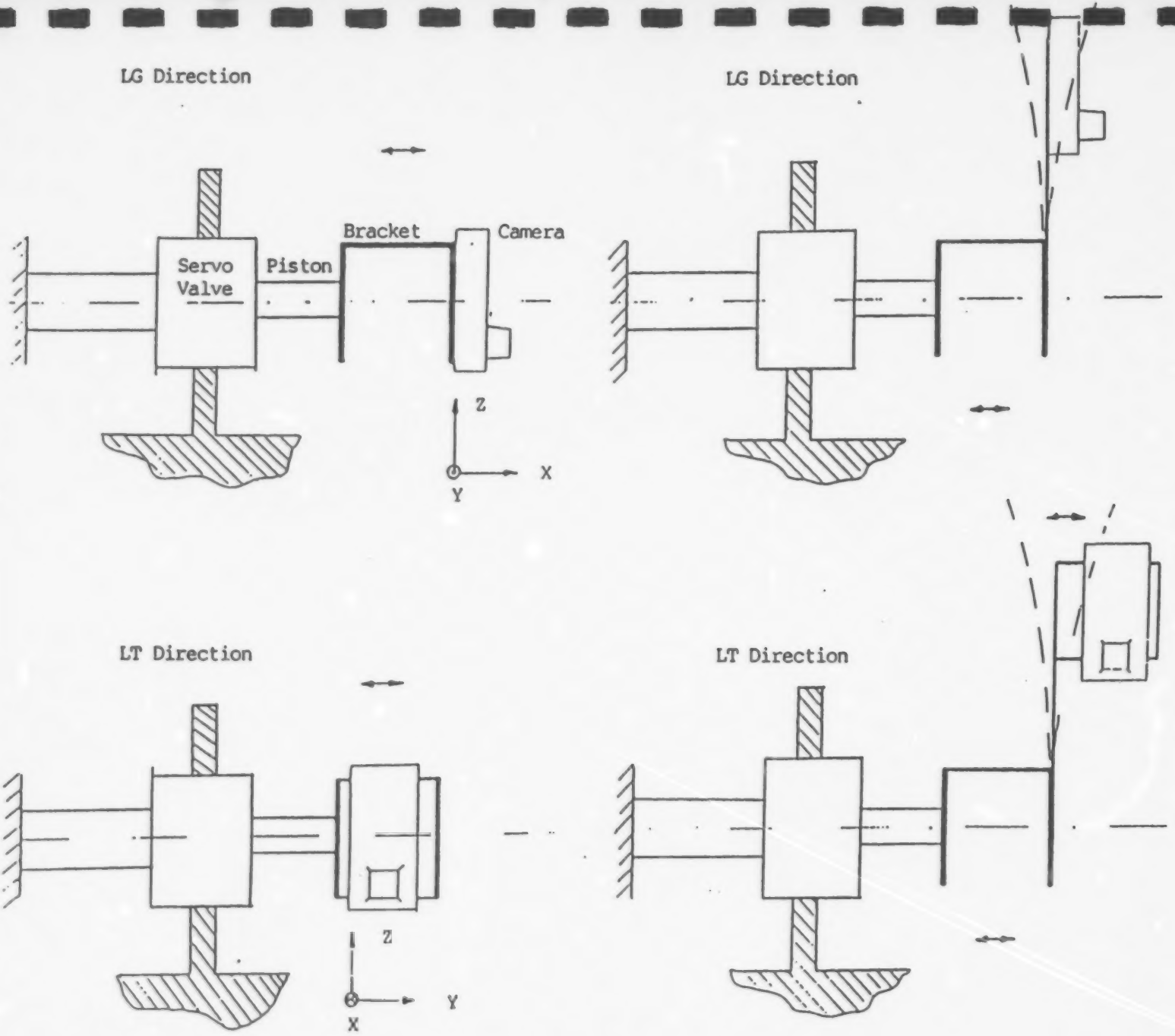

Fig. 4 Camera configurations on the vibration stand. Horizontal actuator

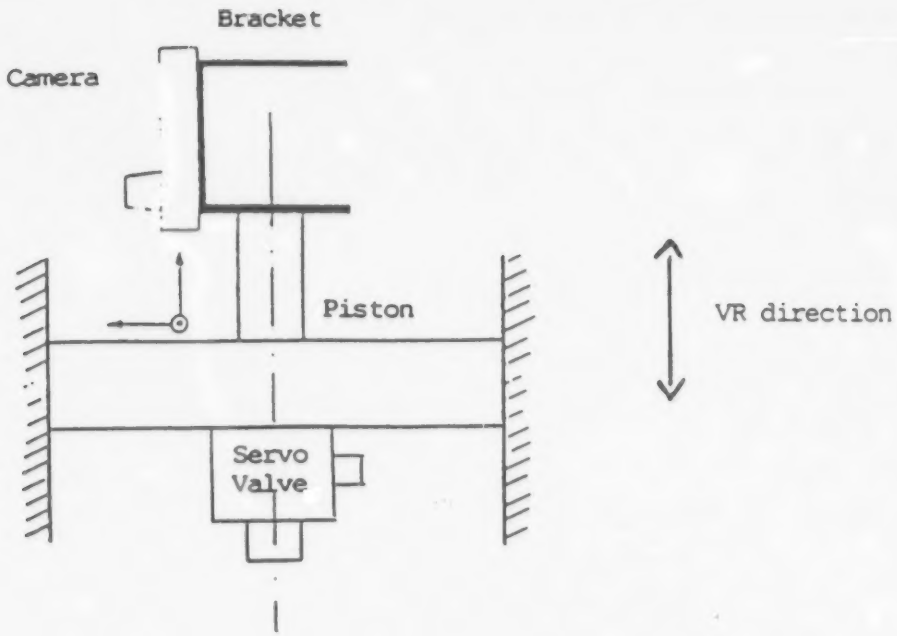

Fig. 5 Vertical actuator

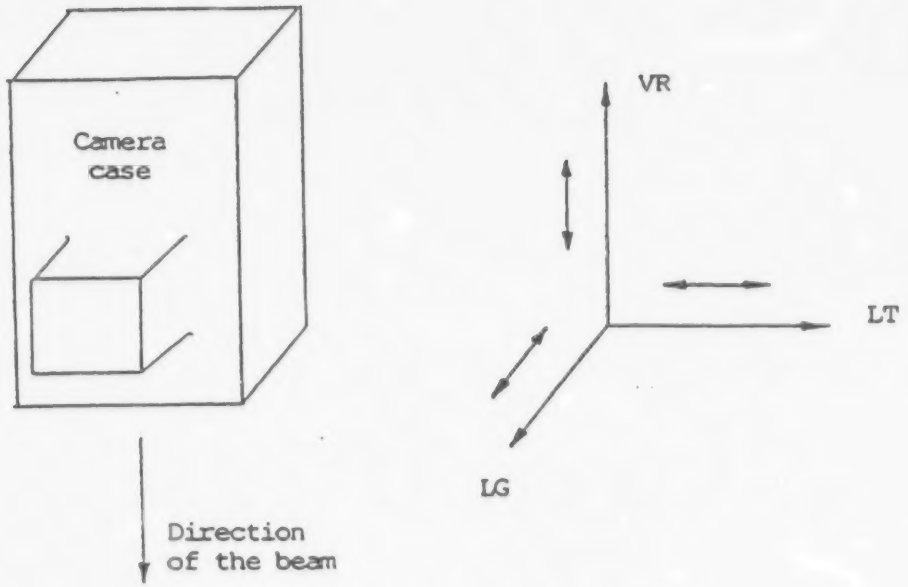

Fig. 6 Saturn III Camera emplacement

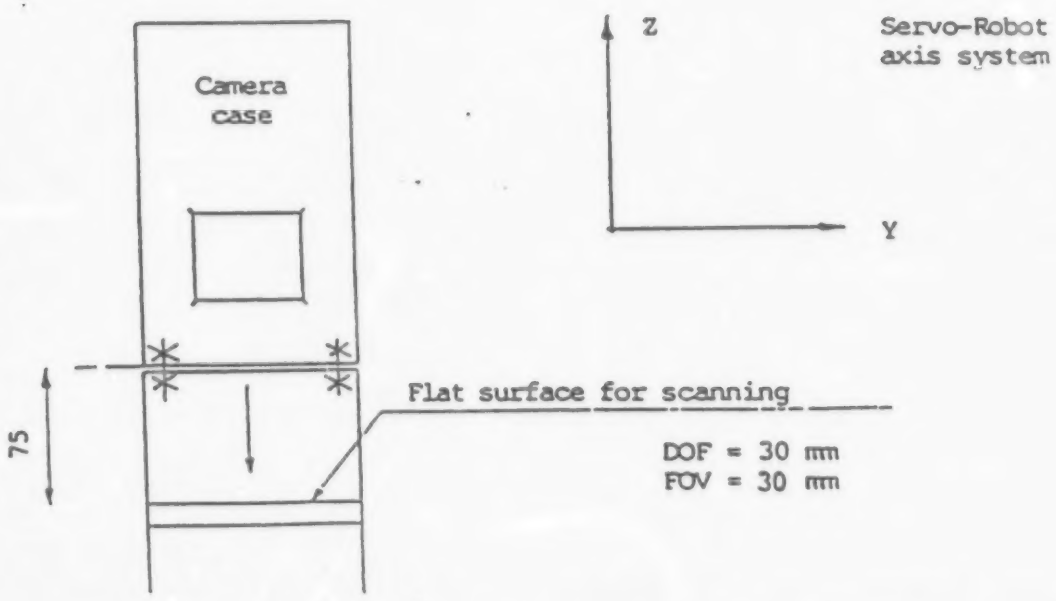

Fig. 7 Target (to be scanned). The target was attached to the camera front

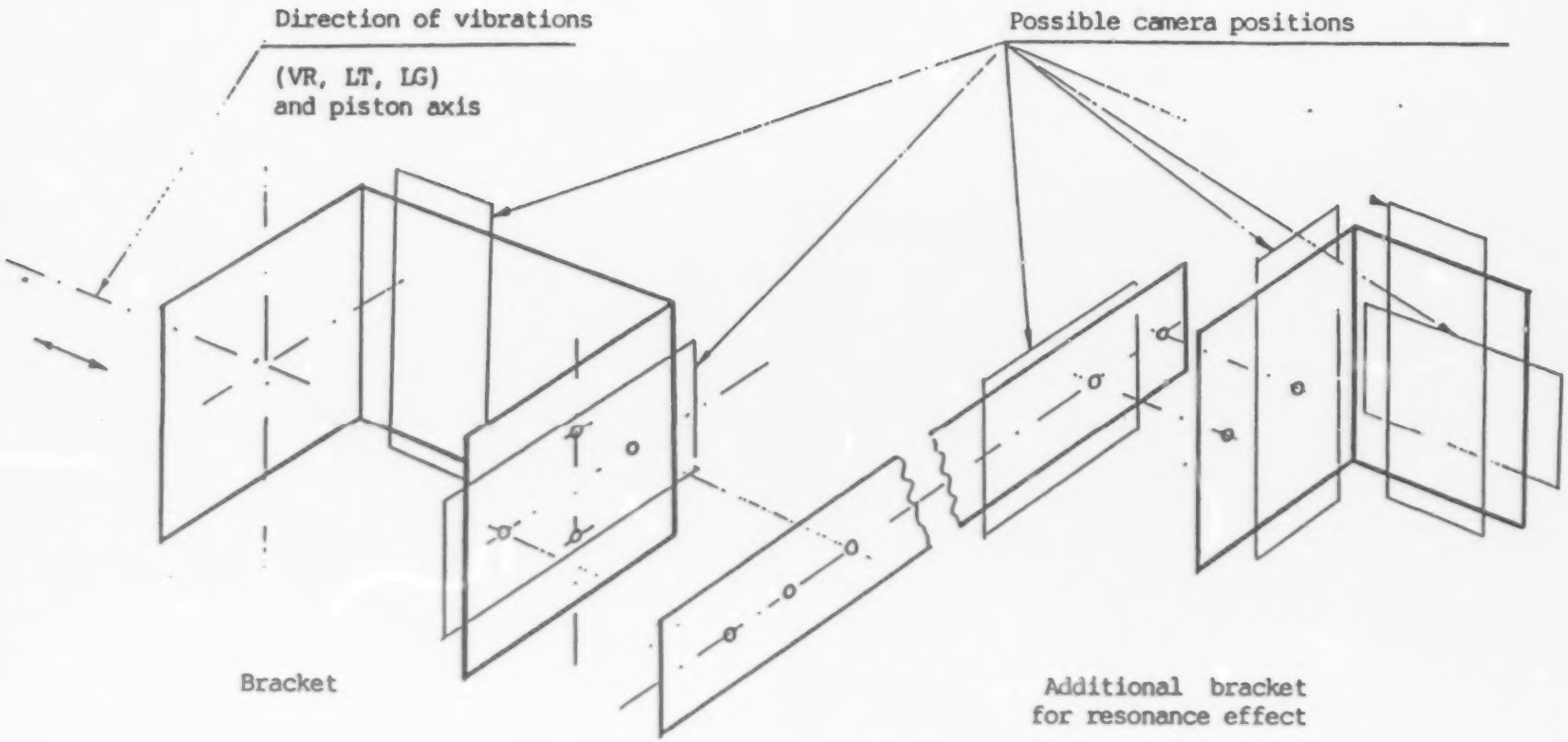

Fig. 8 Special bracket set

Fig. 9
f = 2 HZ
a = 0.183 g
L[illegible]

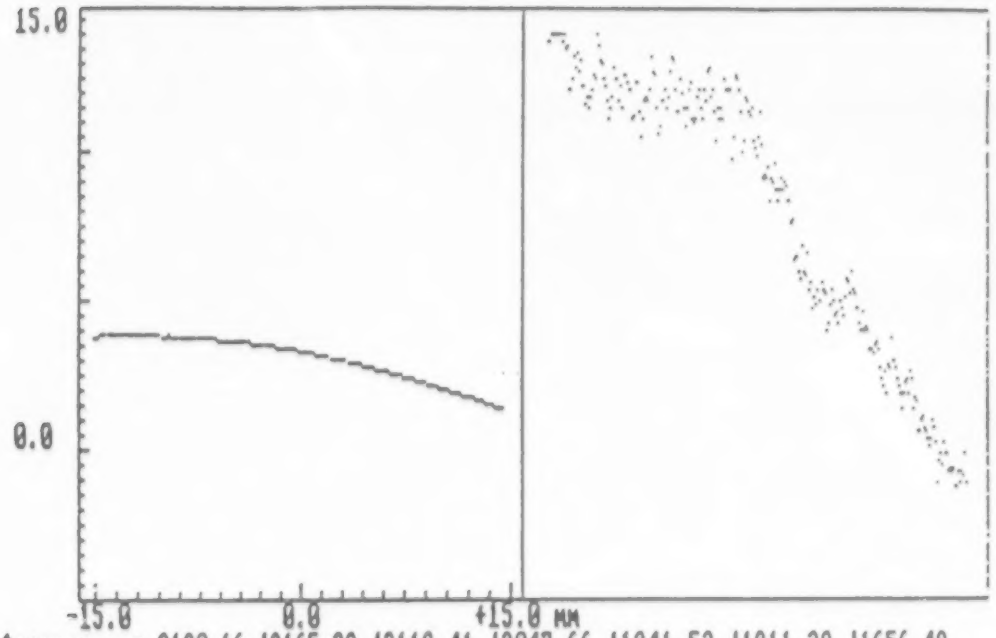

Average = 2180.16 ¦2165.28 ¦2119.41 ¦2047.66 ¦1941.53 ¦1811.39 ¦1656.48
Deviation = 0.90 ¦ 0.79 ¦ 0.72 ¦ 1.01 ¦ 1.31 ¦ 1.71 ¦ 1.91

->_

Fig. 10
f = 4 HZ
a = 0.159 g

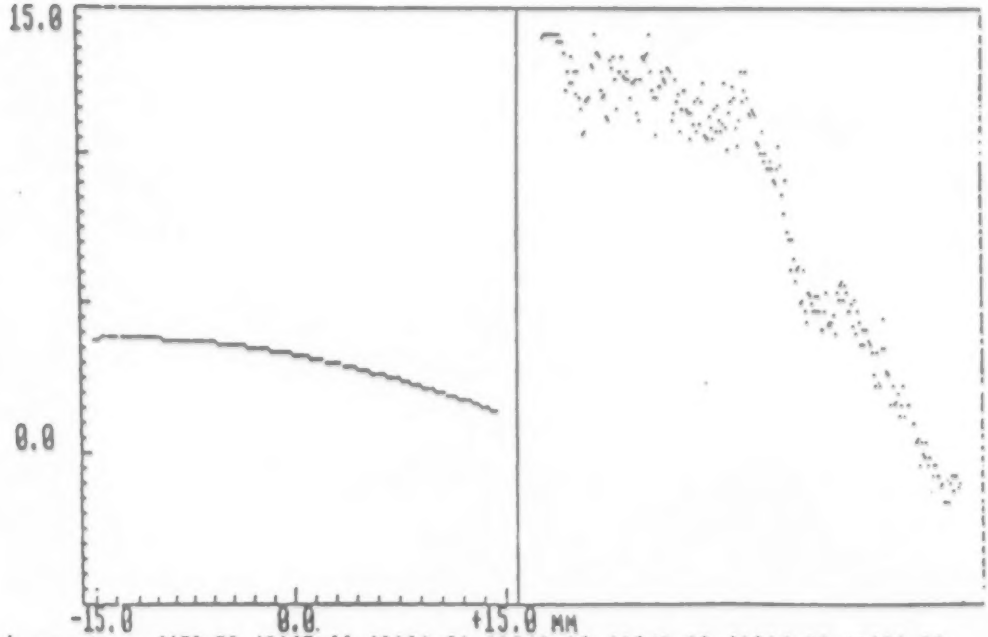

Average = 2179.73 ¦2165.66 ¦2121.01 ¦2048.16 ¦1943.82 ¦1814.29 ¦1656.93
Deviation = 0.85 ¦ 0.82 ¦ 0.82 ¦ 0.95 ¦ 1.31 ¦ 1.29 ¦ 1.70

Fig. 11
f = 10 HZ
a = 0.194 g
LT

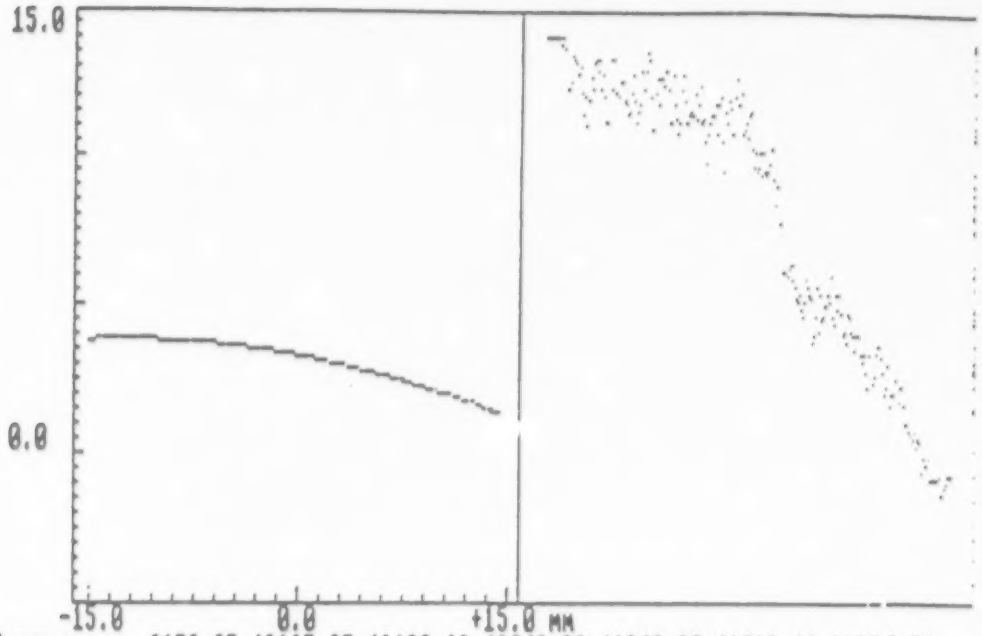

Average =	2179.85	2165.85	2120.63	2048.33	1942.90	1813.44	1656.94
Deviation =	1.02	0.64	0.76	0.93	1.57	1.53	1.61

Fig. 12
f = 25 HZ
a = 0.140 g
LT

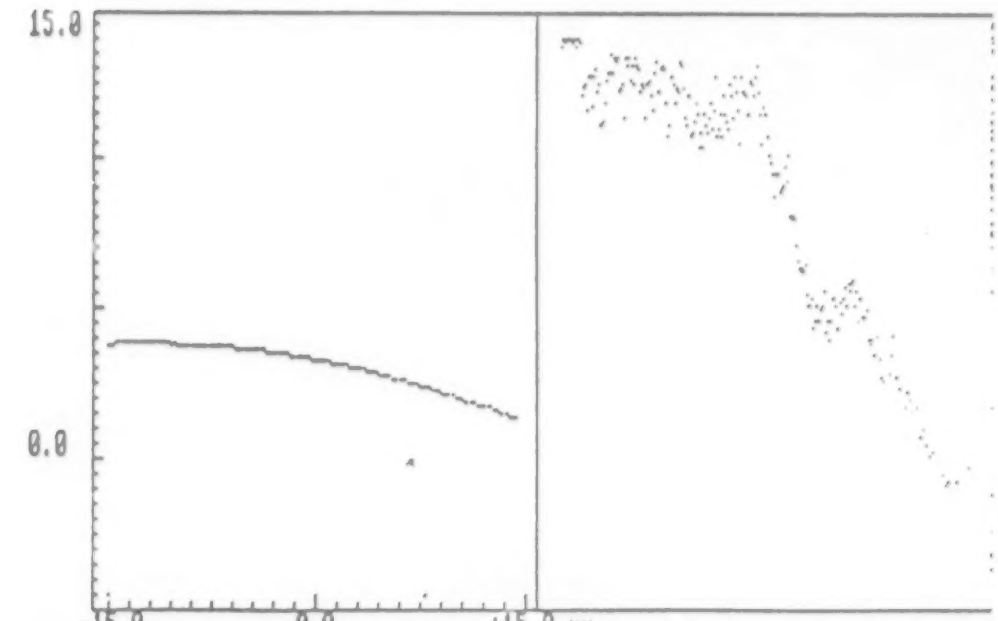

Average =	2179.33	2165.00	2119.18	2047.58	1941.81	1812.42	1656.73
Deviation =	1.01	0.80	0.77	0.84	1.55	1.63	1.74

Fig. 13
f = 50 HZ
a = 0.128 g
LT

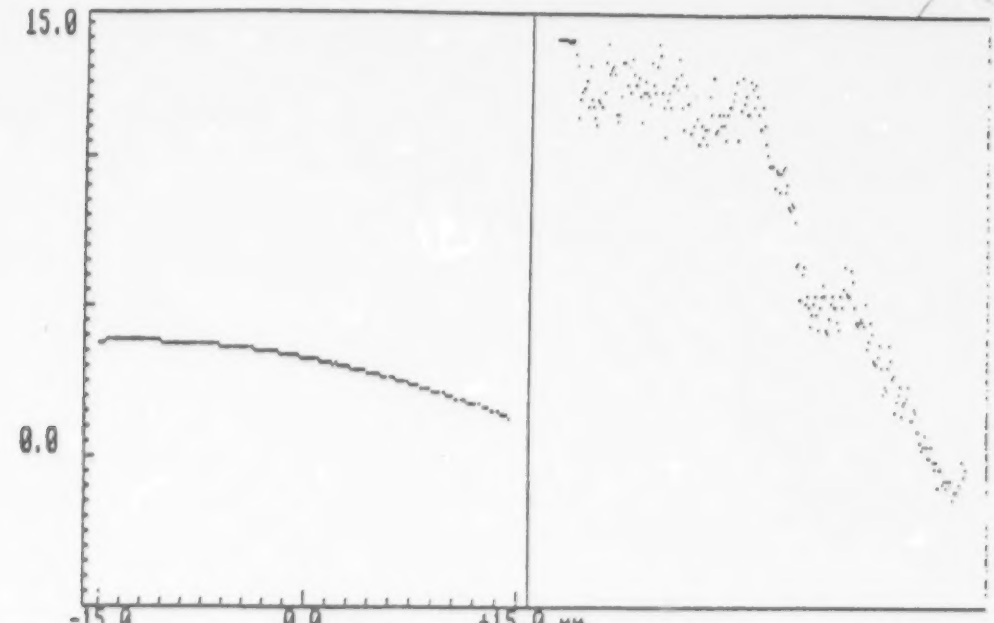

Average	= 2179.90	2164.21	2118.60	2046.83	1940.25	1810.26	1654.53
Deviation	= 1.00	0.83	0.82	1.18	1.28	1.87	1.58

->_

Fig. 14
f = 50 HZ
a = 1.12 g
LT

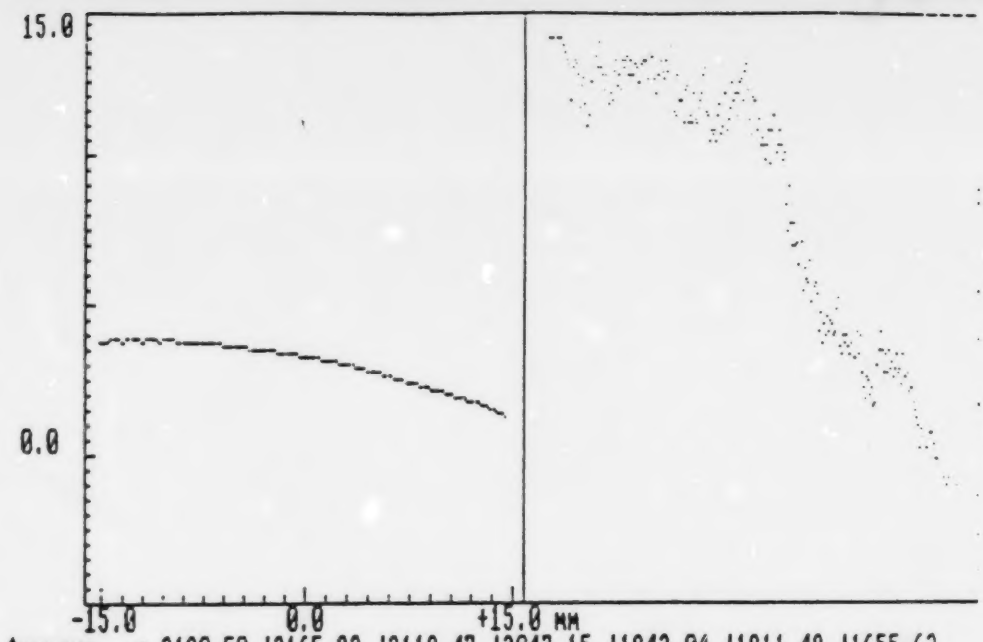

Average =	2180.50	2165.32	2119.47	2047.15	1942.04	1811.48	1655.62
Deviation =	3.75	3.16	3.21	3.86	3.79	3.26	4.20

->_

Fig. 15
f = 50 HZ
a = 2.0 g
LG

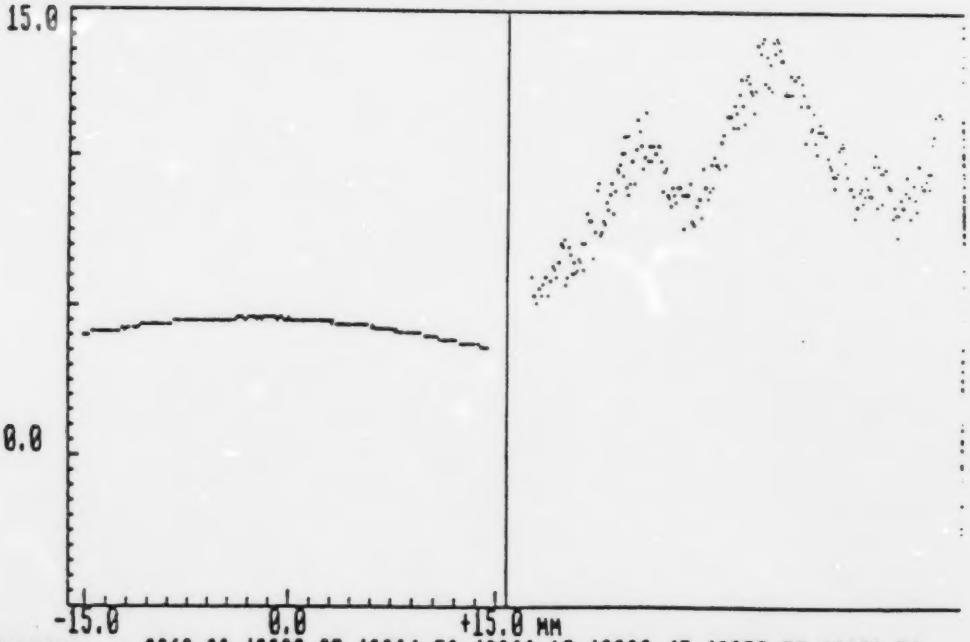

Average =	2268.88	2332.87	2364.58	2366.10	2333.45	2270.77	2191.54
Deviation =	3.76	3.35	2.89	2.14	2.36	2.46	2.73

->_

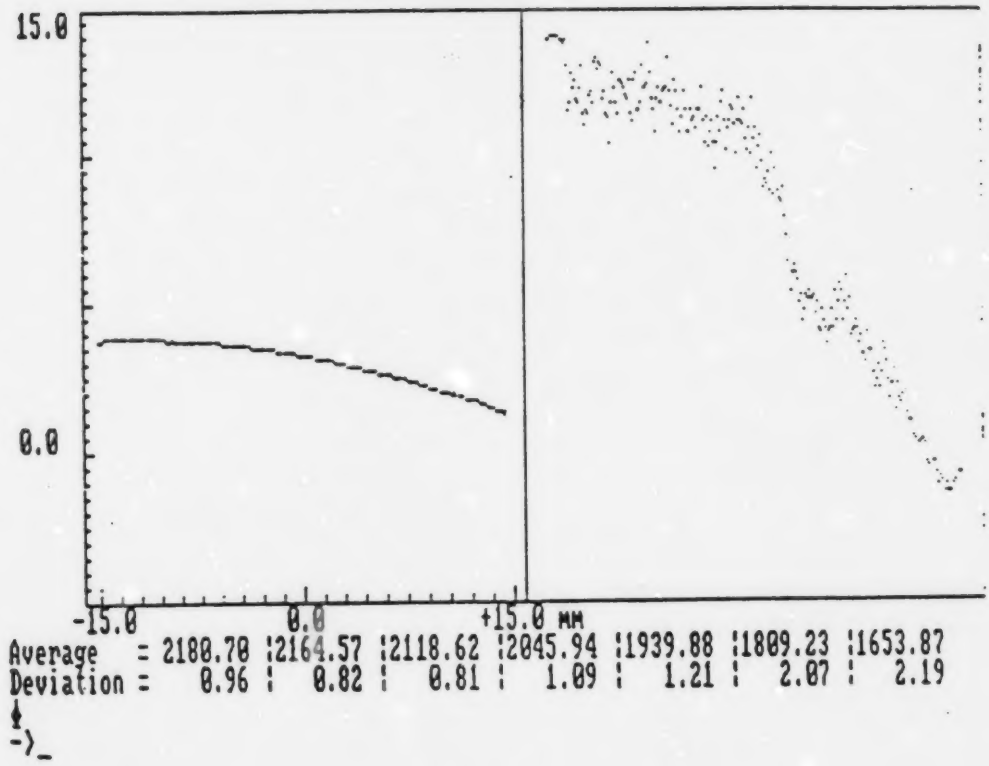

Fig. 16 Typical signal shape for SMC

Fig. 17
LG
f = 75 HZ
a = 3.15 g

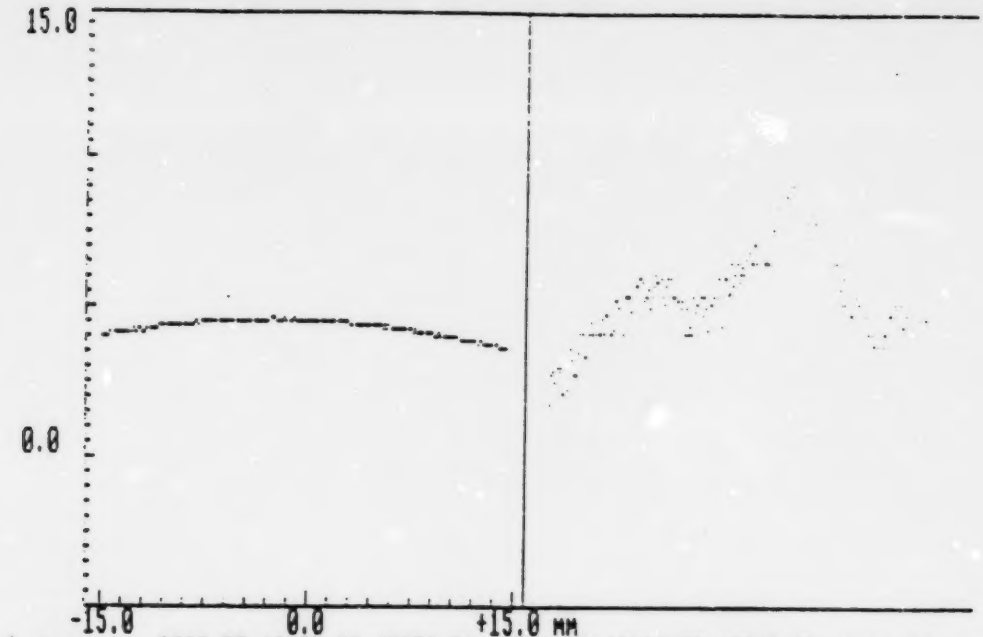

Average = 2268.57 ¦2329.86 ¦2356.90 ¦2361.99 ¦2327.79 ¦2269.59 ¦2191.50
Deviation = 5.56 ¦ 3.97 ¦ 4.03 ¦ 3.08 ¦ 3.09 ¦ 3.05 ¦ 3.07

Fig. 18
LT
f = 150 HZ
a = 2.08 g

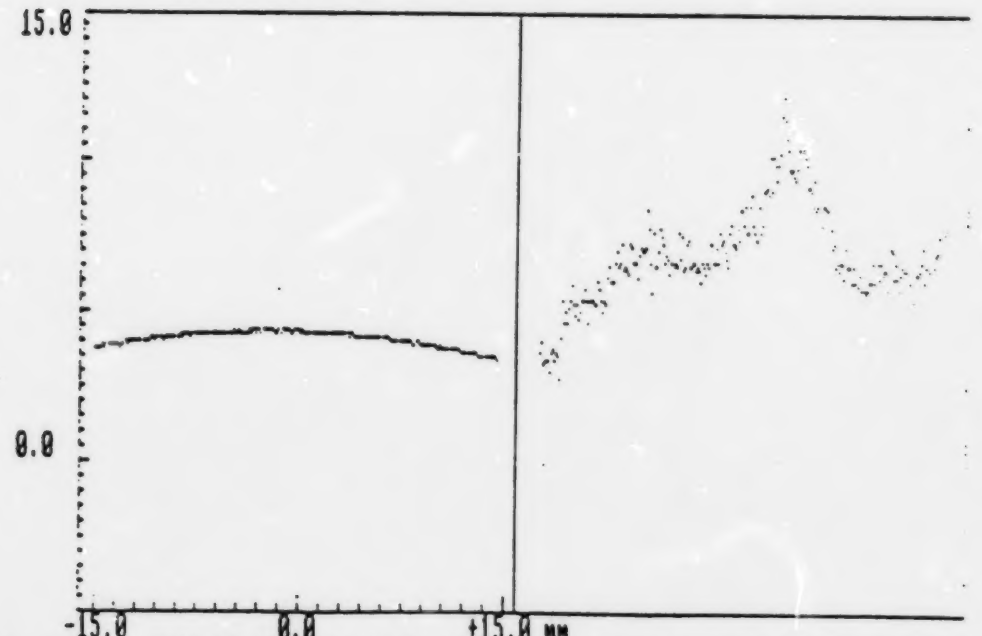

Average = 2210.97 ¦2270.00 ¦2304.15 ¦2307.17 ¦2274.49 ¦2220.02 ¦2137.05
Deviation = 5.81 ¦ 3.47 ¦ 4.80 ¦ 3.07 ¦ 2.64 ¦ 2.92 ¦ 3.31

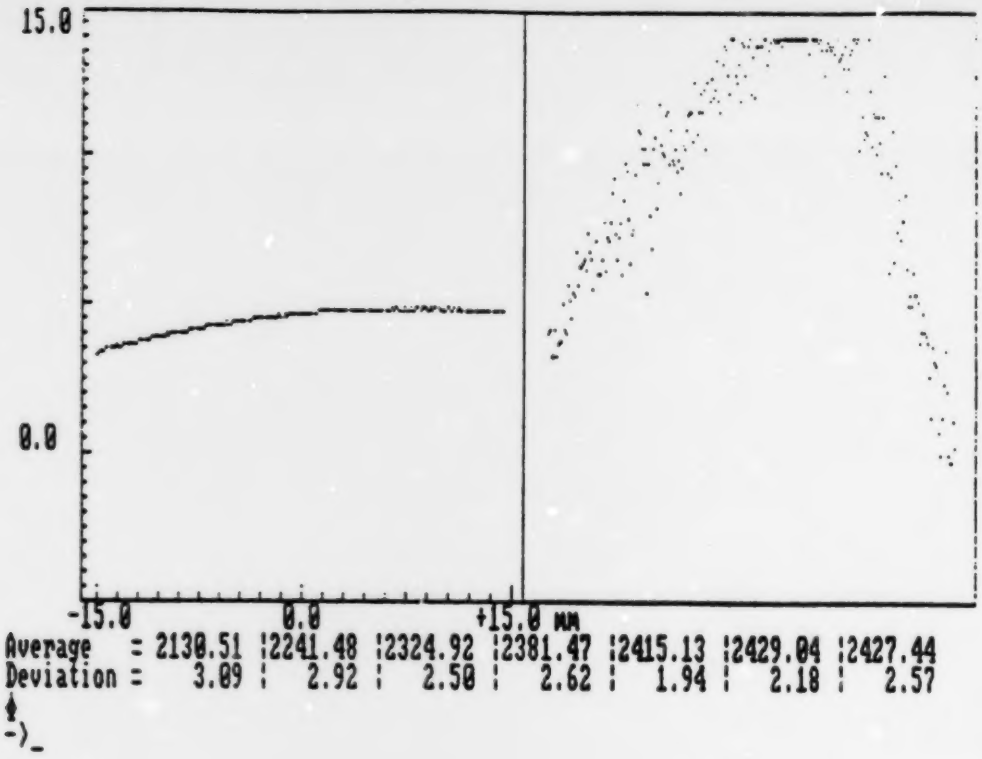

Fig. 19
SMC

Average =	2130.51	2241.48	2324.92	2381.47	2415.13	2429.04	2427.44
Deviation =	3.09	2.92	2.50	2.62	1.94	2.18	2.57

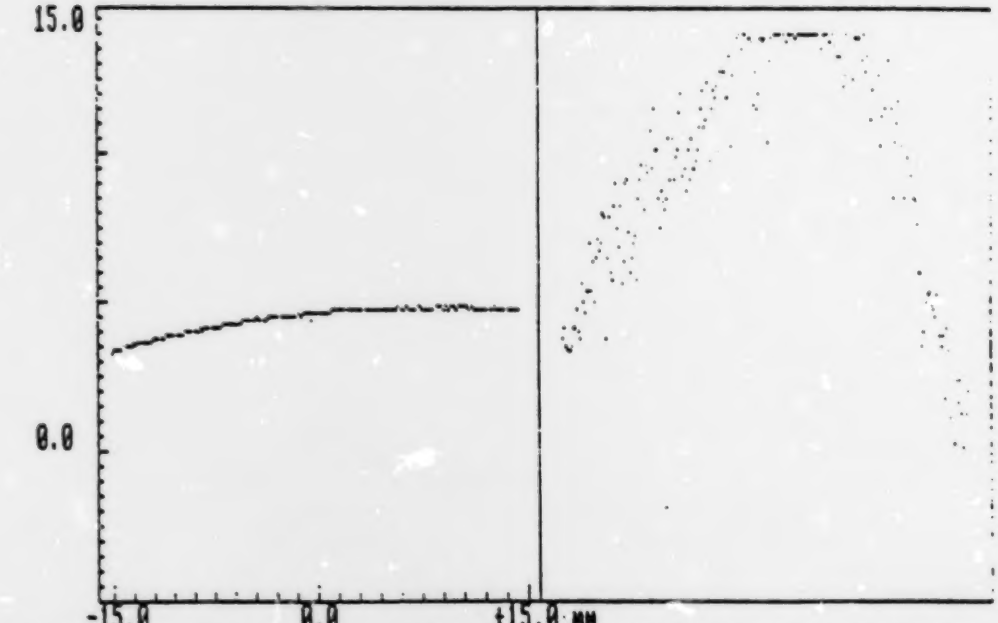

Fig. 20
f = 5 HZ
a = 0.326 g

Average =	2129.91	2241.13	2324.62	2381.98	2415.23	2428.74	2427.49
Deviation =	3.46	2.86	2.73	2.35	2.36	2.39	2.80

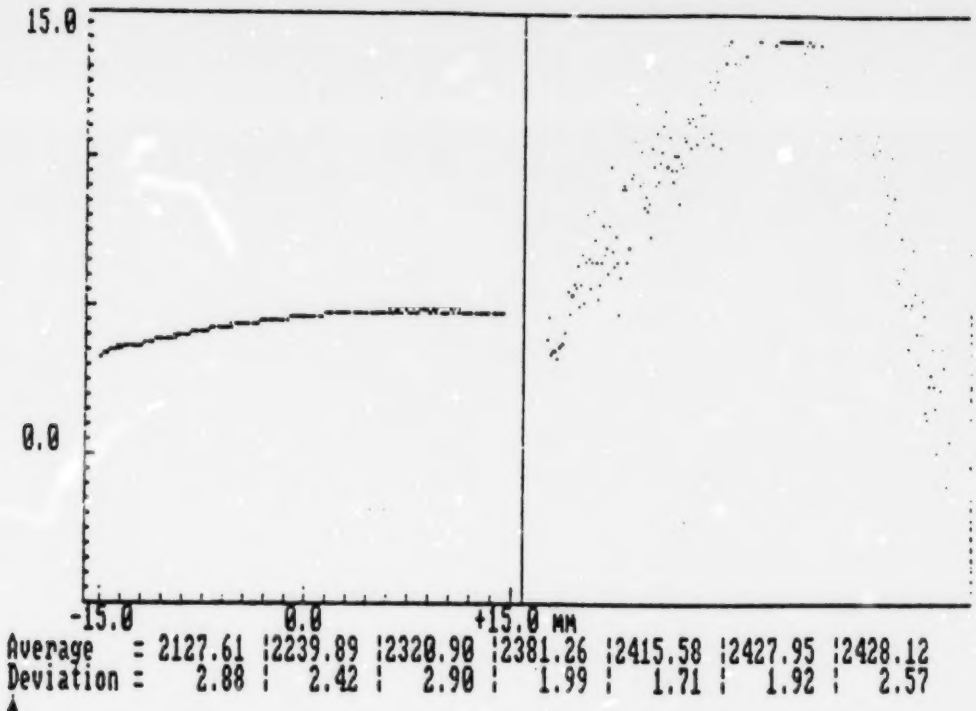

Fig. 21
f = 20 HZ
a = 0.116 g
VR

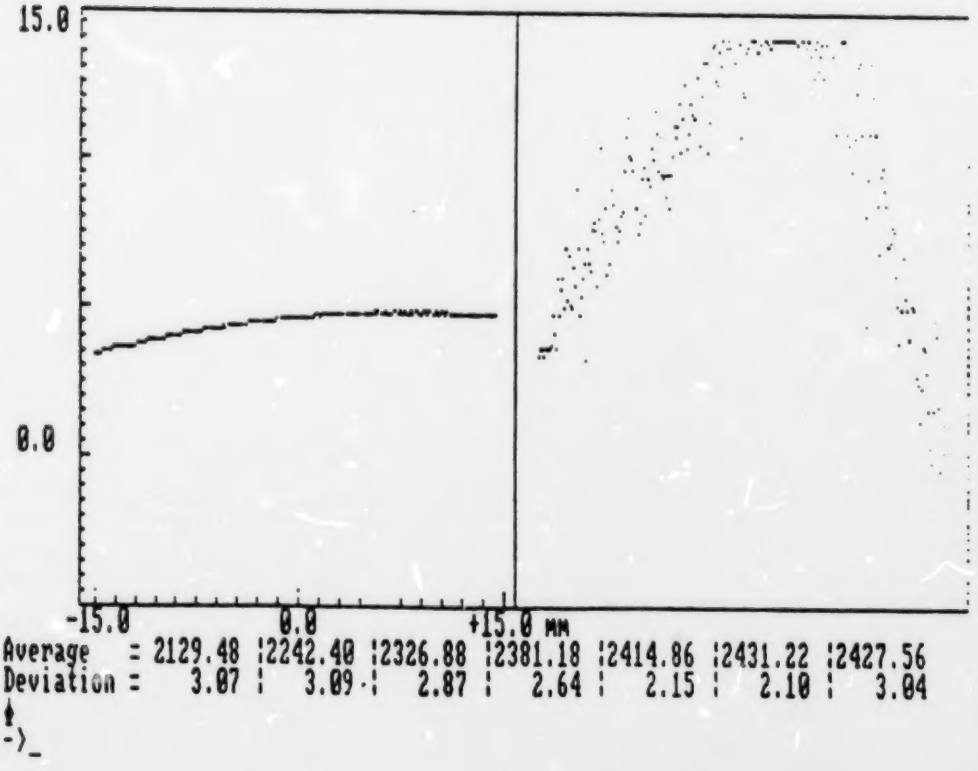

Fig. 22
f = 50 HZ
a = 0.130 g
VR

Fig. 23
f = 50 HZ
a = 0.818 g
VR

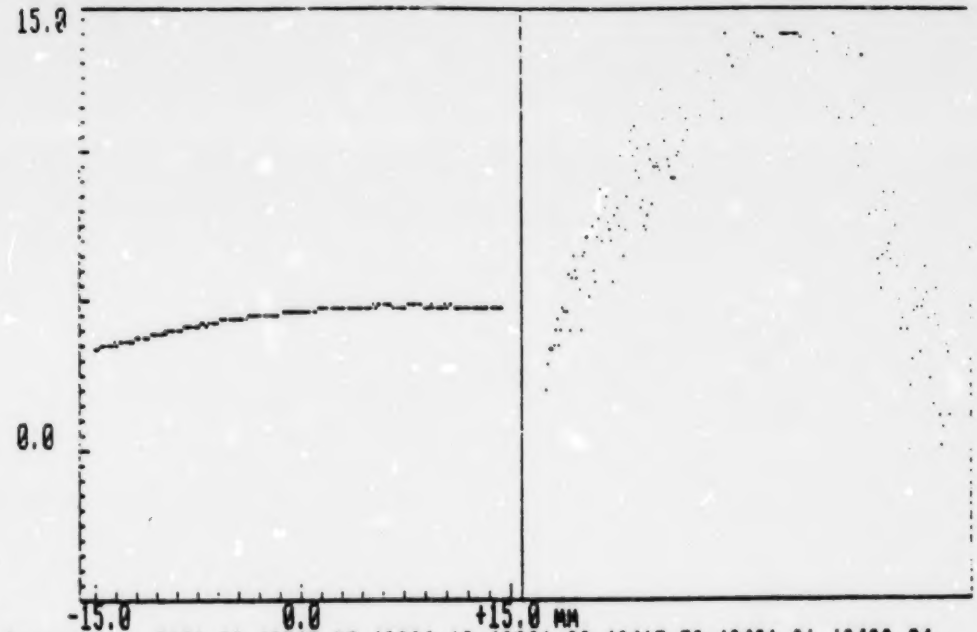

Average =	2131.33	2242.90	2326.12	2381.98	2415.73	2431.91	2428.04
Deviation =	5.34	4.77	4.67	4.97	4.30	4.31	4.96

->_

Fig. 24
f = 100 HZ
a = 0.809 g
VR

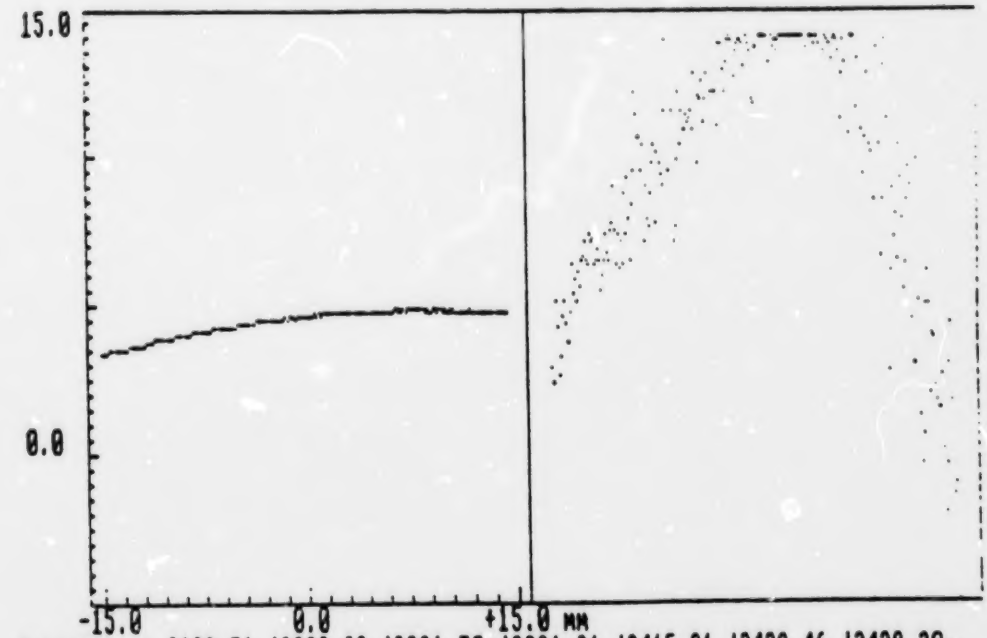

Average =	2128.51	2239.99	2321.70	2381.81	2415.91	2428.46	2428.30
Deviation =	5.86	4.60	5.92	4.23	3.07	4.20	3.68

->_

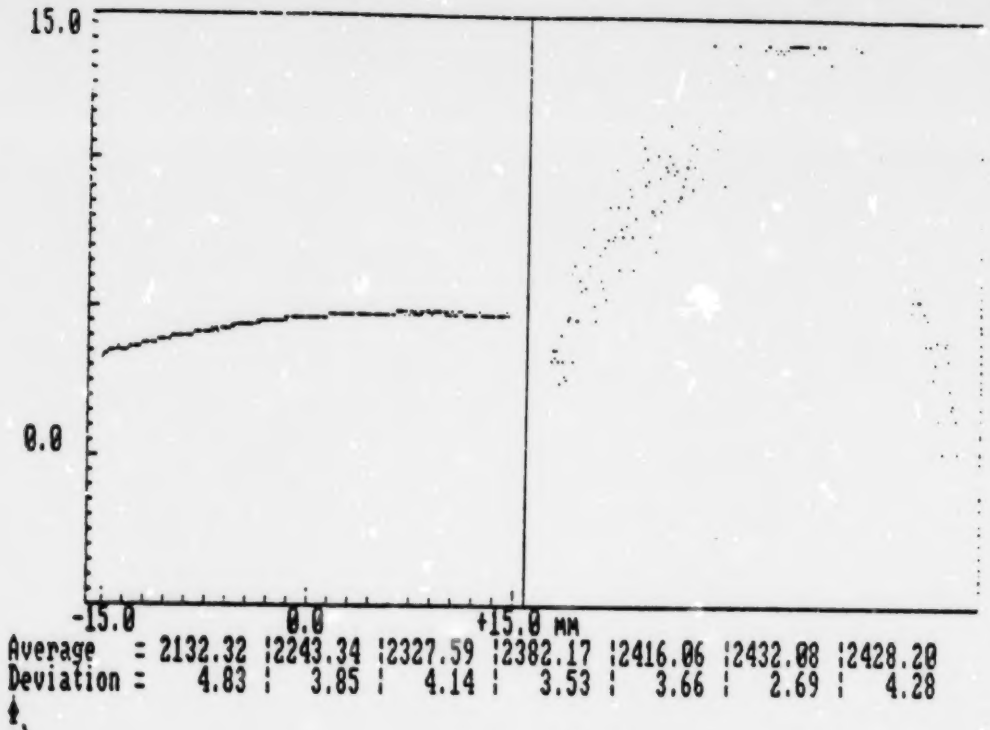

Fig. 25
f = 5 HZ
a = 0.515 g
VR

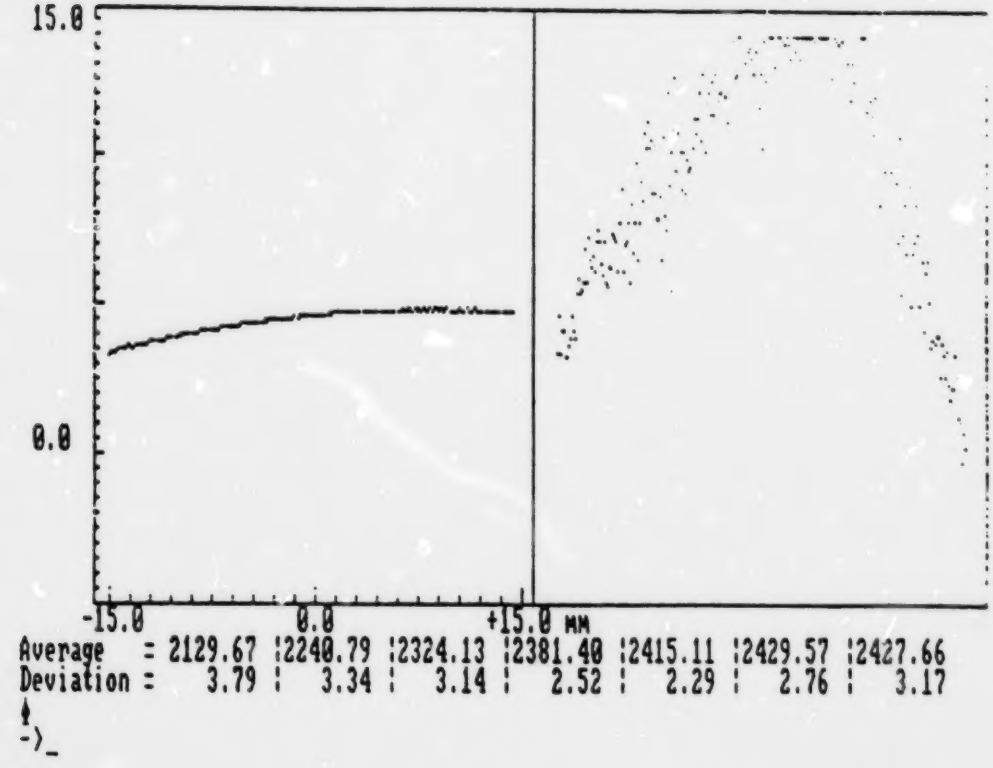

Fig. 26
f = 30 HZ
a = 0.501 g
VR

Fig. 27
f = 30 HZ
a = 1.024
VR

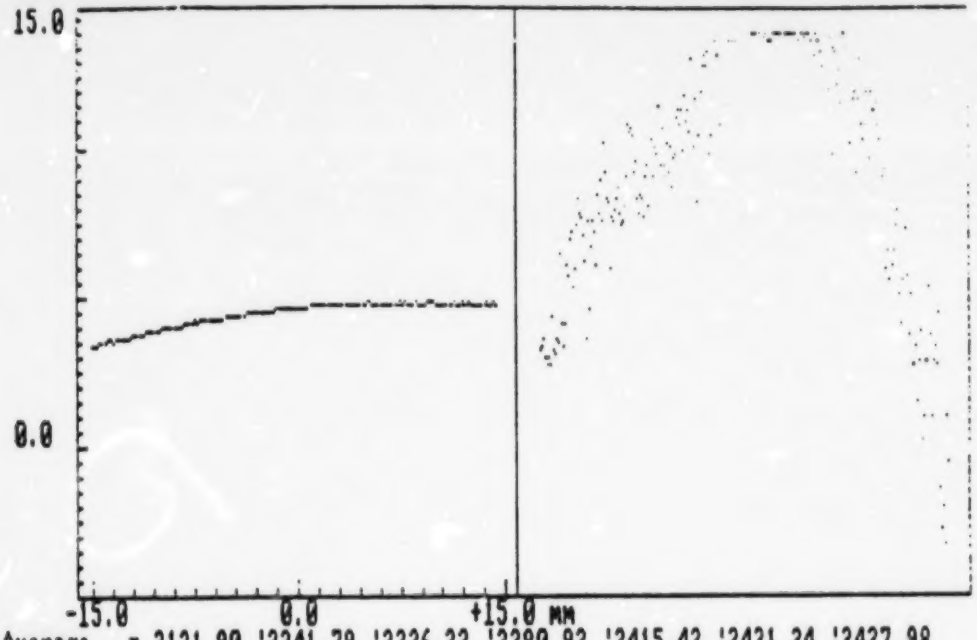

Average =	2131.80	2241.79	2326.22	2380.92	2415.42	2431.24	2427.98
Deviation =	4.06	3.88	3.92	3.23	2.52	3.07	3.81

->_

Fig. 28
f = 50 HZ
a = 1.015 g
VR

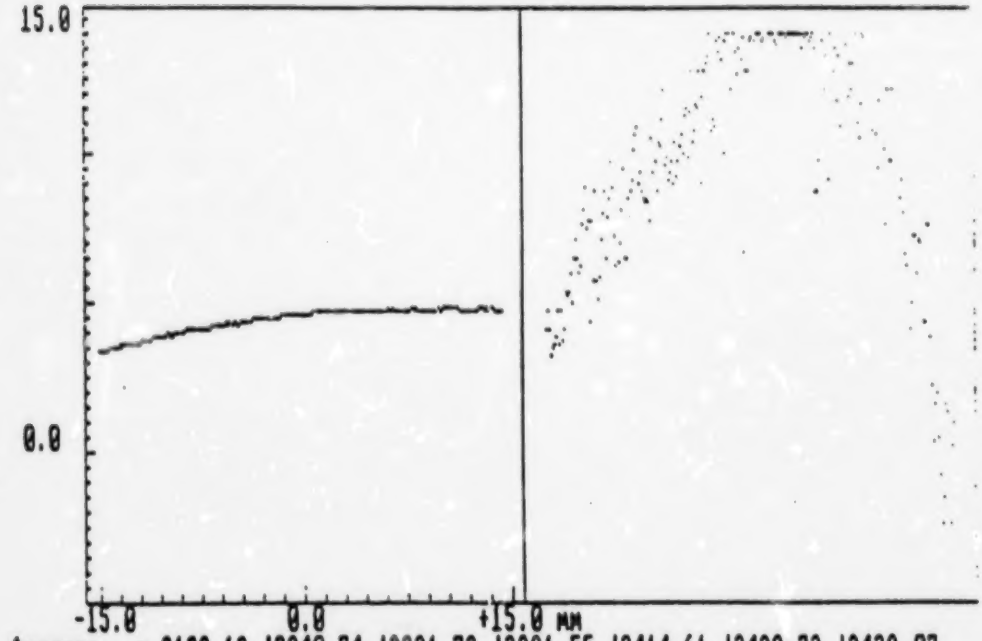

Average =	2129.13	2240.74	2321.73	2381.55	2414.61	2428.73	2429.07
Deviation =	6.96	6.17	6.42	5.44	4.47	5.55	5.85

->_

Fig. 29
f = 100 HZ
a = 1.010 g
VR

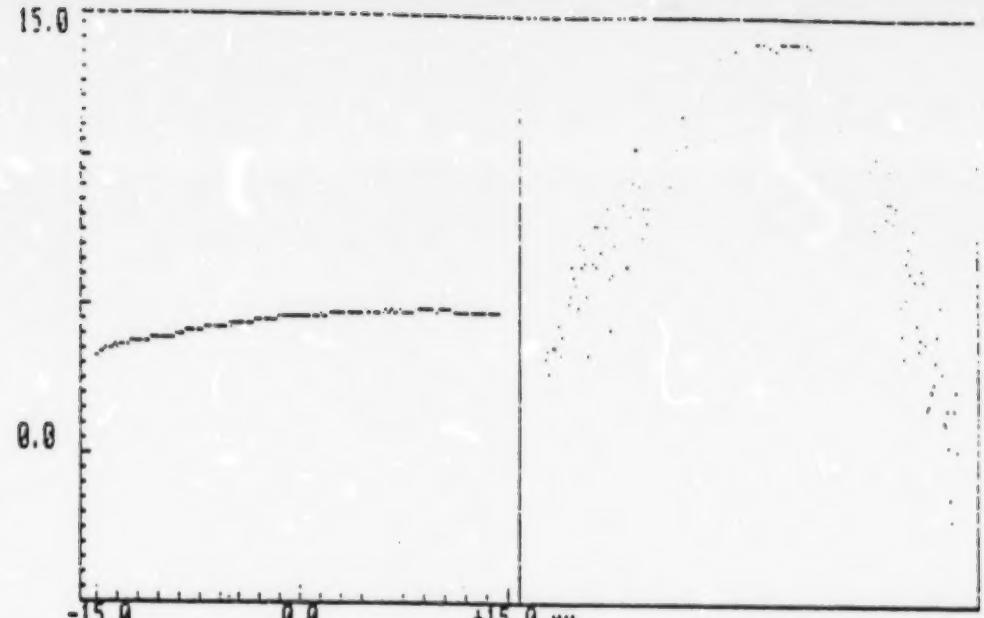

Average =	2131.10	2242.67	2325.25	2382.21	2415.99	2430.22	2427.83
Deviation =	6.84	6.55	6.17	4.57	4.50	5.02	5.14

-)_

Fig. 30
f = 150 HZ
a = 1.024 g
VR

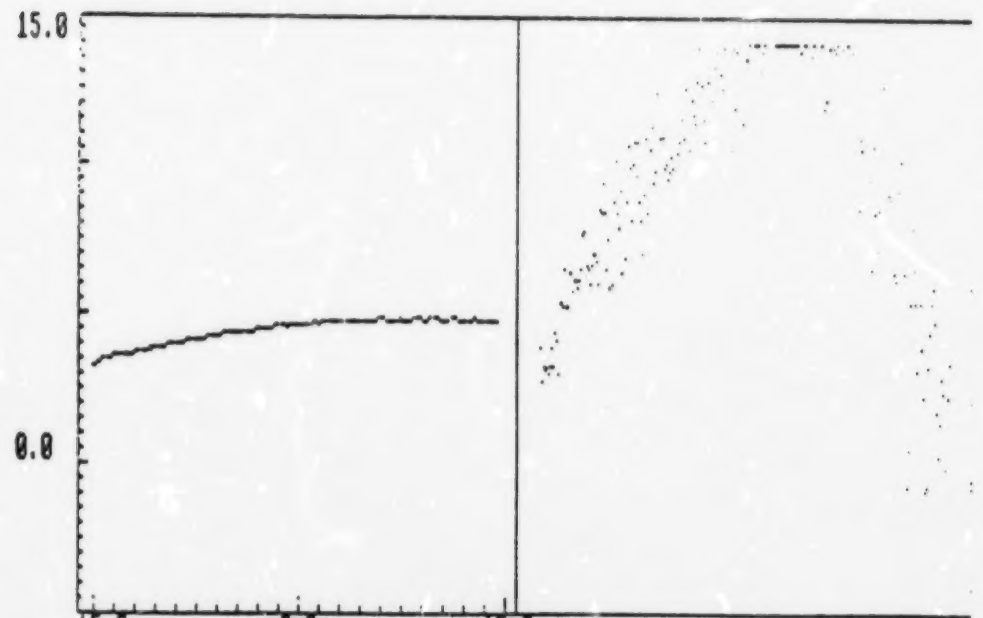

Average =	2129.20	2240.30	2321.64	2380.32	2415.82	2429.70	2429.41
Deviation =	8.13	6.78	6.38	6.76	4.79	4.02	4.90

-)_

Fig. 31

2 T = 0.14s
= 2.10 g
LG

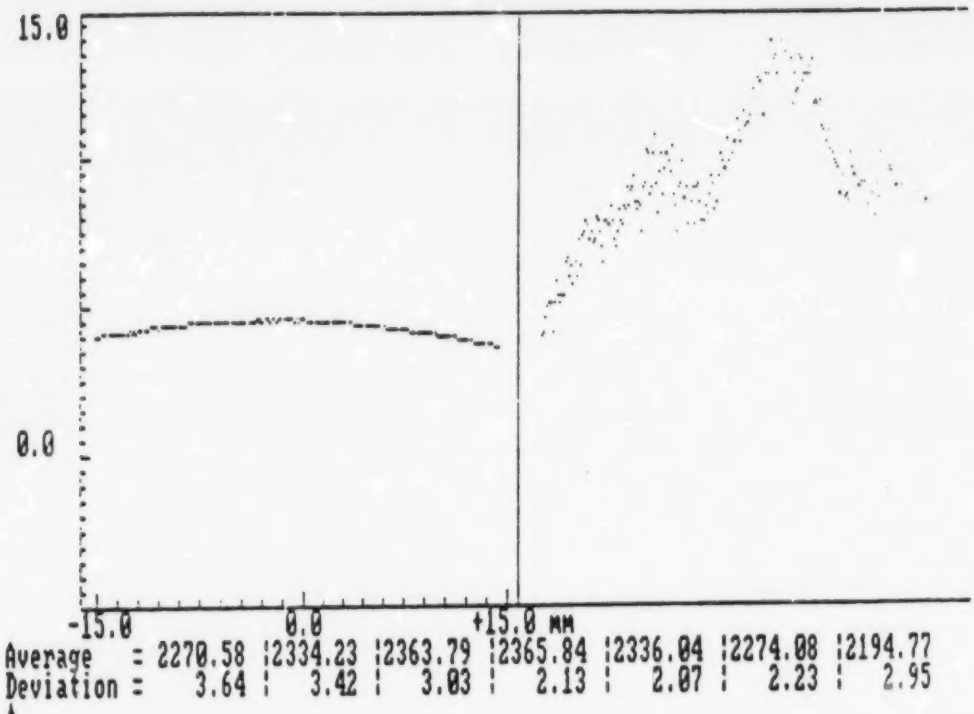

Average =	2270.58	2334.23	2363.79	2365.84	2336.04	2274.08	2194.77
Deviation =	3.64	3.42	3.03	2.13	2.07	2.23	2.95

-)_

g. 32

me conditions like
escribed in fig. 31
but the laser
power is
ltiplied by
66

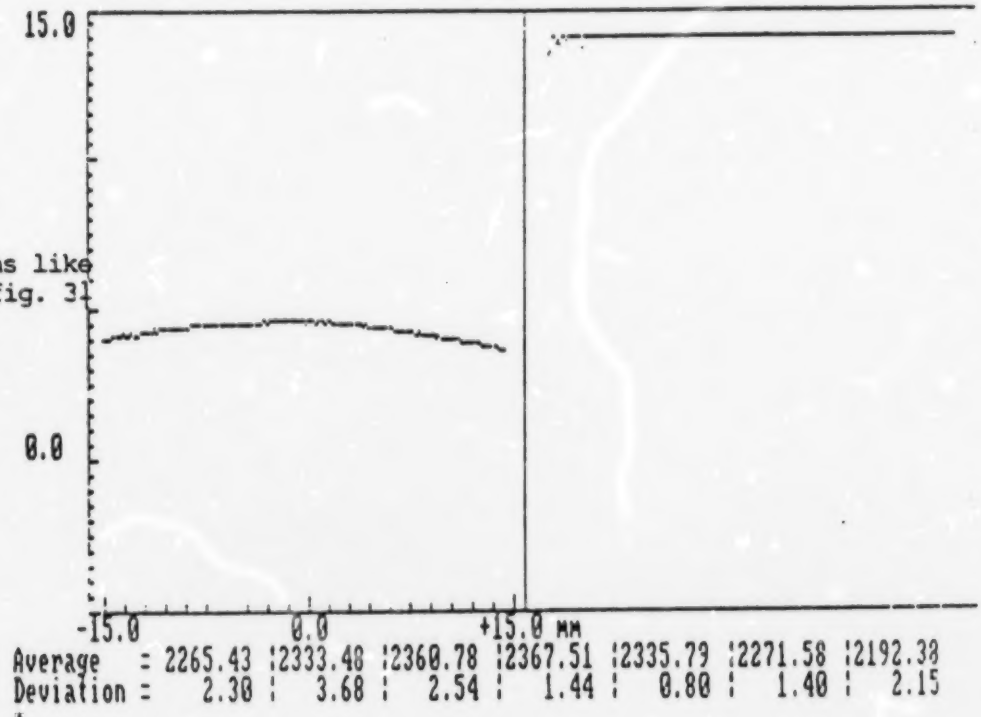

Average =	2265.43	2333.48	2360.78	2367.51	2335.79	2271.58	2192.38
Deviation =	2.30	3.68	2.54	1.44	0.80	1.40	2.15

-)_

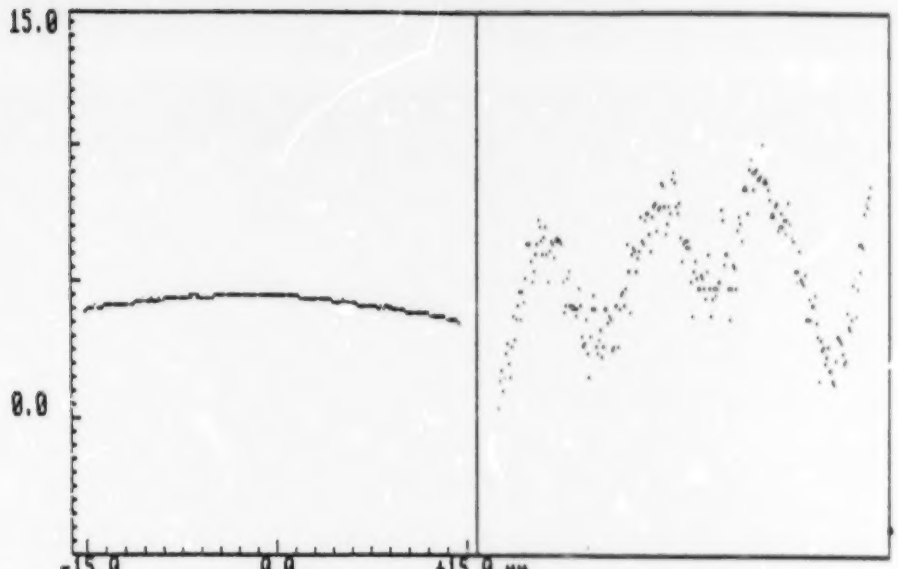

Fig. 33
0.5T = 10ms
= 5.05 g

Average =	2251.98	2316.79	2344.68	2350.51	2319.38	2258.94	2178.47
Deviation =	5.52	4.96	5.35	3.58	4.15	3.67	4.10

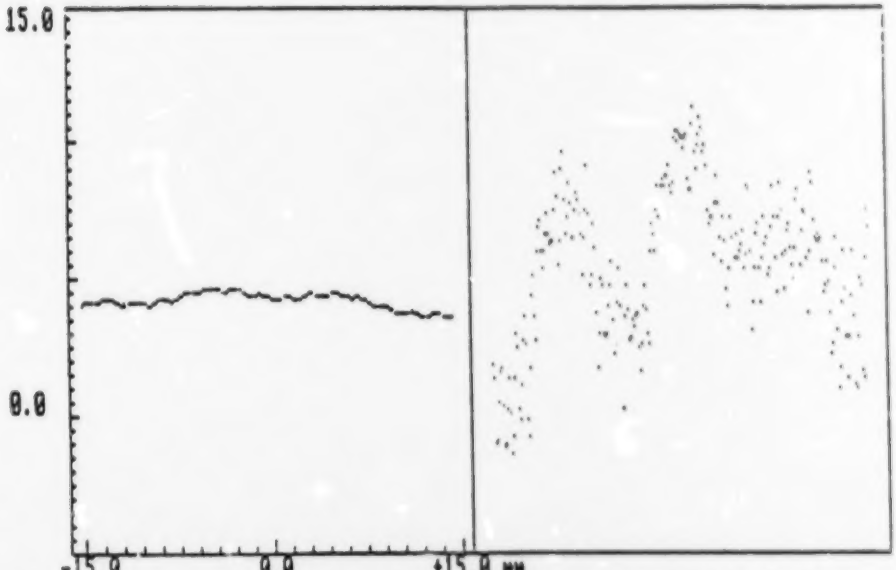

Fig. 34
0.5T = 10ms
= 5.02 g

Average =	2251.35	2313.29	2340.78	2343.44	2312.04	2252.33	2175.61
Deviation =	40.97	21.15	31.14	33.56	38.71	34.31	17.85

Fig. 35
T = 10ms
= 5.03 g
VR

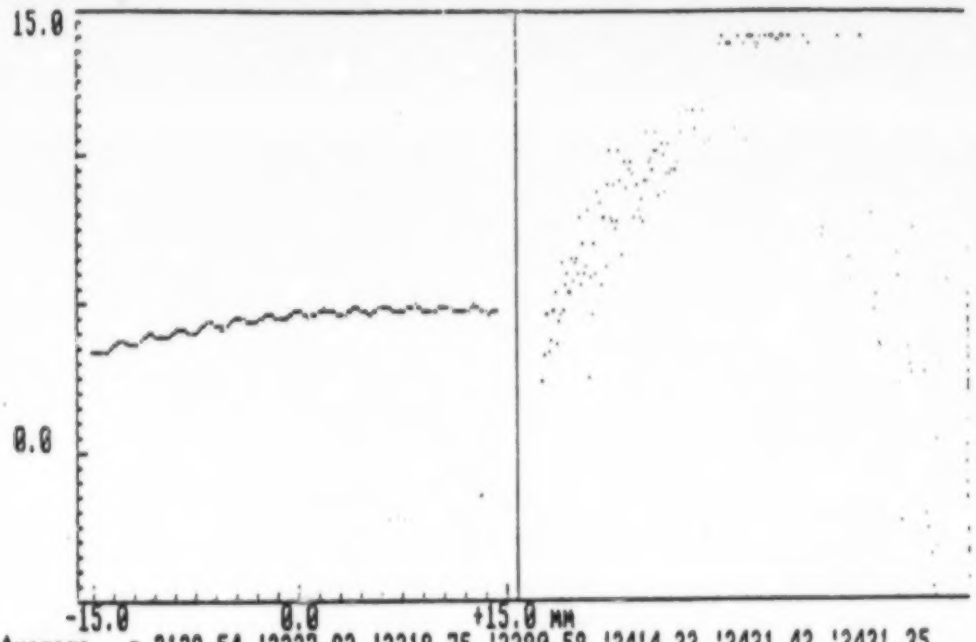

Average	= 2129.54	2237.83	2319.75	2380.59	2414.23	2431.42	2431.35
Deviation	= 22.78	22.76	21.10	19.27	17.84	19.98	20.76

->_

Fig. 36
T = 30ms
a = 2.10 g
V

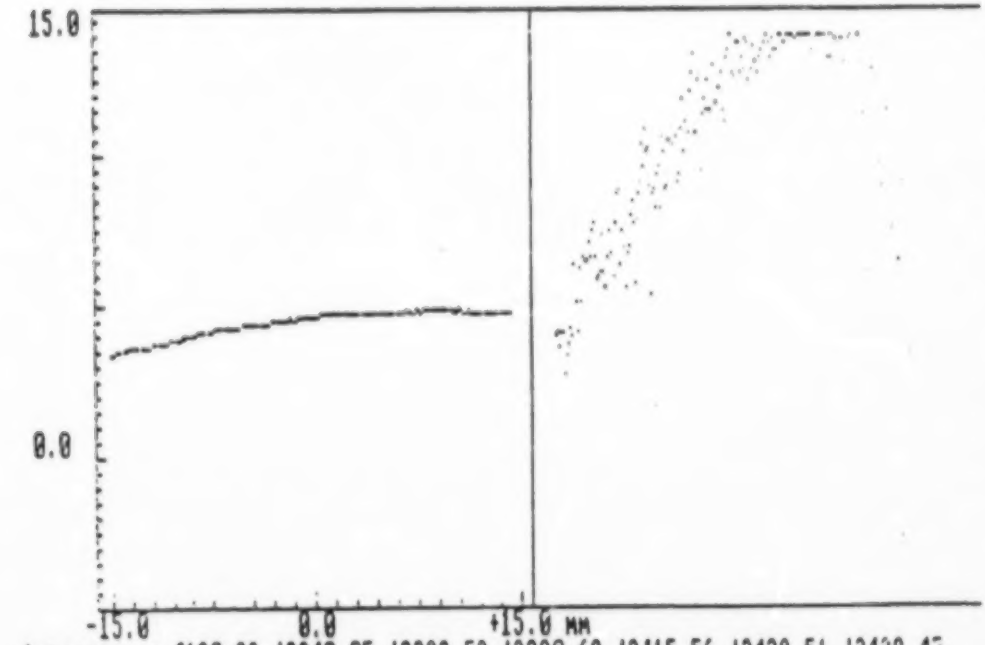

Average	= 2130.38	2240.05	2322.52	2380.69	2415.56	2428.51	2428.47
Deviation	= 7.51	6.62	6.79	5.35	4.93	5.25	5.79

->_

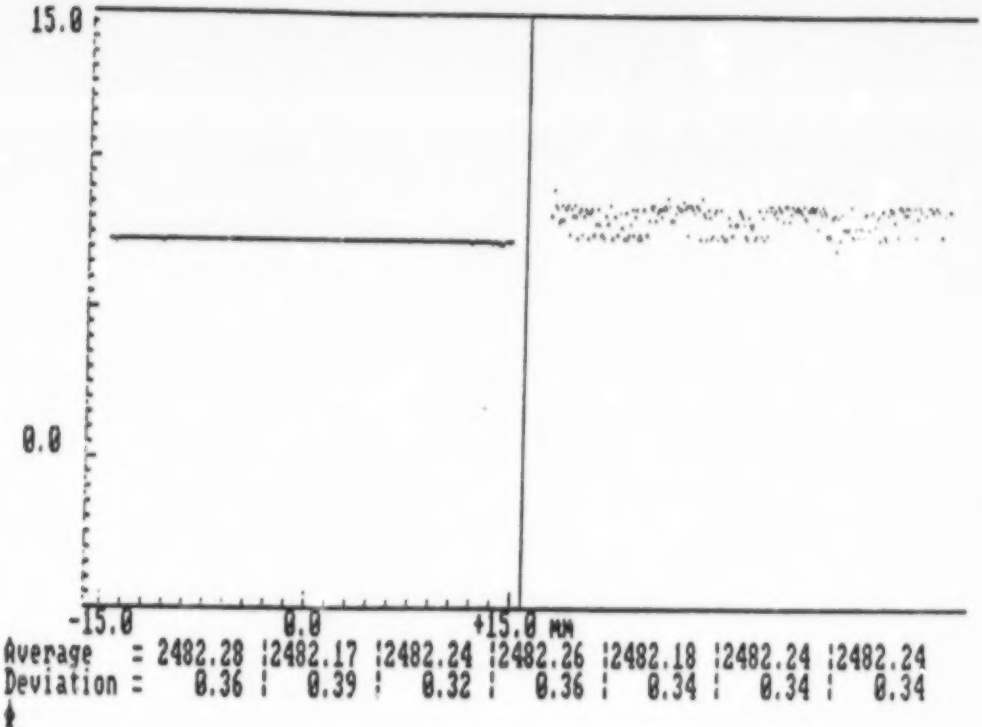

Fig. 37
t_d = 1°C

Salvo is stopped because of the temperature requirements

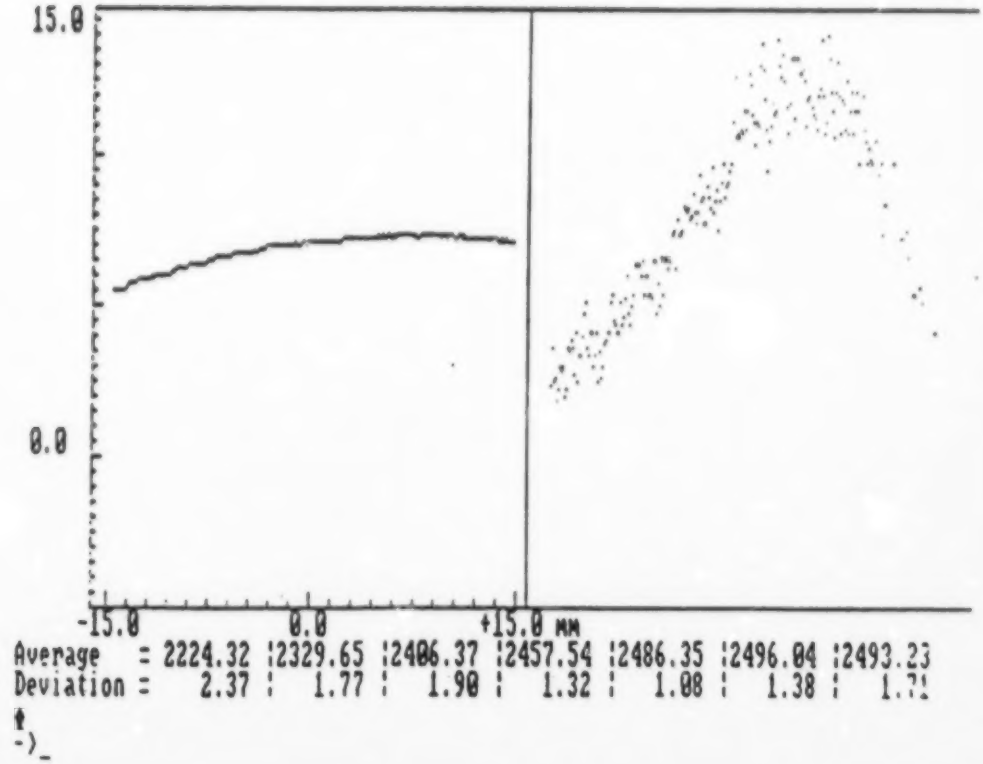

Fig. 38
t_d = 8°C

Fig. 39

t_d = 13°C

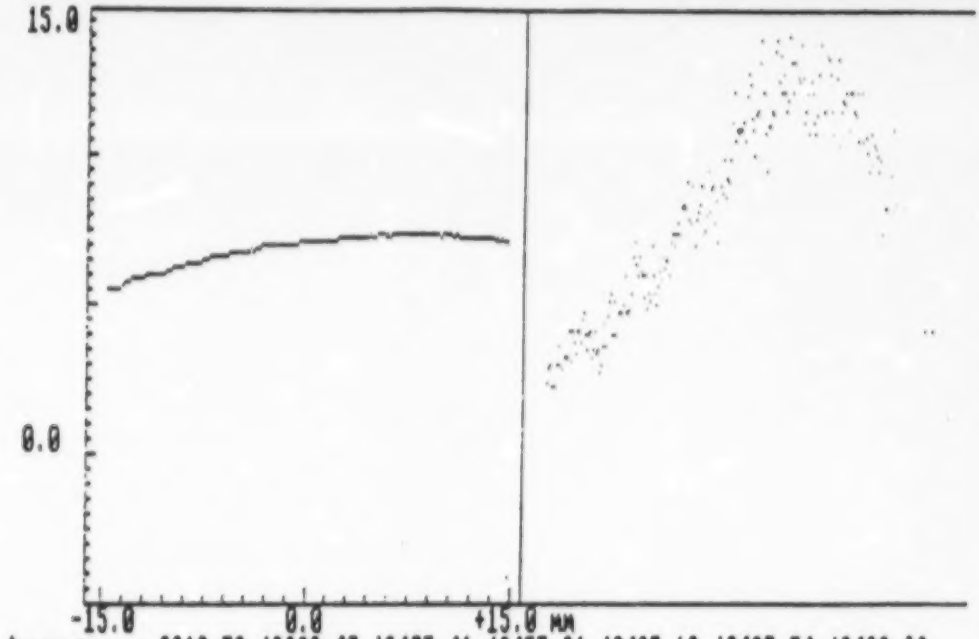

Average =	2219.79	2328.48	2405.41	2457.91	2487.13	2497.54	2493.98
Deviation =	1.94	1.91	1.79	1.37	0.77	1.10	1.69

Fig. 40

t_d = 17°C

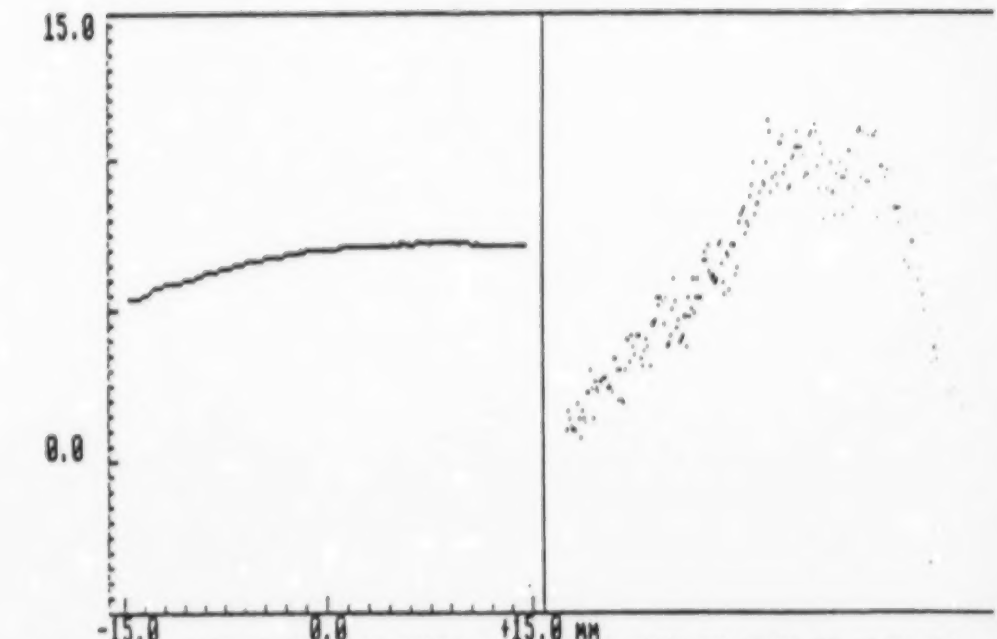

Average =	2195.39	2304.15	2384.51	2438.99	2471.37	2483.50	2481.02
Deviation =	2.36	2.28	2.01	1.37	1.52	1.28	1.65

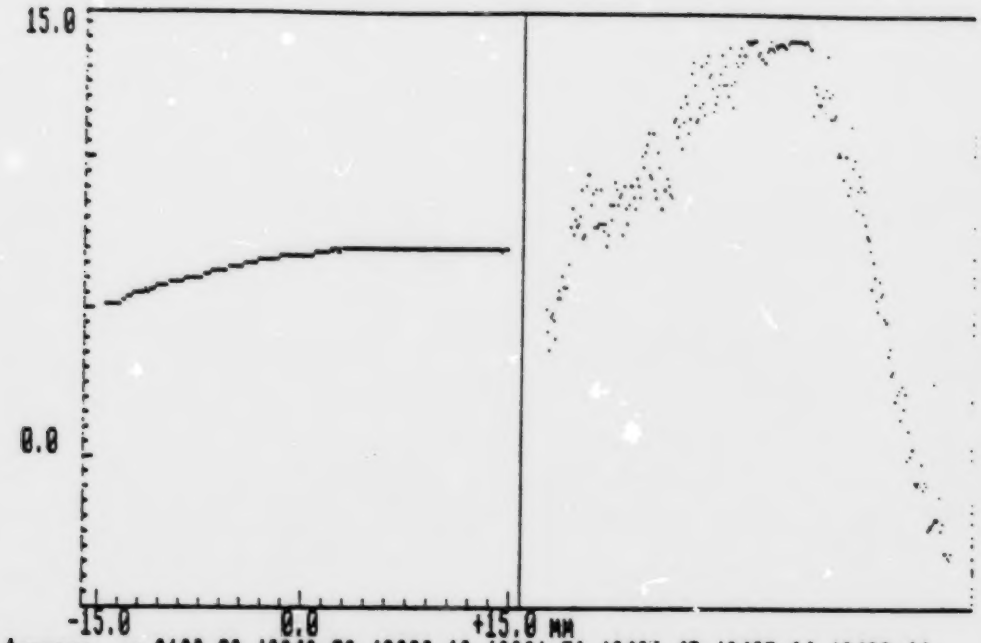

Fig. 41

t_d = 33°C

r = 77%

Average =	2139.02	2249.08	2333.13	2391.56	2426.45	2437.64	2433.66
Deviation =	1.60	1.38	1.84	0.78	1.06	1.34	3.05

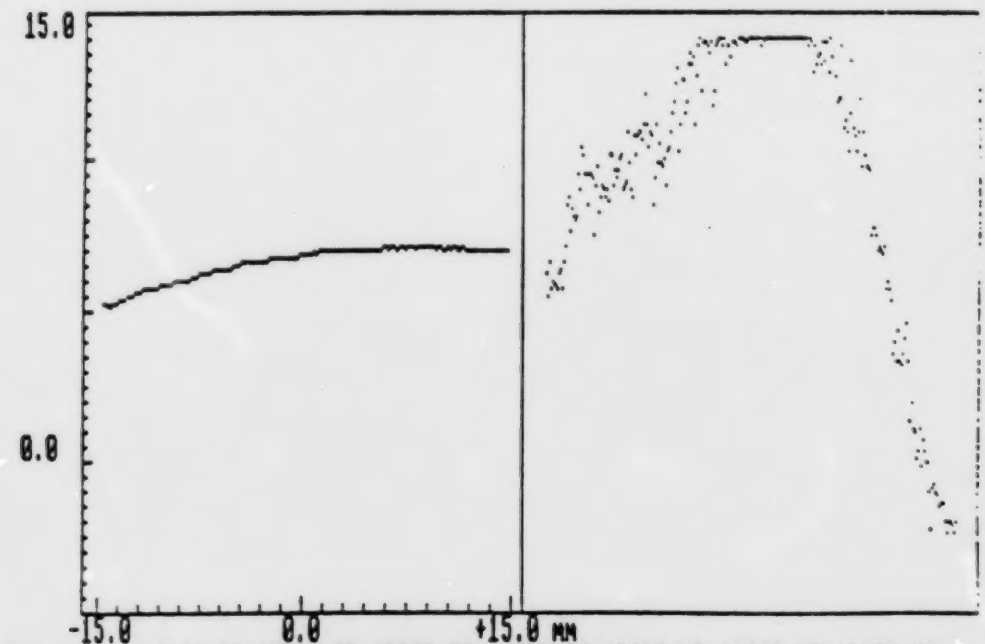

Fig. 42

t_d = 28°C

r = 78%

Average =	2163.93	2263.45	2349.98	2403.30	2437.59	2448.90	2449.53
Deviation =	1.32	1.22	1.69	0.71	1.09	1.79	2.40

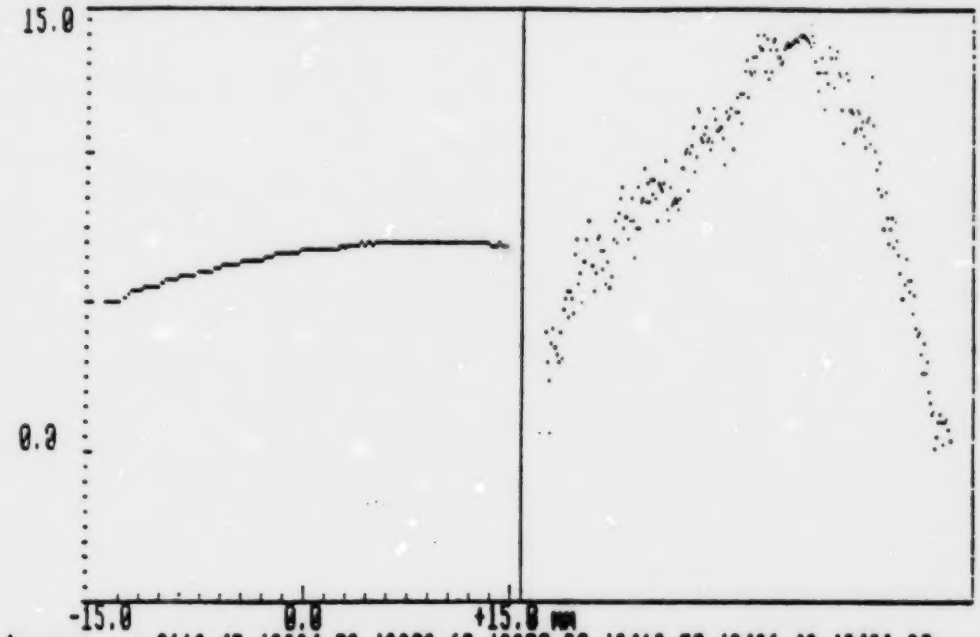

Average =	2112.47	2224.82	2308.60	2370.90	2412.70	2426.49	2426.20
Deviation =	1.68	1.99	1.49	1.43	1.01	1.13	1.82

Fig. 43

$t_d = 40^{\circ}C$

r = 76%

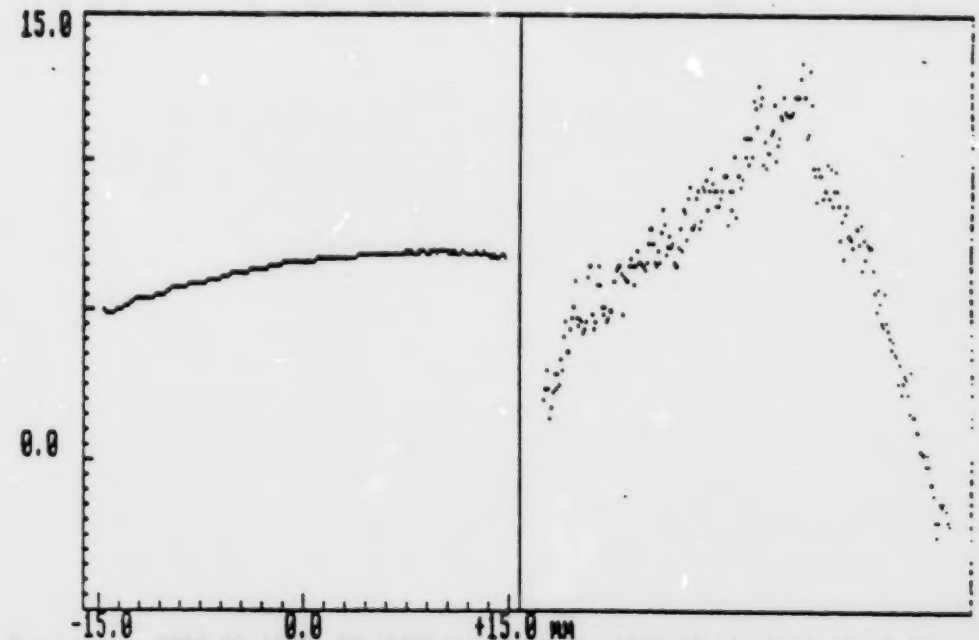

Average =	2095.43	2285.20	2298.44	2356.77	2395.93	2412.62	2412.48
Deviation =	2.01	2.30	1.86	1.83	1.66	2.27	2.59

Fig. 44

$t_d = 44^{\circ}C$

r = 78%

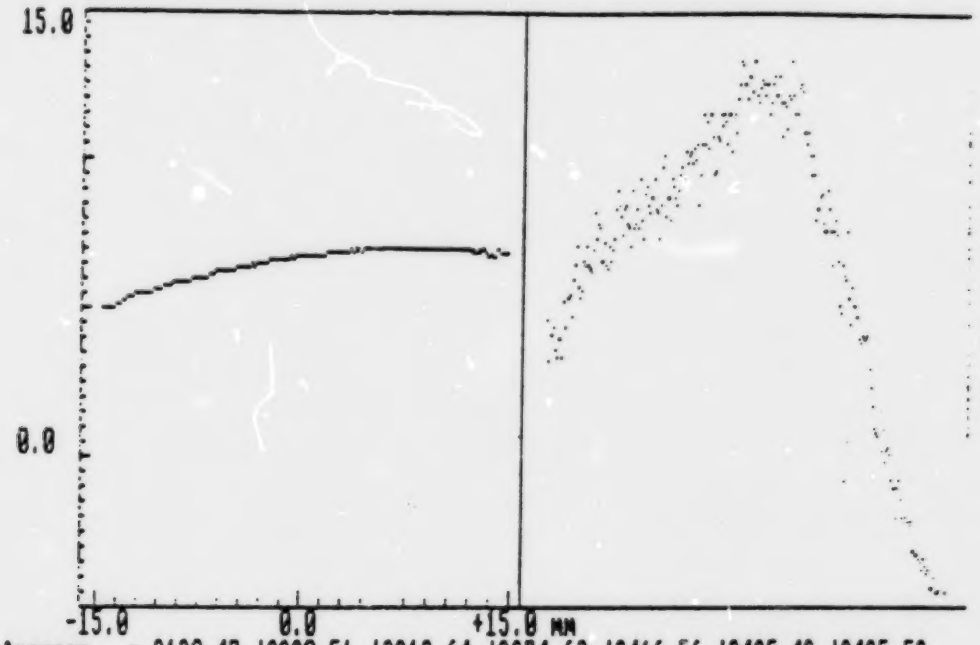

Fig. 45

t_d = 40°C

r = 88%

Average = 2120.47 | 2230.51 | 2318.64 | 2374.69 | 2416.56 | 2425.49 | 2425.52
Deviation = 1.66 | 1.95 | 2.15 | 1.60 | 1.35 | 1.87 | 3.94

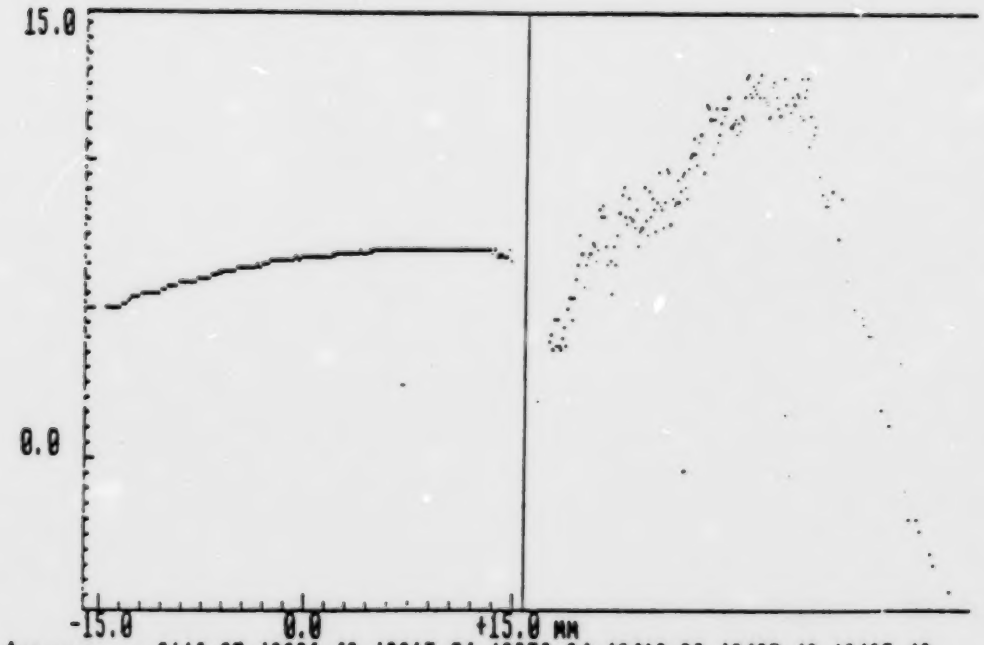

Fig. 46

t_d = 41°C

r = 90%

Average = 2118.37 | 2226.49 | 2317.04 | 2373.34 | 2413.28 | 2427.49 | 2425.48
Deviation = 1.45 | 1.89 | 1.52 | 1.81 | 1.51 | 2.43 | 3.76

Fig. 47

t_d = 38°C

r = 56%

After being left in t_d = 40°C and

r = 60% during 40 hrs

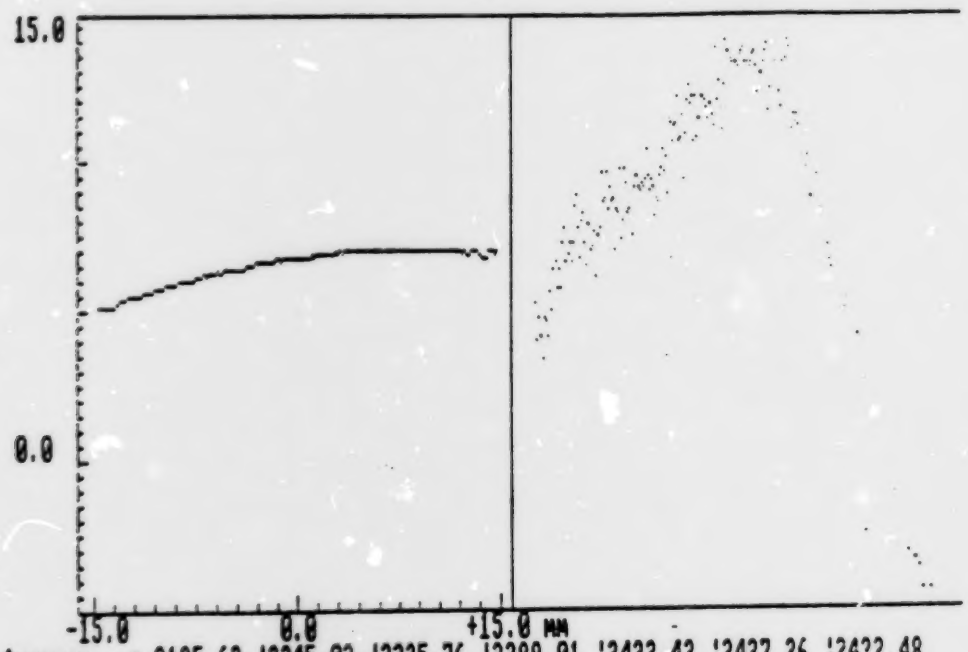

Average =	2135.63	2245.02	2325.76	2389.01	2422.43	2437.26	2432.48
Deviation =	1.94	1.79	1.64	1.48	1.50	2.39	3.73

-)_

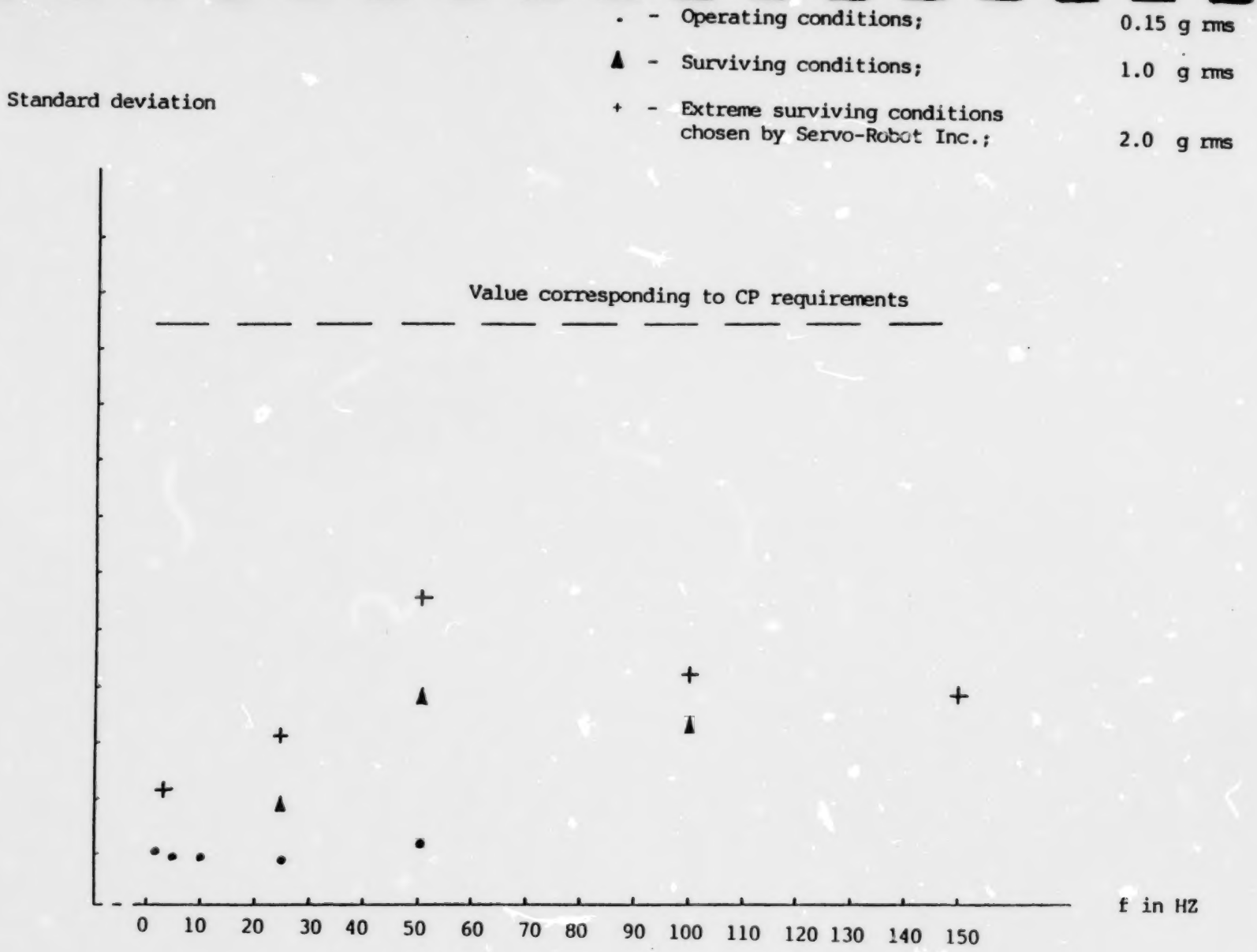
. - Operating conditions; 0.15 g rms
▲ - Surviving conditions; 1.0 g rms
+ - Extreme surviving conditions chosen by Servo-Robot Inc.; 2.0 g rms
Standard deviation
Value corresponding to CP requirements
0 10 20 30 40 50 60 70 80 90 100 110 120 130 140 150
f in HZ

Fig. 48 vibrations - LT direction

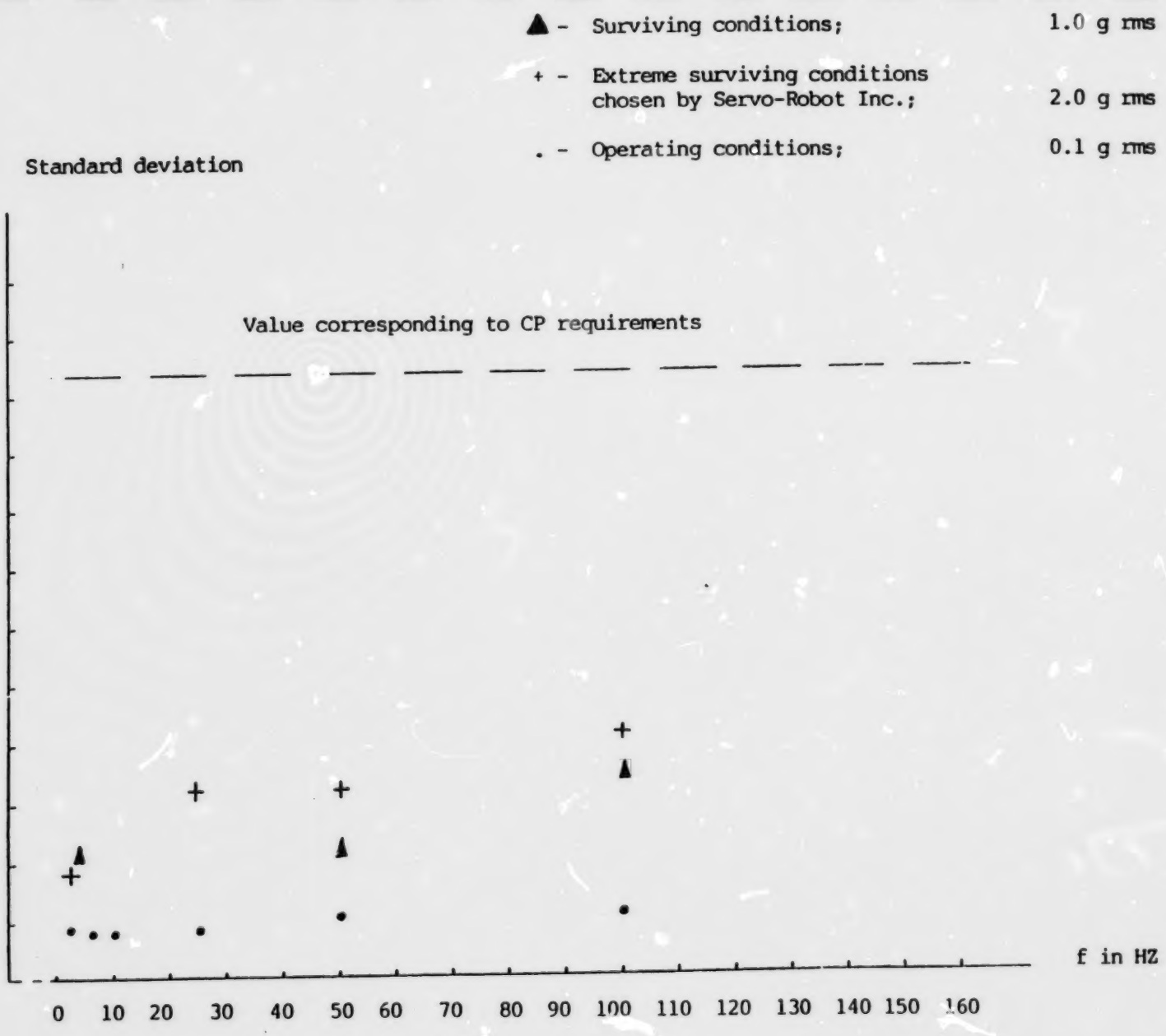
▲ - Surviving conditions; 1.0 g rms
+ - Extreme surviving conditions chosen by Servo-Robot Inc.; 2.0 g rms
. - Operating conditions; 0.1 g rms
Standard deviation
Value corresponding to CP requirements
f in HZ
0 10 20 30 40 50 60 70 80 90 100 110 120 130 140 150 160

Fig. 49 Vibrations - LG direction

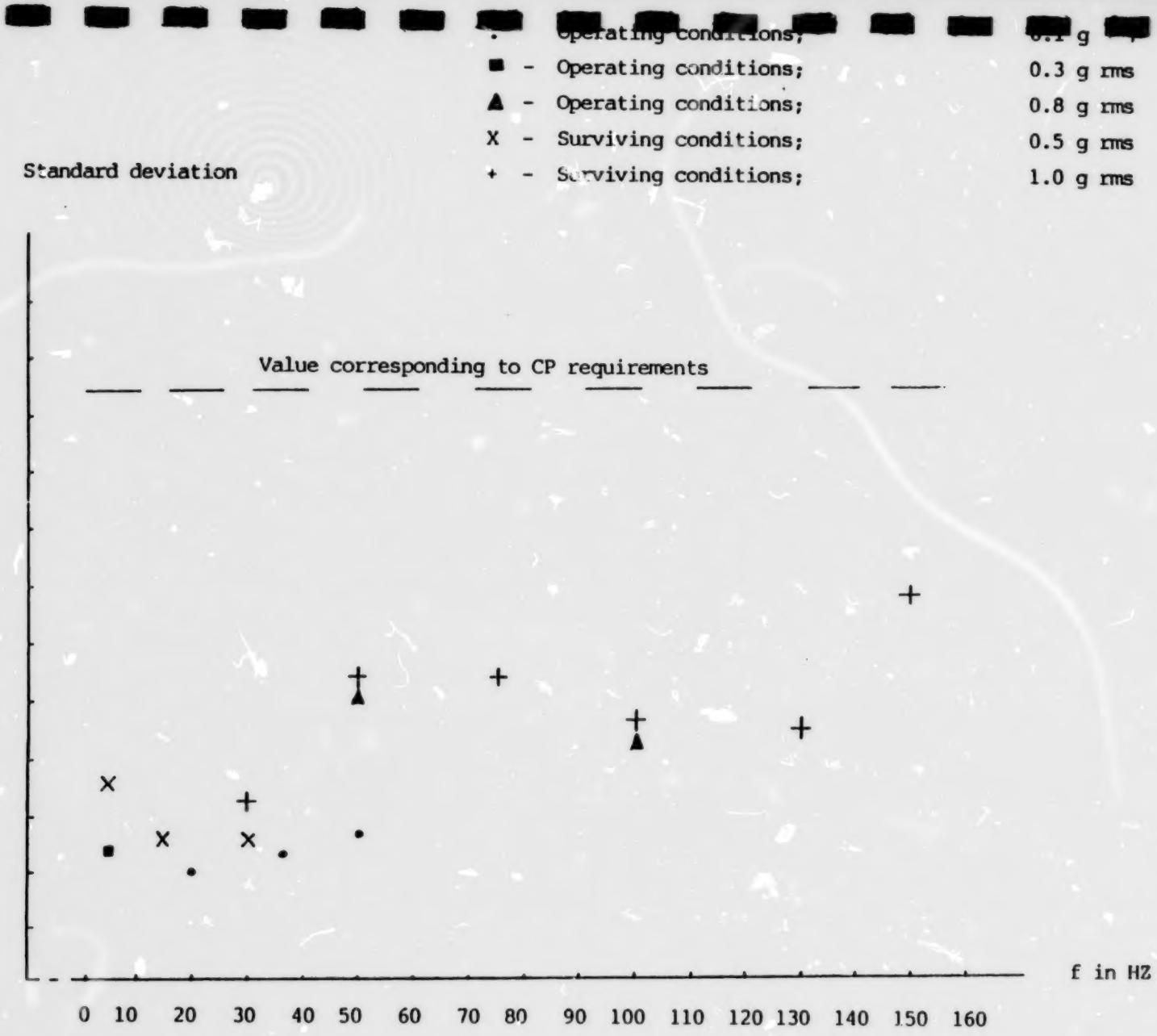
• - Operating conditions; 0.1 g rms
■ - Operating conditions; 0.3 g rms
▲ - Operating conditions; 0.8 g rms
X - Surviving conditions; 0.5 g rms
+ - Surviving conditions; 1.0 g rms
Standard deviation
Value corresponding to CP requirements
f in HZ
0 10 20 30 40 50 60 70 80 90 100 110 120 130 140 150 160

Fig. 50 Vibrations - VR direction

Fig. 51
f = 90 HZ
a = 1.20 g
LT

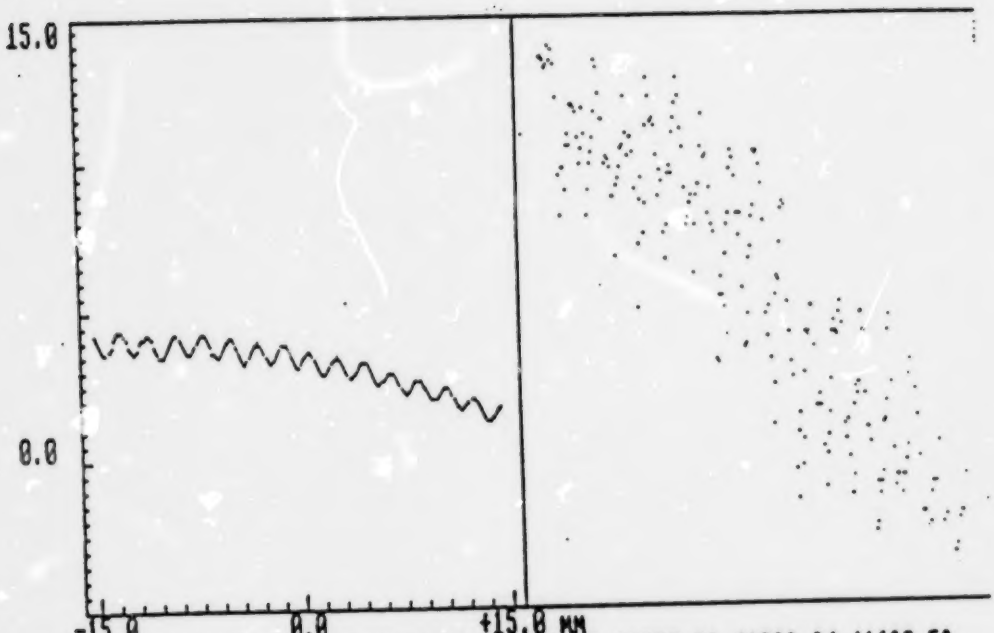

Average =	2212.66	2196.76	2150.96	2075.35	1970.31	1838.94	1680.59
Deviation =	60.26	59.36	58.51	56.12	55.29	52.54	55.18

->_

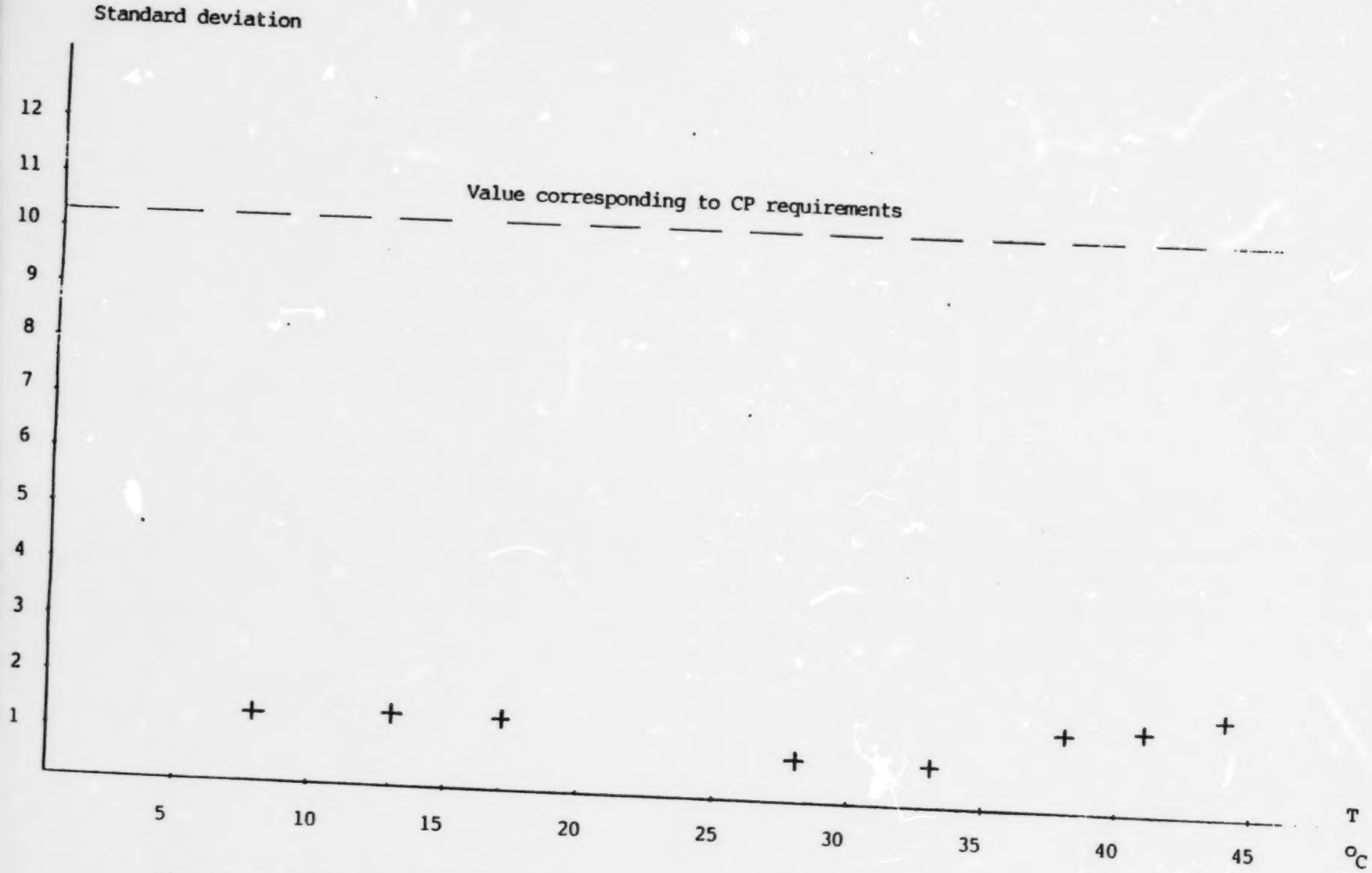

Fig. 52 Standard Deviation vs temperature

Fig. 53

Actual SMC in room conditions

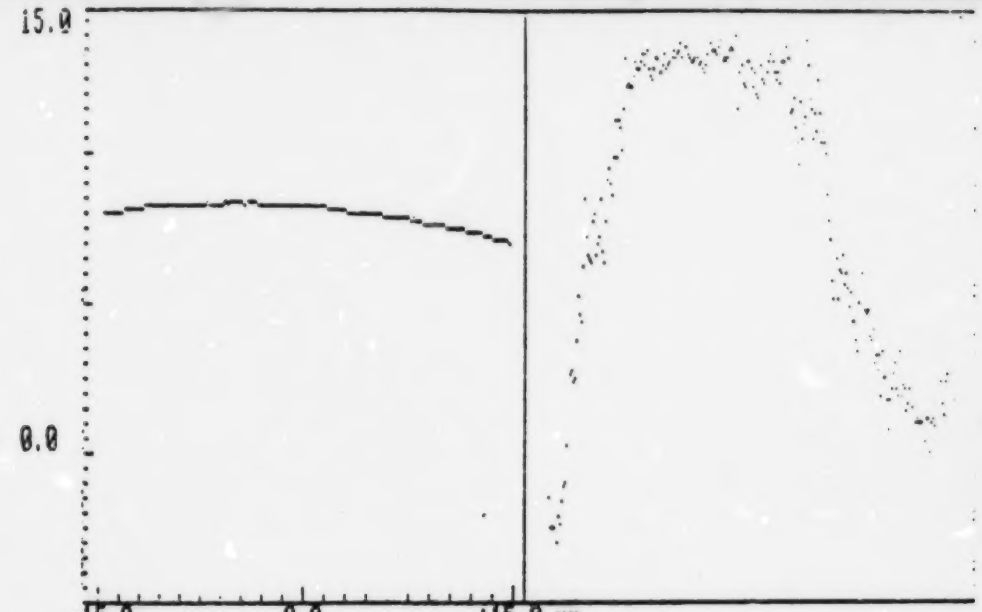


```
Average   = 2694.96 |2716.35 |2719.34 |2701.06 |2663.20 |2608.85 |2530.73
Deviation =    0.26 |   0.20 |   0.21 |   0.21 |   0.26 |   0.34 |   0.48
```

->_

LT and LG vibrations without scanning; operating requirements

TAB 1 LT

f	a	t
2	0.1	25
3		
4		
5		
10		
15		
20		
25		
30		
40		
50		
60		
70		
80		
90		
100		
110		
120		
130		
140		
150	0.1	25

TAB 2 LG

f	a	t
2	0.1	25
3		
4		
5		
10		
15		
20		
25		
30		
40		
50		
60		
70		
80		
90		
100		
110		
120		
130		
140		
150	0.1	25

TAB 3 VR

f	a	t
1 2 3 4 5	0.3 0.3	25 25
5 10 15 20 30 40 50	0.1 0.1	10 25 25
50 60 70 80 90 100	0.8 0.8	25 25

LT, LG and VR vibrations without scanning; survival conditions

TAB 4 LT

f	a	t
5	0.5	25
20	0.5	25
[illegible]	1.0	25
50		
00	1.0	25

TAB 5 LG

f	a	t
5	0.5	25
10		
15		
20		
25		
30	0.5	25
30	1.0	25
40		
50		
70		
90		
100		
120		
150	1.0	25

TAB 6 VR

f	a	t
5	0.5	25
10		
15		
20		
25		
30	0.5	25
30	1.0	25
40		
50		
70		
90		
100		
120		
150	1.0	25

LT and LG vibrations with scanning and signal measurement;
operating requirements

TAB 7 LT

f	a	t
2	0.1	30
3		30
4		30
5		60
10		30
15		30
20		30
25		60
30		30
40		30
50		60
60		30
70		30
80		60
90		60
100		900
110		30
120		30
130		30
140		30
150	0.1	30

TAB 8 LG

f	a	t
2	0.1	30
3		30
4		120
5		120
10		30
15		30
20		30
25		60
30		30
40		30
50		60
60		30
70		30
80		60
90		60
100		720
110		30
120		30
130		30
140		30
150	0.1	60

LT and LG vibrations with scanning and signal measurements;
survival requirements

TAB 9 LT

f	a	t
5	0.5	60
10	0.5	60
15	0.5	60
20	0.5	60
25	0.5	60
30	0.5	60
30	1.0	60
40	|	60
50	|	60
70	|	60
90	|	60
100	|	60
120	|	60
150	1.0	60

TAB 10 LG

f	a	t
5	0.5	60
10	|	60
15	|	60
20	|	60
25	|	60
30	0.5	60
30	1.0	60
40	|	60
50	|	60
70	|	60
90	|	60
100	|	60
120	|	60
150	1.0	60

LT and LG vibrations with scanning and signal measurements survival requirement

TAB 11 LG

f	a	t
1	0.125	15
2	0.183	15
4	0.159	15
10	0.194	15
25	0.140	15
50	0.128	15
50	0.315	25
50	0.761	25
50	1.120	25
50	1.530	25
50	2.150	25
75	0.644	15
75	1.880	25
75	3.150	20
100	0.775	20
100	1.880	20
150	1.750	25
150	0.350	25

TAB 12 LT

f	a	t
4	2.10	60
10	2.05	30
20	1.27	15
25	1.95	25
50	0.200	120
50	1.200	25
75	0.200	60
75	1.200	25
90	1.250	30
90	1.550	30
100	0.100	15
100	0.200	60
100	0.380	20
150	0.320	20
150	1.15	15
150	2.08	25

VR vibrations with scanning and signal measurements

Operating requirements

Tab 13

f	a	t
3	0.328	30
5	0.326	30
20	0.116	30
35	0.121	30
50	0.130	30
50	0.818	30
75	0.816	30
90	0.808	30
100	0.812	30

Survival requirements

Tab 14

f	a	t
5	0.519	30
15	0.511	30
30	0.501	30
30	1.024	30
50	1.018	30
75	1.026	30
100	1.016	30
130	1.018	30
150	1.024	30

TAB 15

	t_d	r	t_{cam}	t_{las}	t_{pel}	P	i_{las}	i_{pel}	t	Remarks
	^oC	%	^oC	^oC	^oC	mW	mA	mA	min	
	1 x	N/A	3.61	20.52	3.26	0.55	70.6	- 780	15	x Only one point on the object measured because of scanner operating requirements after being left in non-operating t_d = - 25° C during 24 hours
	1 x		3.82	21.04	3.40	0.50	70.7	- 780	15	
	1 x		3.86	21.13	3.82	0.50	70.6	- 780	15	
	1 x		3.97	21.29	3.68	0.66	71.6	- 780	15	
	1 x		4.02	21.39	3.68	0.66	71.5	- 780	15	
	1 x		4.02	21.39	3.68	0.66	71.5	- 780	15	
	1 x		4.15	21.52	3.82	0.47	70.1	- 780	15	
	8		10.45	22.60	9.54	0.77	72.6	- 564	15	
	8		10.41	22.61	9.41	0.77	72,6	- 564	15	
	8		10.37	22.59	9.41	0.77	72.6	- 568	15	
	8		10.33	22.60	9.41	0.77	72.6	- 568	15	
	8		10.27	22.60	9.41	0.77	72.6	- 568	15	
	12		10.25	22.46	9.28	0.41	70.7	- 584	15	
	12		10.25	22.46	9.28	0.41	70.7	- 584	15	
	12		10.25	22.46	9.28	0.41	70.7	- 584	15	
	13		10.01	22.51	9.15	0.78	72.5	- 580	15	
	13		10.34	22.51	9.41	0.78	72.6	- 572	15	
	13		10.51	22.58	9.54	0.78	72.6	- 568	15	
	17		16.05	23.58	15.88	1.13	74.5	- 368	15	
	17		16.64	23.77	16.16	0.69	72.7	- 340	15	

TAB 16

	t_d	r	t_{cam}	t_{las}	t_{pel}	P	i_{las}	i_{pel}	t	Remarks
	^oC	%	^oC	^oC	^oC	mW	mA	mA	min	
	28	78	27.69	25.95	25.68	0.94	74.8	64.0	15	
	28	78	27.64	25.93	25.65	0.95	74.8	64.0	15	
	28	78	27.62	25.94	25.56	0.95	74.8	60.0	15	
	33	77	31.88	26.95	30.20	0.86	74.9	260.0	15	
	33	77	31.52	26.83	29.48	0.87	74.9	236.0	15	
	33	77	31.27	26.71	28.91	0.88	74.9	216.0	15	
	33	77	31.27	26.69	28.80	0.89	74.9	208.0	15	
	37	79	34.09	27.20	31.06	0.85	74.9	312.0	15	
	37	79	34.27	27.24	31.15	0.85	74.9	316.0	15	
	37	81	34.30	27.32	31.42	0.84	74.9	328.0	15	
	40	76	36.25	27.80	33.46	0.80	75.0	424.0	15	
	40	76	36.25	27.81	33.49	0.79	75.0	424.0	15	
	40	76	36.21	27.80	33.48	0.79	75.0	424.0	15	
	40	76	36.21	27.81	33.49	0.79	75.0	424.0	15	
	40	88	36.45	27.90	33.99	0.80	75.0	448.0	15	
	40	88	36.49	27.92	33.99	0.80	75.0	448.0	15	condensation traces
	40	88	36.53	27.91	34.02	0.80	75.0	448.0	15	on thecamera case
	40	88	36.53	27.91	34.04	0.80	75.0	448.0	15	
	40	88	36.61	27.95	34.14	0.80	75.0	452.0	15	

TAB 16 Continued

	t_d	r	t_{cam}	t_{las}	t_{pel}	P	i_{las}	i_{pel}	t	Remarks
	^oC	s	^oC	^oC	^oC	mW	mA	mA	min	
	41	90	36.92	28.05	34.43	0.79	75.0	472.0	15	
	41	90	36.92	28.05	34.49	0.79	75.0	468.0	15	condensation on
	41	90	36.92	28.04	34.49	0.78	75.0	468.0	15	the camera case
	41	90	36.92	28.04	34.49	0.79	75.0	472.0	15	
	41	90	36.88	28.05	34.49	0.79	75.0	472.0	15	
	41	90	36.92	28.05	34.49	0.79	75.0	472.0	15	
	44	77	39.73	28.56	36.66	0.73	75.1	568.0	15	
	44	78	39.84	28.65	36.95	0.73	75.1	588.0	15	
	44	78	40.00	28.73	37.29	0.72	75.1	604.0	15	
	44	78	40.14	28.79	39.13	0.71	75.1	612.0	15	* after being left in
	38 *	56	35.20	27.71	32.95	0.81	75.0	396.0	15	t_d= 40 during 40 hrs